

INFORMATION TO USERS

This was produced from a copy of a document sent to us for microfilming. While the most advanced technological means to photograph and reproduce this document have been used, the quality is heavily dependent upon the quality of the material submitted.

The following explanation of techniques is provided to help you understand markings or notations which may appear on this reproduction.

1. The sign or "target" for pages apparently lacking from the document photographed is "Missing Page(s)". If it was possible to obtain the missing page(s) or section, they are spliced into the film along with adjacent pages. This may have necessitated cutting through an image and duplicating adjacent pages to assure you of complete continuity.
2. When an image on the film is obliterated with a round black mark it is an indication that the film inspector noticed either blurred copy because of movement during exposure, or duplicate copy. Unless we meant to delete copyrighted materials that should not have been filmed, you will find a good image of the page in the adjacent frame.
3. When a map, drawing or chart, etc., is part of the material being photographed the photographer has followed a definite method in "sectioning" the material. It is customary to begin filming at the upper left hand corner of a large sheet and to continue from left to right in equal sections with small overlaps. If necessary, sectioning is continued again—beginning below the first row and continuing on until complete.
4. For any illustrations that cannot be reproduced satisfactorily by xerography, photographic prints can be purchased at additional cost and tipped into your xerographic copy. Requests can be made to our Dissertations Customer Services Department.
5. Some pages in any document may have indistinct print. In all cases we have filmed the best available copy.

**University
Microfilms
International**

300 N. ZEEB ROAD, ANN ARBOR, MI 48106
18 BEDFORD ROW, LONDON WC1R 4EJ, ENGLAND

8014980

PEARL, MIRILEE LESLIE

STUDIES ON THE ROLE OF ACTIN MICROFILAMENTS IN THE ACTION
OF VASOPRESSIN IN TOAD URINARY BLADDER

City University of New York

PH.D.

1980

University
Microfilms
International

300 N. Zeeb Road, Ann Arbor, MI 48106

18 Bedford Row, London WC1R 4EJ, England

Copyright 1979

by

Pearl, Mirilee Leslie

All Rights Reserved

PLEASE NOTE:

In all cases this material has been filmed in the best possible way from the available copy. Problems encountered with this document have been identified here with a check mark .

1. Glossy photographs
2. Colored illustrations _____
3. Photographs with dark background
4. Illustrations are poor copy _____
5. Print shows through as there is text on both sides of page _____
6. Indistinct, broken or small print on several pages _____ throughout

7. Tightly bound copy with print lost in spine _____
8. Computer printout pages with indistinct print _____
9. Page(s) _____ lacking when material received, and not available from school or author _____
10. Page(s) _____ seem to be missing in numbering only as text follows _____
11. Poor carbon copy _____
12. Not original copy, several pages with blurred type _____
13. Appendix pages are poor copy _____
14. Original copy with light type _____
15. Curling and wrinkled pages _____
16. Other _____

STUDIES ON THE ROLE OF ACTIN
MICROFILAMENTS IN THE ACTION OF VASOPRESSIN
IN TOAD URINARY BLADDER
BY
MIRILEE LESLIE PEARL

A dissertation submitted to the Graduate
Faculty in Biomedical Sciences in partial
fulfillment of the requirements for the
degree of Doctor of Philosophy, The
City University of New York.

© COPYRIGHT BY
MIRILEE LESLIE PEARL

1980

Studies on the Role of Actin Microfilaments in the Action of Vasopressin in
Toad Urinary Bladder

by

Mirilee Leslie Pearl

Thesis Advisor, Professor Ann Taylor

Vasopressin -(VP) induced water movement across toad urinary bladder epithelium (TUBE) was inhibited by dihydrocytochalasin B, suggesting that actin plays a role in the VP response. An actin-like protein was therefore isolated from TUBE. Crude extracts of isolated cells show a prominent band on SDS gels that comigrates with rabbit muscle actin. This fraction was purified on DEAE-cellulose and the polymerized pellet resulting from the column step was highly enriched in the 45,000 dalton component. This material was further purified on Sephadex G-150. Electron microscopy (EM) of polymerized, negatively stained samples derived from such extracts revealed 50-70 A filaments similar to those formed by rabbit actin. In sectioned material, many such filaments were seen in the apical subplasmalemmal region of whole TUBE cells. When bladders were glycerinated and subsequently exposed to heavy meromyosin (HMM), EM of this region revealed filaments decorated with arrowhead figures similar to those formed by HMM and rabbit actin. HMM-decorated filaments were also seen in the smooth muscle layer of toad bladders. These findings are consistent with the concept that 1) an actin-like protein is a major component of TUBE cells; and 2) an actin-like protein may play a functional role in VP-induced water movement.

ACKNOWLEDGEMENTS

Many individuals helped make by predoctoral training a fruitful and pleasurable experience. Among these I would first like to thank my advisor, Ann Taylor, whose intelligence, integrity, and kindness have made her a joy to work with. Ann not only provided a comfortable space in which to work, but also gave freely of her time during these years. She is one of the finest persons I have been lucky enough to know, and I sincerely hope that the future will allow us to work together again.

Over the years I have been greatly impressed by the friendly atmosphere in the Department of Physiology at Cornell. I wish to thank Erich Windhager whose own graciousness seems to set the casual but intense tone of the department. Dr. Windhager always made me feel a welcome member of Cornell, and I am grateful for this treatment.

Elizabeth Eich in my lab used to work with Roger Greif at Cornell, and when I first came to Cornell. Elizabeth helped me set up biochemical systems in the lab, using equipment from Dr. Greif's lab. These two individuals have also given generously of time and advice, without which I never would have gotten through these years. I especially want to thank Liz for buying milk in the morning. I want to thank, in addition, the other members of the Department of Physiology at Cornell who were individually helpful during my graduate training.

None of this would have happened were it not for the particular philosophy of Irving Schwartz, who permitted me to do my dissertation research at Cornell. I am grateful for having had this opportunity. Sandy Masur at Mount Sinai was

responsible, actually, for my getting to know Ann Taylor, and acted throughout these years as my official advisor and, more personally, as intermediary to smooth the bureaucratic complications caused by working in two institutions. I want to thank Sandy also for keeping the faith throughout the hard times.

Most of the microscopy in this thesis was done in Bill Marovitz's laboratory. Bill not only trained me as a microscopist, but is also my friend. I wish to thank him for allowing me to feel at home in his lab, and for endless helpful conversations, supplies and warm feelings.

Friendship and moral support during these years, especially from Michael Toma, Rita Margolies, Catherine Ross, Naomi Rhoads, Frank King and others has helped keep me together and moving along the path.

Sara Leake, Kathleen Tobin and Theresa Neal all helped me deal with administrative tasks and reams of paper generated during the course of the work. Rochelle Lester typed the thesis manuscript beautifully and minimized the trauma which this caused me. For all this help and good feeling, I am deeply grateful.

TABLE OF CONTENTS

	<u>Page</u>
List of Tables	xi
List of Figures	xii
INTRODUCTION	1
The Role of Vasopressin in Osmoregulation and its Cellular Mechanism of Action	4
Biochemical Pathways in Vasopressin Action	5
Mechanism of Water Permeation	9
Cellular Events in the Action of Vasopressin	11
Route of Water Movement	11
Exo- and Endocytosis	11
Intramembranous Particle Aggregates	13
Microtubules and Microfilaments	15
Microfilaments	16
METHODS	22
I. Functional Studies	22
Measurement of Osmotic Water Movement: Studies with Dihydrocytochalasin B	22
Measurement of the Effective Osmotic Gradient	23
Calculations	23
Dihydrocytochalasin B	24
II. Biochemical Studies	24
Protein Determinations	24
SDS-Polyacrylamide Gel Electrophoresis	28

<u>Table of Contents, continued</u>	<u>Page</u>
Myosin ATPase Activity	32
Preparation of Stock Proteins	35
Rabbit Psoas Muscle Actin	35
Rabbit Muscle Myosin	41
Heavy Meromyosin	46
Isolation of Actin from Toad Bladder Epithelial Cells	49
Isolation of Epithelial Cells	49
Extraction of Toad Bladder Actin	50
DEAE-Cellulose Chromatography	51
Polymerization of Actin-like Protein	52
Preparation of G-150 Column	53
Chromatography of Actin-like Protein on G-150 Sephadex	54
III. Morphological Studies	55
Glycerination and Heavy Meromyosin Treatment of Toad Urinary Bladders	55
Sample Preparation for Electron Microscopy	57
Thin Section Electron Microscopy	57
Negatively Stained Samples	59
RESULTS	61
I. Effect of Dihydrocytochalasin B on Osmotic Water	61
Effect on Basal Water Flow	61
Effect on Vasopressin-Induced Water Flow	63

<u>Table of Contents, continued</u>	<u>Page</u>
II. Isolation and Purification of Actin-like Protein from Toad Bladder Epithelial Cells	63
Preliminary approaches	63
Hartwig and Stossel Procedure	63
Extraction from Acetone Powder	72
Isolation of Actin-like Protein by Column Chromatography	76
DEAE Cellulose Chromatography	77
Polymerization Cycle	79
Chromatography of Toad Bladder Actin- like Protein on G-150 Sephadex	83
Filament Formation	86
Estimates of Actin Content and Yields	93
III. In Situ Labeling of Actin Filaments with Heavy Meromyosin	94
Results of HMM Labeling of Epithelial Cells	99
The Granular Cell	99
Other Epithelial Cells	111
Mitochondria-Rich Cell	111
Basal Cells	114
Smooth Muscle Cells	122
Dimensions of Toad Bladder Acto-HMM	128
DISCUSSION	130
I. Functional Studies with Dihydrocytochalasin B	130

<u>Table of Contents, continued</u>	<u>Page</u>
II. Biochemical Studies	134
Isolation of Actin-like Protein	134
Evidence for a Toad Bladder Myosin-like Protein	139
III. Morphological Studies: In situ Labeling with HMM	141
Glycerin Treatment	141
Heavy Meromyosin Decorated Bladders	143
Comparisons with Other Studies on Toad Bladder Actin	144
Organization of the Microfilament Lattice	146
Correlations and Conclusions	147
The Cytoskeletal Lattice	147
Microfilament-membrane Associations	147
REFERENCES	150

LIST OF TABLES

<u>Table No.</u>	<u>Title</u>	<u>Page</u>
1	Reproducibility of Standard Protein Curve	26
2	Activation of Myosin Mg^{++} -ATPase by Rabbit Muscle Actin	41
3	ATPase Activities of Rabbit Muscle Myosin	46
4	Effect of Dihydrocytochalasin B and DMSO on Basal Osmotic Water Movement	62
5	Effect of Dihydrocytochalasin B on Vasopressin-Stimulated Water Movement	65
6	Theoretical and Observed Yields of Toad Bladder Actin-like Protein	93
7	Filament Periodicity and Width of Toad Bladder Acto-HMM	129
8	Average Lengths of HMM-Decorated Filaments	146

LIST OF FIGURES

<u>Figure No.</u>	<u>Title</u>	<u>Page</u>
1	Chemical Structure of Cytochalasin B and Dihydrocytochalasin B	20
2	Average Standard Protein Determinations (Lowry), 1977-1979	27
3	Electrophoretic Mobility of Standard Proteins on 5% SDS Gels	33
4	Myosin ATPase Activity: Standard Curve	36
5	Filament Formation by Purified Rabbit Muscle Actin	40
6	Filament Formation by Purified Rabbit Muscle Myosin	45
7	Interaction of Rabbit Muscle Actin with Heavy Meromyosin	48
8	Effect of Dihydrocytochalasin B on VP-induced Osmotic Water Movement	64
9	Densitometry of Fractions of Toad Bladder Actin-like Proteins Isolated by the Method of Hartwig, et al.	68
10	Outline of Isolation Procedure for Toad Bladder Actin-like Protein Modified after the Method of Hartwig, et al.	69
11	SDS Gels of Toad Bladder Actin-like Protein Isolated by the Method Modified from Hartwig, et al.	70
12	Outline of Isolation Procedure for Toad Bladder Actin-like Protein by Extraction from an Acetone Powder	73
13	SDS Gels of Toad Bladder Actin-like Protein Isolated from an Acetone Powder	75

List of Figures, continued

<u>Figure No.</u>	<u>Title</u>	<u>Page</u>
14	Outline of Isolation Procedure for Toad Bladder Actin-like Protein Modified after the Method of Gordon, et al.	78
15 A & B	Elution of Rabbit Muscle Actin and Toad Bladder Actin-like Protein from DEAE-Cellulose	81
16	Gel Profile of Selected DEAE- Cellulose Column Fractions	82
17	SDS Gels of Toad Bladder Actin-like Protein Purified on DEAE-Cellulose	84
18	Chromatography of Actin on G-150 Sephadex	85
19	SDS Gels of Toad Bladder Actin-like Protein Purified on DEAE-Cellulose and G-150 Sephadex	87
20	Filament Formation by Actin-like Protein Purified on DEAE-Cellulose	88
21	Filament Formation by Peak I of G-150 Sephadex Column	90
22	Filament Formation by Peak II of G-150 Sephadex Column	92
23	Interaction of Material from Peak II with Heavy Meromyosin	92
24	Electron Micrograph of Typical Intact Toad Bladder	96
25	Apical Region of Normal Granular Epithelial Cell	97
26	Apical Region of Glycerinated Granular Cell	100
27	High Power EM of Glycerinated Granular Cell Treated with HMM and ATP	101

List of Figures, continued

<u>Figure No.</u>	<u>Title</u>	<u>Page</u>
28 A & B	Apical Region of Granular Cell Treated with HMM	104, 105
29	Basolateral Region of Granular Cell Treated with HMM	108
30	Apical Region of Granular Cell Treated with HMM including Granule-Associated Decorated Filaments	109
31	Normal Morphology of a Toad Bladder Mitochondria-Rich Cell	112
32 A & B	Apical Region of HMM-Decorated Epithelial Cell Tentatively Identified as Mitochondria-Rich Cell	115, 116
33	Central Area of HMM-Decorated Epithelial Cell Tentatively Identified as Mitochondria-Rich Cell	117
34	Normal Morphology of a Toad Bladder Basal Epithelial Cell	119
35	Basal Cell Treated with HMM	120
36	Normal Morphology of Toad Bladder Smooth Muscle	123
37	Smooth Muscle Treated with HMM and ATP	124
38 A & B	Toad Bladder Smooth Muscle Treated with HMM	125, 126

To the memory of Sarah

Ah, it is the fault of our science
that it wants to explain all; and if
it explain not, then it says there
is nothing to explain. But yet we
see around us every day the growth
of new beliefs, which think them-
selves new; and which are yet but
the old, which pretend to be young --
like the fine ladies at the opera. *

*Dracula, Bram Stoker (1897). Tempo Books, New York, 1979, p. 256.

INTRODUCTION

Actin is the major protein of both striated and smooth muscle. In skeletal muscle, actin filaments 50 - 70 A in diameter interact with the ATPase of parallel myosin filaments and provide the force-generating mechanism which is the basis of muscle contraction. A similar situation pertains in smooth muscle, although the structural relationships between actin and myosin have not yet been clearly defined. Muscle actin has been extensively characterized over the years, and a great deal of information is available about its structure and interactions with myosin and regulatory muscle proteins (64, 141, 142).

The molecular basis of the motility and contractility of nonmuscle cells is not so well understood. However, the investigations of the last decade have clearly shown that the movements of cells, and in many cases of their constituent organelles, are mediated through the organized activity of contractile proteins and microtubules (47, 115, 125). Microfilaments composed of actin-like protein subunits are present in all eukaryotic cells (115) and are believed to interact, in many cases, with myosin (25) and elements of calcium-based regulatory mechanisms (25, 38). These interactions of nonmuscle contractile proteins thereby form the basis of cellular processes controlling cell shape (25) and cellular motility (25, 134). In nonmuscle cells, actin filaments are closely associated with cell membranes (26, 103, 122) and appear to be of critical importance in regulating their surface topography (26, 139). The cooperative functioning of microfilaments and microtubules has been implicated in regulation of the spatial distribution and lateral mobility of surface receptors on lymphocytes and fibroblasts (39, 137); and these organelles may play a cooperative role in surface processes such as the capping of antibodies (26,

39). The functional integrity of microfilaments is also necessary for exo- and endocytosis (4, 39).

The neurohypophyseal hormone, vasopressin, has two major cellular actions. It influences smooth muscle contractility (5), and it promotes trans-cellular water movement in responsive epithelial tissues (53, 57, 77). This latter action underlies its primary physiological role, which is the regulation of water balance (7, 53). Microfilaments (50 - 70 A and 100 A diameter) and also microtubules are known to be present in vasopressin-sensitive epithelial cells, as in other nonmuscle cells. In the past few years, several laboratories have provided evidence that vasopressin-stimulated osmotic water movement (the hydrosmotic response) is dependent on the structural and/or functional integrity of these cytoskeletal elements. Thus, agents that interact with tubulin and disrupt microtubules, such as colchicine, vinblastine and podophyllotoxin, inhibit the action of vasopressin on water movement in amphibian epithelia (36, 130, 131, 133). There is convincing evidence that the inhibitory effects of these agents are due to their interaction with tubulin (and/or cytoplasmic microtubules) within the epithelial cells. Similarly, cytochalasin B, an agent which inhibits many cellular processes dependent on a functionally intact microfilament network, specifically impairs vasopressin- (and oxytocin-) stimulated water flow in anuran urinary bladder (19, 29, 51, 130, 132). Though data obtained from experiments with cytochalasin B must be interpreted with caution, one may reasonably conclude from recent work in this field (16, 17, 89), that the 50 - 70 A microfilaments present in toad bladder epithelial cells (24, 109) may participate in the hydrosmotic action of the

hormone (19, 29, 51, 130, 132).

The specificity of the interaction between cytochalasin B and actin microfilaments in nonmuscle cells has long been a subject of controversy. Indeed, the drug has been shown also to interfere with the transport of hexoses and nucleosides across the plasma membranes of many cell types (75, 114). Recently, a new cytochalasin analogue, dihydrocytochalasin B (H₂CB), has been developed (87). Experiments in various cell types indicate that this drug interferes in a similar fashion to cytochalasin B with nonmuscle cell functions requiring actin, but that it has no effect on hexose or nucleoside transport (9, 87).

The availability of this agent now makes it possible to specifically test the hypothesis that actin-containing microfilaments are involved in the hydros-motic action of vasopressin. However, an actin-like protein has never been isolated from, nor specifically localized within, the target cells of vasopressin-sensitive epithelia.

The studies presented below are concerned with the role of actin microfilaments in mediating the hydros-motic response to vasopressin in the urinary bladder of the toad. The findings cover three areas: 1) functional studies on the inhibition of vasopressin-induced water movement by dihydrocytochalasin B indicate that this drug is effective in inhibiting the hydros-motic response in the toad urinary bladder; 2) biochemical studies provide evidence that an actin-like protein which forms 50 - 70 Å microfilaments is a major consti-tuent of the bladder epithelial cells; and 3) morphological studies of the inter-action of bladder epithelial cell microfilaments with heavy meromyosin pro-

vide unequivocal evidence that actin is present in the bladder epithelium, and give information about its localization within the epithelial cells.

The Role of Vasopressin in Osmoregulation and Its

Cellular Mechanism of Action

The regulation of internal water balance, including the osmolality and, to some extent, the volume of body fluids, is mediated, in terrestrial vertebrates, through the action of vasopressin (antidiuretic hormone). This octapeptide is manufactured in the lateral and ventromedial hypothalamus (119). Projections of the hypothalamic nuclei, which pass through the pituitary stalk, transport hormone-containing vesicles to storage sites in the neurohypophysis. Under conditions of hyperosmolarity, or during episodes of acute volume depletion, the activation of sensitive cells in the supraoptic nucleus, perhaps directly by osmotic shrinkage, signals the neurohypophysis to release vasopressin into the peripheral circulation (119). Upon release, vasopressin circulates at a concentration of 10^{-12} - 10^{-11} M and eventually binds to specific receptors on the plasma membranes of its target cells (72). The concerted events resulting from the action of vasopressin serve as links in the servo-regulatory mechanism that functions to maintain a normal effective circulating blood volume. The hormone causes the contraction of some smooth muscles and the relaxation of others (5). Its effects on the epithelial tissues of the mammalian kidney (7, 8, 34), and on the urinary bladders and skin of amphibians (8, 62, 82), lead to the absorption of water (and, in mammals, to the production of concentrated urine) according to osmotic necessity.

Studies of the mechanism of action of vasopressin in renal target tissues are complicated by the problems encountered in dealing with so complex an organ as the kidney. For this reason, the amphibian urinary bladder and skin have been extensively employed as model epithelial systems. Information about the cellular mechanism of action of vasopressin has largely been obtained through the use of toad and frog bladder as experimental systems. The data thus obtained have, in large part, aided in developing an understanding of the functions of the mammalian distal nephron. The information derived from the present studies may therefore be expected to provide insights into the mechanism of action of vasopressin in hormone-sensitive cells of mammalian as well as amphibian origin. To facilitate understanding of the development of ideas in this field, the discussion of the cellular action of vasopressin which follows will consider data obtained from the use of sensitive anuran epithelial systems, supplemented with relevant information from studies of mammalian renal tissues.

Biochemical Pathways in Vasopressin Action

The cellular action of vasopressin is initiated by hormone binding to responsive epithelial cells. The localization of the vasopressin receptor to basolateral cell membranes was originally inferred from the fact that, under physiological conditions, the hormone is only effective when presented to the serosal side of its target epithelial cells (11, 77, 82). Stronger evidence for this hypothesis has come from recent studies of canine renal medullary membranes examined after separation by free-flow electrophoresis (123). Enzy-

matic analysis of fractions obtained by this method indicated that vasopressin-sensitive adenylate cyclase activity was present only in the membrane fraction identified as being derived from the basolateral plasma membranes of the medullary epithelial cells (123).

The concept that vasopressin acts by altering cyclic adenosine monophosphate (cAMP) levels in toad bladder epithelium was originally proposed by Orloff and Handler (107, 108), who showed that addition of cAMP or theophylline to isolated toad bladders mimicked the vasopressin response. Subsequently, Handler et al. (52) demonstrated that vasopressin increases intracellular cAMP levels in whole toad bladders; and these findings have been confirmed in preparations of isolated epithelial cells (106). Recent experiments in toad bladder (151, 152) and renal medulla (153) have now provided evidence that the vasopressin-stimulated increase in cAMP is modulated (damped) through feedback regulation involving prostaglandins. Apparently, vasopressin causes an increase in the synthesis of prostaglandin E₂, and this in turn is believed to regulate cAMP production through inhibition of vasopressin-sensitive adenylate cyclase activity (151-153).

It is generally accepted that cAMP exerts its effects by activation of protein kinases (80). In vasopressin-sensitive epithelia, elements of one or more cAMP-dependent protein kinase system(s) have also been described (31, 36, 40, 67, 73, 123). Jard and Bastide (67) first obtained evidence for a protein kinase in toad bladder epithelial cells, using exogenous histones as an acceptor; later studies by Kirchberger et al. (73) and Dousa et al. (36) demonstrated cAMP-dependent protein kinase activity in a soluble fraction of toad

bladder epithelial cells and in renal medullary plasma membranes, respectively. These workers showed that phosphorylation of exogenous substrates was increased in the presence of cAMP. In contrast, DeLorenzo and Greengard (31) and others (40) found that phosphorylation of a specific membrane protein (protein D) (32) from toad bladder was decreased after exposure to cAMP, apparently through the action of a specific membrane-associated cAMP-dependent phosphatase. Protein D (P-50) was later demonstrated by Greengard and co-workers in a wide variety of cell types (32). Schwartz et al. (123) using renal medullary membranes purified by free flow electrophoresis, described a cAMP-mediated self-phosphorylating system consisting of a protein kinase and substrate associated with the luminal plasma membrane fraction. However, these workers were unable to demonstrate any cAMP-dependent phosphatase activity in this system. Recently, Huang (63) has characterized cAMP-dependent protein kinase in renal medullary tissue, and has demonstrated both Type I and Type II kinases in the soluble fraction, together with cAMP-dependent kinases which were membrane-bound. Both soluble and particulate fractions contained kinases which were self-phosphorylating. Further work on the membrane-bound self-phosphorylating (Type II) kinase revealed that it consisted of a catalytic and regulatory subunit, and that the latter appeared to be identical with Protein D. In the presence of cAMP, the catalytic subunit phosphorylated its regulatory subunit; and the latter (protein D) was subsequently dephosphorylated by the phosphatase described by DeLorenzo et al. (31, 32). Thus, cAMP was shown to control net dephosphorylation of protein

D at the substrate level, i. e., cAMP-dependent phosphorylation of protein D rendered this protein susceptible to the action of the phosphatase which had originally been observed in the earlier studies by DeLorenzo et al. In sum, these studies demonstrating cAMP-dependent activation of protein kinases in vasopressin-sensitive systems show that while such a pathway plays a role in the action of this hormone, the precise relationship of protein kinase activation to the sequence of events leading to hormone-induced changes in membrane permeability remains to be determined.

In amphibian urinary bladder vasopressin (and exogenous cAMP) increases the permeability of the apical epithelial cell membrane to water and also to sodium, urea and certain other small molecules (8, 34). These effects are mediated by separate pathways, and can be differentially inhibited during the course of transport experiments. Thus, hormone-stimulated water movement is blocked by methohexital(84) and by colchicine and cytochalasin B (130), while sodium and urea transport are unaffected (19, 29, 130). Similarly, hormone-stimulated sodium transport can be blocked by treatment of the bladder with amiloride (13), without any effect on the hydrosmotic response. Finally, incubation of bladders with phloretin (83) inhibits hormone-stimulated urea transport without affecting the increase in the transport of water or sodium. The subject of this thesis is primarily concerned with the cellular pathway leading to increased water permeability of the apical membrane of bladder epithelial cells, and the data available concerning the activation of this transport pathway will now be discussed in detail.

Mechanism of Water Permeation

Classical studies by Hevesy et al. (62) and Koefoed-Johnsen and Ussing (77) of the isolated amphibian skin showed that the diffusional flow of water measured as the isotopic flux of D_2O in the presence of vasopressin was insufficient to account for the observed rate of osmotic water movement when the skin was exposed both to hormone and an osmotic gradient. These authors concluded that a mechanism of bulk flow must therefore be operating to account for the rate of osmotic water movement. Andersen and Ussing(6) later postulated that a diffusional and bulk flow barrier were present in series in the skin to account for the specificity of action of vasopressin on water movement. Subsequently, Hays and Leaf (57) carried out similar studies in the toad bladder and arrived at similar conclusions.

However, questions about the nature of water permeation through these membranes still remained. The bulk flow hypothesis was questioned with the discovery that a significant increase in the rate of water diffusion through frog skin could be achieved by vigorous stirring of the solutions bathing the experimental membrane, and that under these conditions, diffusional flow closely approximated the observed rate of osmotic water flow (27). Experiments by Cass and Finkelstein (21) on lipid bilayers further revealed that eliminating the effect of an unstirred fluid layer facing the artificial membrane allowed the rate of diffusional water permeability to approximate the rate of osmotic water transfer. The conclusions of these workers were substantiated in experiments in the toad bladder by Hays and Franki (58), which demonstrated that with rapid stirring, hormone-stimulated diffusional water flow approxi-

mated that achieved in the presence of an osmotic gradient. These authors therefore suggested that it was not necessary to postulate either a dual barrier or the existence of large aqueous pores in the luminal membrane of vasopressin-sensitive epithelia. With the subsequent demonstration that urea transport could be dissociated from water movement (83), the pore theory, as originally stated, became completely untenable. Hays et al. (59) finally concluded that the vasopressin-induced transfer of water could occur through a system of pores no larger than 2 Å, i. e., slightly larger than the radius of the water molecule, but smaller than that of urea.

On the basis of studies on non-electrolyte permeability of toad bladders, Pietras et al. (111, 112) suggested that vasopressin might cause a nonspecific increase in the fluidity of the lipid bilayer of the membrane, thus reducing its resistance to water flow. In testing this hypothesis, Finkelstein (41) found that increasing the fluidity of artificial lipid bilayers led to proportional increases in the permeability to water and to all hydrophilic molecules. However, vasopressin treatment of toad bladders produced large increases in the diffusional permeability to water with only modest increases in the diffusion of other hydrophilic molecules. With this evidence that vasopressin could not alter the rate of water permeability simply by inducing a nonspecific increase in membrane fluidity, Finkelstein (42) reached the same conclusion as Hays et al. (59), viz: that in the resting toad bladder, water traversed the luminal membrane primarily through pores having dimensions not much larger than the water molecule (about 2 Å), and that vasopressin increased the number, but probably not the size, of pores available for transport.

While these studies of the biophysical aspects of water movement through membranes provide little direct evidence concerning the cellular mechanism of vasopressin-stimulated osmotic water flow, they do reveal some of the characteristics that must be considered as a part of any model of water flow. Thus whatever the intermediate cellular steps leading to enhanced water flow in the hormone-stimulated state, they must provide a discrete and specific pathway by which water traverses the apical cell membrane of sensitive tissues, in the absence of solute flow.

Cellular Events in the Action of Vasopressin

Although the exact mechanism by which vasopressin selectively increases the water permeability of sensitive epithelial membranes is not known, investigations into this problem have provided much information about the cellular events occurring between vasopressin stimulation of protein kinase activity and the ultimate permeability change at the apical membrane.

Route of Water Movement

Evidence that transepithelial water movement occurred through rather than between the epithelial cells of the frog skin, and that the apical membrane is the rate-limiting barrier, came originally from experiments by MacRobbie and Ussing (93) and Peachey et al. (109). These investigators observed that exposure to the hormone, in the presence of a dilute mucosal medium, caused the epithelial cells to swell. In other experiments, Hays et al. (57) showed that the non-inulin space of toad bladder epithelial cells increased by nearly 50% after stimulation with vasopressin. Later experiments by DiBona et al. (35) de-

monstrated that the granular cell was the specific route of vasopressin-stimulated osmotic water movement in the toad bladder, since only these cells swelled when fixed in the presence of an osmotic gradient favoring mucosal to serosal water flow, whereas all the cells swelled in the presence of a reverse osmotic gradient. Evaluation by these criteria provided evidence for the hypothesis that water moved osmotically through the granular cell, and did so at a rate that depended on the osmotic gradient and on the specific water permeability of the granular cell apical membrane.

Exo- and Endocytosis

Many hormone-dependent events have been recently demonstrated to occur at the apical surface of the granular cell. Masur and coworkers first showed that both exo- and endocytosis are stimulated in the presence of hormone (99, 100). In particular, they observed increased exocytosis of membrane-limited granules after hormone treatment of isolated toad bladders (100). These workers therefore suggested that vasopressin (or cAMP)-induced changes in membrane permeability might be the result of addition to the apical membrane of the contents and/or membranes of the granules by a mechanism of granule fusion. Further work by Gronowicz et al. (50) has now shown the magnitude and time course of the sequential stimulation of exo- and endocytosis in the toad bladder. Prior to the onset of hormone-stimulated endocytosis, there is an effective doubling of the amount of luminal membrane of the granular cells. These studies therefore provide convincing evidence for the addition of membrane to the apical aspect of the granular cells, that may play a role in the vasopressin-

dependent increased permeability at this site.

Other workers have shown that vasopressin stimulates the release of "lysosomal" hydrolases at the mucosal surface of the frog bladder (112). Pietras et al (113) found that colchicine, but not lumicolchicine, inhibits the appearance of lysosomal hydrolases in the mucosal fluid of vasopressin - treated frog bladders. These workers also showed that the hormone-sensitive redistribution of concanavalin A binding sites on the apical membranes of bladder epithelial cells was inhibited in bladders incubated with colchicine (113). It is noteworthy that both this phenomenon, and the exo- and endocytic events described above (99, 100) are blocked if bladders are pre-treated with colchicine (50).

A number of recent studies with the scanning electron microscope have demonstrated that vasopressin induces changes in surface morphology of toad bladder epithelial cells. After exposure to the hormone the ridge-like microvilli, typical of granular cells in the resting state, are transformed into individual, finger-like projections (28, 51, 102).

Intramembranous Particle Aggregates

In the past 5 years, a number of freeze-fracture studies of amphibian urinary bladder have provided direct evidence for the appearance of new membrane components in the granular cell apical membrane after exposure to vasopressin (23, 68, 69, 140). The original finding by Chevalier et al. (23) of an increase in specific intramembranous particle aggregates in the P face of apical membranes of frog bladders exposed to hormone or cAMP has been

confirmed in the toad bladder (68). Kachadorian and coworkers (68, 69) have found that a linear correlation exists between the frequency of particle aggregates and osmotic water flow, although aggregates are present even in the absence of water flow. These findings have led to the view that the particle aggregates are associated with the increase in water permeability induced by the hormone, and may even contain the channels through which water moves across the membrane (69). The appearance of new intramembranous particle aggregates is inhibited if tissues are pretreated with either colchicine or cytochalasin B (69).

More recent investigation into the origin of the intramembranous particle aggregates has uncovered the existence of a new class of cytoplasmic vesicles in the apical regions of the granular epithelial cells. These vesicles contain (preformed) particle aggregates similar to those found in freeze-fracture replicas of apical membranes of both resting and hormone-stimulated bladders (140), and are found in both control and hormone-treated preparations. Preliminary evidence suggests that the intramembranous particles in the luminal membrane of hormone-treated bladders may arise by addition of vesicle membrane containing the preformed aggregates from this cytoplasmic store (140). Thus, the addition (and deletion) of new membranous material to the apical surface of vasopressin-sensitive epithelia appears to be crucial to the development, maintenance and decline of increased permeability, as was originally postulated by Masur et al. (100) and extended by the results of recent freeze-fracture studies (23, 68, 69).

Microtubules and Microfilaments

Over the last several years many workers have investigated the role of the cytoplasmic organelles, microtubules and microfilaments, in the cellular action of vasopressin. These organelles have been demonstrated to play a crucial role in the control of surface events, membrane particle distribution and exo- and endocytosis in many cells (125).

The selective inhibition of the hydrosmotic response to vasopressin by the antimitotic agent, colchicine, in anuran tissues has been well documented by Taylor and coworkers (117, 130, 132, 133, 147) and others (19, 54). The concentration dependence, specificity, and time and temperature dependence for this inhibition correlate well with data on the interaction of colchicine with brain and toad bladder tubulins (133). No inhibition of hormone-induced water flux was found with lumicolchicine, an isomer that does not interact with tubulin or microtubules. Morphological studies designed to compare the number of microtubules in colchicine-treated toad bladders with those in their untreated controls, showed a dose-dependent reduction in the volume density of assembled microtubules in the colchicine-treated tissue (117). The microtubule disrupters, vinblastine and podophyllotoxin (130, 131) and nocodazole (60) have similar effects on vasopressin-induced hydrosmotic water flow.

The binding of colchicine to the 39,000 x g supernatant fraction of toad bladder epithelial cells has also been investigated (147). In isolated epithelial cell preparations, over 98% of the total binding activity of ³H-colchicine was found in the supernatant, with less than 2% recovered in the particulate fraction. Comparison of the binding properties of the soluble colchicine-binding

fraction from toad bladder with those of purified samples of chick brain tubulin revealed that these preparations behaved identically in their ability to bind colchicine (147).

As mentioned above, colchicine has also been shown to inhibit both hormone-dependent granule exocytosis (50) and lysosomal enzyme release (113), as well as the appearance of apical membrane intramembranous particle aggregates in the granular epithelial cells (69).

Taken together, these data strongly support the hypothesis that colchicine impairs the response to vasopressin by interacting with tubulin, disrupting cytoplasmic microtubules and preventing the hormone-induced events at the luminal membrane.

Microfilaments

The notion that microfilaments may play a functional role in the action of vasopressin is based largely on experiments using cytochalasin B (CB). The effect of this drug upon water, sodium and urea transport has been tested in both frog and toad urinary bladder (19, 29, 33, 51, 130, 132). Functional studies of the effect of the drug on oxytocin- or vasopressin-sensitive water and solute transport in these tissues indicate that hormone-dependent water flow is specifically and reversibly inhibited by cytochalasin B (19, 29, 33, 130). (Neither basal nor hormone-stimulated sodium transport is affected by the drug, although in two studies (19, 29) the drug caused a decrease in potential difference across the tissue.)

Comparison of the extent of inhibition of hormone-induced water movement by cytochalasin B reported by different laboratories shows considerable variation. For example, in Bufo marinus Taylor et al. (131) found an inhibition of 20% with a drug dose of 5 $\mu\text{g}/\text{ml}$, while DeSousa (33) reported 85-100% inhibition with a dose of 1 $\mu\text{g}/\text{ml}$. Dose-response data from Taylor et al. (132), on the effect of CB in the Colombian toad (Bufo marinus), indicated a linear correlation between the dose of CB and the inhibition of the hydrosmotic response up to an inhibition of 60% with 50 μM CB, the maximum concentration tested. A double-reciprocal plot of these data indicated that the drug was interacting with a single affinity class of binding sites having an apparent inhibition constant of $3 \times 10^{-5}\text{M}$. These data correspond closely to the low affinity binding site originally described by Lin et al. (87) in studies of CB binding and inhibition of microfilament-related cell movement.

Morphological studies of anuran bladder following exposure to CB have also given variable results. Thus, differing effects on cytoplasmic and microvillus fine structure and microfilament organization have been reported by various investigators (19, 29). On the other hand, scanning electron microscope studies (29, 51) have consistently shown that the appearance of the apical membrane is minimally distorted by exposure to CB, or CB and vasopressin, in the absence of water flow. However, in CB-treated bladders, when an osmotic gradient, and hence water flow, was present, the normal transformation of the granular cell microvilli (28, 51, 102) was blocked; instead these cells appeared flattened and essentially devoid of microvilli (29, 51).

In sum, these experiments on anuran epithelium support the notion that microfilaments participate in effecting the vasopressin-induced water permeability change. Conceivably, these cytoskeletal elements may play a role in the processes leading to the insertion of specific intramembranous particles and/or granules into the granular cell apical membrane.

It has been tempting to speculate that the effects of CB in inhibiting vasopressin-induced osmotic water flux are due to its disruption of microfilaments within the epithelial cells. However, several problems in interpreting the data have prevented precise elucidation of the nature of this effect. Studies of many different cell functions have shown that the effects of cytochalasin B may be mediated through at least two major affinity classes of binding sites (87). Doses of CB below 5×10^{-6} M block the uptake of hexoses, and in some cases nucleosides, in many cell types; these effects are mediated by the high-affinity binding site for the drug. At concentrations of 5×10^{-6} M to 5×10^{-5} M, however, microfilament-related functions are also inhibited. Therefore, in order to implicate microfilaments in any cell function sensitive to cytochalasin B, it is necessary to rule out the involvement of binding sites not related to microfilaments, e. g. , ones similar to those related to hexose transport.

Recently, Lin et al. (88) have prepared and purified a reduced cytochalasin derivative, dihydrocytochalasin B (H_2CB) by reduction of the native mold metabolite with sodium borohydride and ethanol. (Dihydrocytochalasin B was

analyzed by mass spectroscopy and found to be reduced across the double bond between C₂ and C₃ (Figure 1.) H₂CB has been used to distinguish between microfilament-related and hexose transport-related binding sites. When this drug was employed on the same red blood cell assay in which a dose-dependent inhibition of glucose transport had been demonstrated with cytochalasin B (85), no inhibition by the reduced derivative was found, and H₂CB did not displace tritiated cytochalasin B from the membrane. Yet importantly, H₂CB was shown to be as effective as CB in affecting cell motility and morphology; thus, H₂CB inhibited clot retraction of human platelets, cytoplasmic streaming in Elodea, and cytokinesis in fertilized sea urchin eggs--all microfilament-related functions normally inhibited by CB (9, 86). Most recently, studies with H₂CB have permitted the identification of specific membrane-associated cytochalasin-binding sites related to actin microfilaments (see Discussion).

The studies to be presented here were designed to further investigate the possibility that the 50-70 A microfilaments in epithelial cells of the toad urinary bladder may play a role in the stimulation and maintenance of water movement induced by vasopressin. Functional studies are presented that demonstrate inhibition of vasopressin-stimulated water movement by dihydrocytochalasin B, that is similar to that observed with the less specific cytochalasin B; biochemical studies of an actin-like protein from isolated bladder epithelial cells show that this protein is similar to other nonmuscle actins; morphological studies of bladders treated with heavy meromyosin will directly

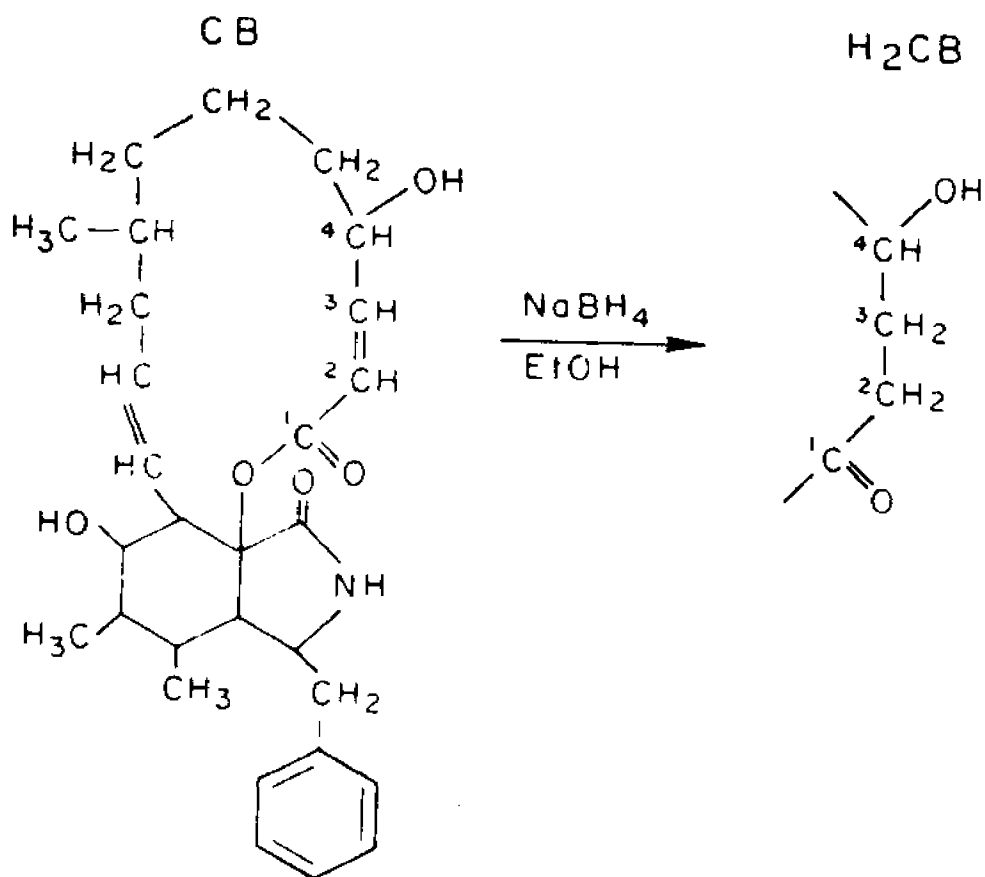


Fig. 1. Chemical structures of cytochalasin B (CB) and the reduced derivative, dihydrocytochalasin B (H₂CB). Exposure of CB to sodium borohydride and ethanol results in reduction of the double bond across C₂ and C₃.

demonstrate the existence of actin in the epithelial cells as well as provide clues to the state of organization of the microfilaments within them.

METHODS

FUNCTIONAL STUDIES

Measurement of Osmotic Water Movement: Studies with Dihydrocytochalasin B

Osmotic water movement was measured using the gravimetric method of Bentley (11). Female Dominican toads (Bufo marinus, National Reagents, Bridgeport, Conn.) were double pithed and the hemibladders were excised and attached to glass tubing. After mounting, the bladders were each washed four times in deionized water and then filled with 5 ml of deionized water. The experimental hemibladder and its paired control were each placed into a 25 ml bath of Ringer's solution containing Na, 114; Cl, 120; K, 3.4, HCO₃, 2.4; and Ca, 1.78 mEq/L. The osmolality of the solution was 209 mOsm/L and the initial pH was 8.0. The solution was continuously bubbled with air, and this caused the pH to increase to a final value of 8.5 after several minutes. All studies were carried out at 23°C. After immersion in Ringer's solution, the hemibladders were weighed on a Mettler H35 balance every 15 min for 1 h to establish a baseline rate of water flow. (Weight loss is taken as a direct measure of water flow.) At the end of this period, an aliquot of dihydrocytochalasin B (H₂CB) was added to the serosal bathing medium of each experimental hemibladder. An equivalent volume of dimethyl sulfoxide (DMSO), not exceeding 0.2% of the total bath volume, was added to each control hemibladder in a similar fashion. The bladders were then incubated 30 min, with weighings each 30 min, to monitor the effect of H₂CB on the basal rate of water flow. After this incubation period, arginine vasopressin was added to

the serosal medium bathing each hemibladder to a final concentration of 20 mU/ml. Osmotic water movement was measured at 15 min intervals for 1 hr.

Measurement of the Effective Osmotic Gradient

In order to monitor the effect of H₂CB on the osmotic gradient to which the hemibladders were exposed, aliquots of both the mucosal and serosal solutions were removed from each experimental and control hemibladder at the end of the 90 min incubation period, prior to addition of hormone, for measurement of osmolality. Two hundred microliters was removed, and the fluid was replaced each time with 200 μ l of the appropriate solution (either deionized water or Ringer's solution). After the addition of vasopressin, similar aliquots were removed for measurements of osmolality (Advanced Instruments, Needham Heights, Mass.) after each 15 min weighing in the experimental hemibladders, and after the 30 and 60 min weighings in the controls. The effective osmotic gradient was calculated from the mean of the differences in osmolality of the serosal and mucosal bathing solutions for each individual hemibladder.

Calculations

Osmotic water flow was calculated for each hemibladder before and after vasopressin treatment. Water movement was determined as the mean flow for the 90 min incubation period prior to the addition of hormone, and for the 60 min period which followed the addition of vasopressin. Since the gradient dissipated only after initiation of hormone-induced water flow, the results are expressed in mg/min/mOsm for this period only. Inhibition of vasopressin-induced osmotic water flow was calculated as the ratio of experimental to con-

trol flows expressed as above, subtracted from unity, and multiplied by 100 to give the percent inhibition for each experimental hemibladder relative to its paired control. The mean inhibition of the response to vasopressin plus or minus the standard error of the mean was calculated for each concentration of H₂CB used. The statistical significance of the inhibition of water movement was estimated using Student's t-test for paired data.

Dihydrocytochalasin B

Dihydrocytochalasin B was a generous gift from Prof. S. Lin, Department of Biophysics, Johns Hopkins University, Baltimore, Md. To 2.1 mg of the purified, lyophilized powder, prepared in Prof. Lin's laboratory, 420 μ l of DMSO (Fisher) was added. This resulted in a stock solution of H₂CB of 5 mg/ml. The solution was stored at 4°C. For each experiment, 25 or 50 μ l of stock solution was added to the serosal bathing medium of each experimental hemibladder. Equivalent quantities of DMSO were added to the controls.

BIOCHEMICAL STUDIES

Protein Determinations

In all cases where an estimate of protein concentration was necessary, the following method, adapted after Lowry et al. (91) was used.

Four stock solutions were kept, consisting of: 1) bovine serum albumin (BSA), 1 mg/ml in water, stored at 4°C; 2) 2% CuSO₄, stored at 23°C; 3) 1% sodium-potassium-tartrate, stored at 23°C; and 4) 2% sodium carbonate, stored at 23°C. A standard curve of the concentration of BSA was constructed

each time estimates of protein concentration was determined. The procedure was run as follows:

Zero, 10, 25, 50, 75, 100 μ l (and occasionally 200 μ l) of BSA was pipetted into individual 13 x 100 mm glass culture tubes, and the volume adjusted in each case to 200 μ l by the addition of 0.1 N NaOH as necessary. These aliquots provided concentrations of protein equal to 0, 0.05, 0.13, 0.25, 0.37, 0.5 and 1.0 mg/ml. Tubes containing aliquots of unknowns containing protein were prepared similarly. At this time, 200 μ l of each of 2% CuSO₄ and 1% Na-K-tartrate were mixed, and to this solution was slowly added 10 ml 2% Na₂CO₃. One milliliter of the resulting light blue solution was pipetted from a 5 ml pipette into each assay tube. The mixtures were then vortexed and allowed to incubate for 10 min. During the incubation period, an aliquot of 2 N Folin reagent (Sigma) was mixed with an equal volume of water. One hundred microliters of the resulting 1 N Folin reagent was then added to each assay tube, and the samples were well vortexed. After an incubation period of at least 30 min but not exceeding 2 h, the optical density of both standard and unknown solutions were read at 750 nm on a Zeiss PMQ II spectrophotometer, using deionized water as a blank.

After subtracting a measured value as the blank, obtained from the optical density of the standard sample from which protein was omitted, a standard curve was constructed from the known concentrations of the BSA solutions. Points were plotted and the curve constructed by eye where possible, and by least squares regression analysis whenever scatter in the points made this treatment of the data necessary. Estimates of protein concentrations in the

unknowns were made by subtracting the blank value from the O.D. reading for each sample and comparing this reading to the standard curve. This method was found to be highly reproducible both from standard curve to standard curve, and from duplicate and/or repeated measurements made on the unknowns. In cases where the unknowns contained so much protein that they were either off the standard BSA curve or way into the nonlinear portion of the curve, the concentrated sample was diluted 1:1 with water prior to reading in the spectrophotometer. All incubations and measurements were made at 23°C.

A standard curve of protein concentrations was included each time measurements of protein concentrations were made. In order to know the degree to which the estimates of protein concentration varied from run to run, five standard curves run over a 2 year period were chosen at random, and the mean and standard error of the mean were computed. These data are shown in

Table 1.

Conc.	O.D. - O.D. BL					Mean ± S.E.
	1	2	3	4	5	
.05	.102	.100	.098	.090	.112	.100 ± .004
.13	.196	.214	.255	.240	.249	.321 ± .011
.25	.345	.375	.316	.424	.465	.385 ± .027
.37	.478	.531	.532	.517	.555	.523 ± .013
.50	.608	.665	.740	.659	.757	.686 ± .028

When these values were subjected to linear regression analysis, the line determined by the equation $y = 1.28x + 0.0525$ resulted. The points were plotted as shown in Fig. 2, and gave a correlation coefficient of $r^2 = .9985$

AVERAGE STANDARD PROTEIN DETERMINATIONS 1977 - 1979

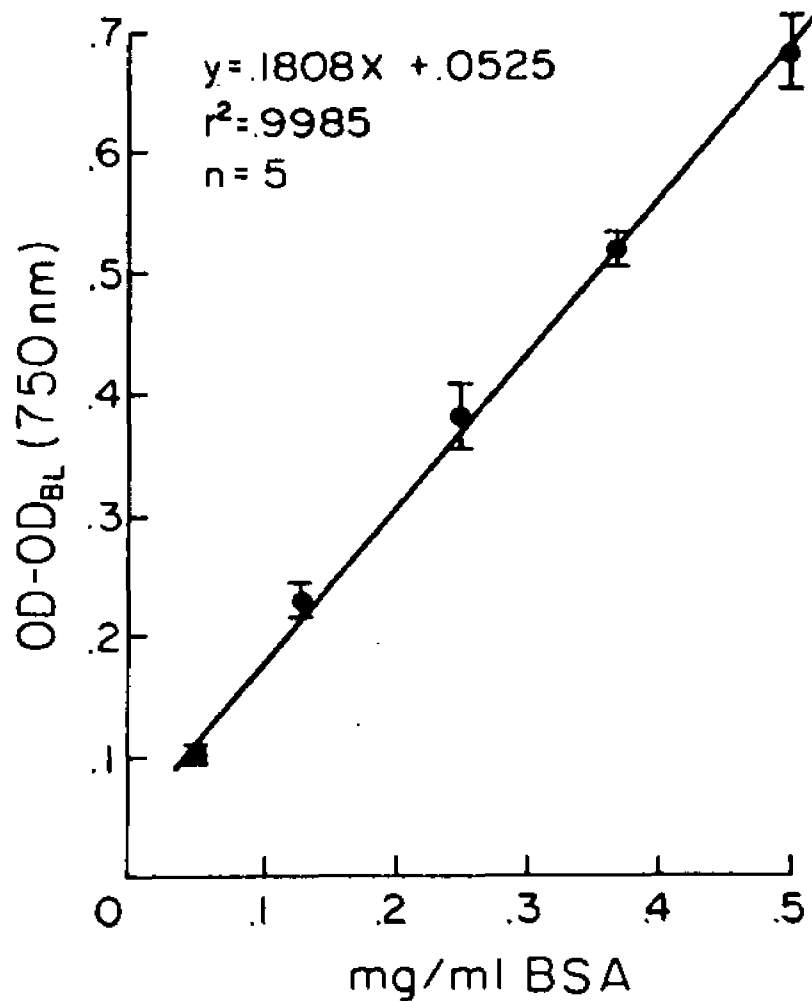


Fig. 2. Regression analysis of standard protein estimations to determine reproducibility of the method. Points represent the mean \pm the standard error of the mean for 5 determinations selected at random over a two-year period.

with respect to the regression line. Thus, protein concentration from experiments carried out early in the course of the work are comparable to those measured at a later time.

SDS-Polyacrylamide Gel Electrophoresis

For general analytical purposes throughout this work, SDS-polyacrylamide cylindrical gels, formed in phosphate buffer after the method of Weber and Osborn (143), were used. In most cases, the acrylamide concentration in the gel was kept at 5%, as this density gave a good separation of the molecular weight species of interest. Occasionally, as for the identification of the low molecular weight light chains of rabbit myosin, it was necessary to increase the density of the gels to 10% acrylamide. In all other cases, 5% gels were used.

Stock Solutions

Gel buffer (double strength)

0.1 M Phosphate buffer, pH 7.0

1.0% Sodium lauryl sulfate

Sample buffer

0.01 M Sodium phosphate, pH 7.2.

1.0% Sodium lauryl sulfate

1.0% β -mercaptoethanol

Acrylamide stock (10%) 37:1 = acrylamide:methylene bis

22.2 g Acrylamide

0.6 g Methylene bis acrylamide

to 100 ml with deionized water

Staining solution

1.125 g (0.25%) Coomassie Brilliant Blue

227 ml methanol

46 ml Glacial acetic acid

Methanol was added to the Coomassie powder, and the mixture was stirred. The acetic acid was slowly added with stirring, and the mixture was made up to 500 ml with deionized water. Staining solution was stored at 23°C for up to several months and reused each time gels were run.

Destaining solution

5% Methanol

7.5% Glacial acetic acid

87.5% water

Preparation of gels

Twelve 7 x 130 mm gel tubes were soaked in acid, rinsed with deionized water and dried. Fifteen milliliters of double strength gel buffer was pipetted into a 125 ml Erlenmeyer flask. To this was added 6.75 ml each of stock acrylamide and water. The mixture was swirled, and then degassed for 10 min by suction from a water aspirator. During this time the gel tubes were placed in a stand and straightened by eye. Two milliliters of a 15 mg/ml solution of ammonium persulfate was prepared, and two 1 ml syringes equipped with 25 gage needles which had been bent were filled with water. The acryla-

amide solution was carefully removed from the aspirator, and 1.5 ml of the persulfate solution was pipetted into the flask. Forty-five microliters of N,N,N',N'-tetramethylethylenediamine (TEMED) was then pipetted into the mixture, and the flask was gently swirled to mix the reagents. The gel-forming mixture was then taken up into a 50 ml syringe fitted with P.E. 90 tubing. The gel tubes were filled from the syringe up to about 1.5 cm from the tops of the tubes. Water from the 1 ml syringe balanced on top of the gel tube was allowed to drip down the side of the tube to flatten the gel meniscus as it formed. After several minutes the gels were topped up with water, covered with Parafilm, and stored on the bench. Ten percent gels were made in the same manner, except that 13.5 ml stock acrylamide was used, and water was omitted from the gel mixture. Samples for gel electrophoresis were prepared in the following manner: into 13 x 100 mm culture tubes were added 5 μ l β -mercaptoethanol, 5 μ l 0.05% Bromphenol blue tracking dye, 50 μ l gel sample buffer and enough enzyme grade sucrose to make the solution much more dense than the gel running buffer. Five to fifty microliters of each of the samples were then added. The tubes were vortexed and heated in a boiling water bath for 1-2 min to insure that the protein was sufficiently complexed with SDS. Samples were then layered on top of the gel tubes which had been placed in the gel apparatus. The tubes were topped up with single strength gel buffer, and the reservoirs were filled with the remaining buffer. Electrodes were attached, and the wires were connected to the output of a Bio Rad model 400 gel electrophoresis apparatus. Samples were allowed to enter the gel at a current of 2 mA/tube. After about 30 min, the current was increased

to 7 mA/tube, and the gels were electrophoresed 4-5 h in the constant current mode until the tracking dye had traveled 2/3 - 3/4 down the length of the gel tube.

Gels were removed from the tubes by rimming the inside of the gel tube with a stream of water from a syringe fitted with a blunt needle. The ejected gels fell into a pan of water, and were subsequently placed into staining tubes (Bio Rad), which fitted into 1.5 x 15 cm test tubes filled with a solution of Coomassie Brilliant Blue. Gels were soaked in this solution for 2-12 h, which served to fix the proteins within the gels, as well as stain them. The gels were then washed in destaining solutions, and finally placed in the diffusion destainer (Bio Rad) for at least 48 h, or until the background cleared. Upon occasion, to detect the presence of minor bands, gels removed from the destainer were restained and destained a second time. Gels were subsequently scanned on a Joyce Loebel Chromoscan densitometer and/or photographed. Gels themselves were stored in capped tubes in 7.5% acetic acid.

The relative mobilities of the various molecular weight species on 5% SDS-PO₄ gels was calculated by the method of Weber and Osborn (143) according to the following equation:

$$\text{Mobility (M)} = \frac{\text{Length from top of gel to protein band}}{\text{Length of gel after destaining}} \times \frac{\text{Length of gel before destaining}}{\text{Length from top of gel to dye front}}$$

According to this equation, a protein which does not migrate at all in this gel system would have a mobility of 0, while a protein that migrates with the dye front would have a mobility equal to the ratio of lengths of the gels before and

after destaining.

Standard solutions of actin, myosin, and tubulin were included in each experimental gel run. While the mobility of any protein in this system increased slightly with increased loading of protein on the gel, the bands of interest were always sufficiently separate from each other so that differences in mobility due to different gel loadings did not become a problem. In general, it was found that rabbit actin migrated in this system with an electrophoretic mobility of 0.7, brain tubulin had a mobility of 0.63, and rabbit muscle myosin heavy chains migrated with a mobility of 0.16. When these values were plotted against the logarithms of the molecular weights of each of these proteins, the resulting line, generated by least squares regression analysis, is that given by the equation, $y = -0.817 x + 4.49$. The data points were fitted to this line with a correlation coefficient of .9994, indicating a linear separation of a large molecular weight range using this gel system. These statistics are shown plotted Fig. 3.

Myosin ATPase Assays

Myosin ATPase activity was measured by the method of Marsh (98), as modified by Puszkin (116).

The following stock solutions were kept stored at 4°: 50 mM imidazole, pH 7.0; 10 mM MgCl₂; 10 mM CaCl₂; 3 M KCl; 20 mM ethylenediamine tetraacetic acid (EDTA); 20% trichloroacetic acid (TCA); acid molybdate; and sodium citrate. To prepare acid molybdate, 20g sodium molybdate was mixed with deionized water, and 50 ml concentrated HCl was added slowly to the

ELECTROPHORETIC MOBILITY OF STANDARD PROTEINS ON 5% SDS GELS

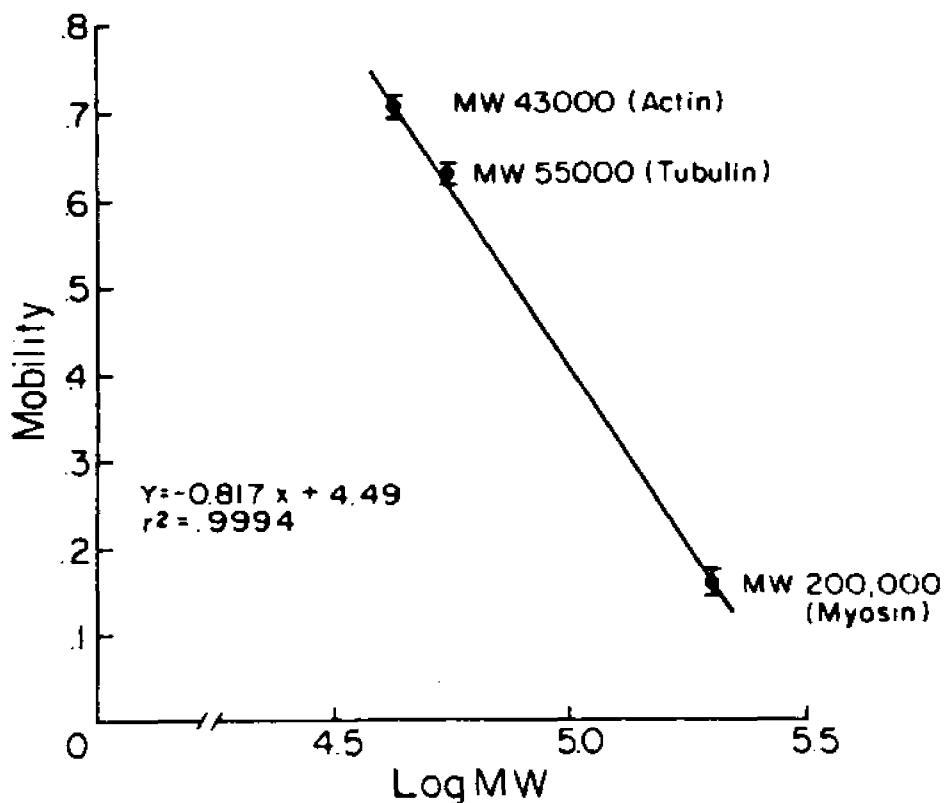


Fig. 3. Separation of proteins by molecular weight on 5% SDS-phosphate gels. Mobility calculated as in (143) is plotted as a function of the logarithm of the molecular weight of each protein. Points represent the mean \pm the standard error of the mean for 5 determinations.

stirring mixture. The solution was then brought up to 500 ml with deionized water. For the sodium citrate solution, 200 g of the dihydrate was mixed with water and titrated to pH 7.0 with concentrated HCl. The mixture was made up to 1 L. n-Butanol was redistilled from the reagent-grade bottle and stored refrigerated. Methanol was kept at 23°C. Twenty millimolar ATP neutralized with imidazole was stored frozen. All ATPase activities were run in duplicate using separate blanks. Blanks were prepared exactly the same way as the experimental samples except that the sample protein was added after the reaction had been stopped.

Each assay tube received 0.5 ml imidazole, and 100 μ l of either $MgCl_2$ or $CaCl_2$, depending on whether the magnesium or calcium ATPase activity of myosin was being tested. For K^+ -EDTA activity, 0.2 ml 3M KCl and 100 μ l 20 mM EDTA was pipetted into the tube. Five to ten micrograms of myosin or test material was added, and the tubes were vortexed. At precise 10 sec intervals, 100 μ l of 20 mM ATP was added to each tube, which was then placed in a 37°C water bath. Precise timing of the incubation period was found to be a critical factor in obtaining acceptable duplicate values of ATPase activity. The samples were incubated for 30 min, and the reaction was stopped by the addition (again at 10 sec intervals) of 0.4 ml TCA to each tube. The tubes were then vortexed and placed on ice. Protein was added to the blanks at this time. One milliliter of sample was then added to 2 ml of redistilled butanol and 200 μ l molybdate, which had been pipetted into fresh tubes. Each tube was then vortexed for 10 sec to extract free phosphate into the butanol phase. Then 0.4 ml of citrate solution was added to complex the remaining ATP and ADP. The

nucleotide-citrate complex was then extracted into water by the addition of 1.4 ml H₂O to each sample. The samples were vortexed, and the butanol layer, containing the UV-absorbing phosphate-molybdate complex, was pipetted into a fresh glass test tube. Two hundred microliters of methanol was added to each tube to clarify any cloudiness (which can result from traces of water in the hydrophobic medium), and the absorbance of the complex was measured at 310 nm in a Zeiss PMQ II spectrophotometer using quartz cuvettes. The concentration of phosphate liberated by the action of the myosin ATPase was determined by comparing values obtained in the experimental assay mixture with those derived from a standard curve constructed for known concentrations of KH₂PO₄. The standard curve is depicted in Fig. 4.

Preparation of Stock Proteins

Rabbit Psoas Muscle Actin

A stock of muscle actin was maintained as a standard for gel electrophoresis, electron microscopy, and calibration of columns. It was prepared as described below, from an acetone powder, as adapted for use in the physiology class at the Marine Biological Laboratories (MBL), Woods Hole, Mass., and communicated to me by Mooseker (104).

Preparation

A 3-4 lb white New Zealand rabbit (Triple - R Rabbitry, Manesquan, N.J.) was killed by cervical dislocation or pentobarbital injection. The psoas muscles were dissected away and placed in ice-cold 0.9% saline. Connective

Myosin ATPase Standard Curve

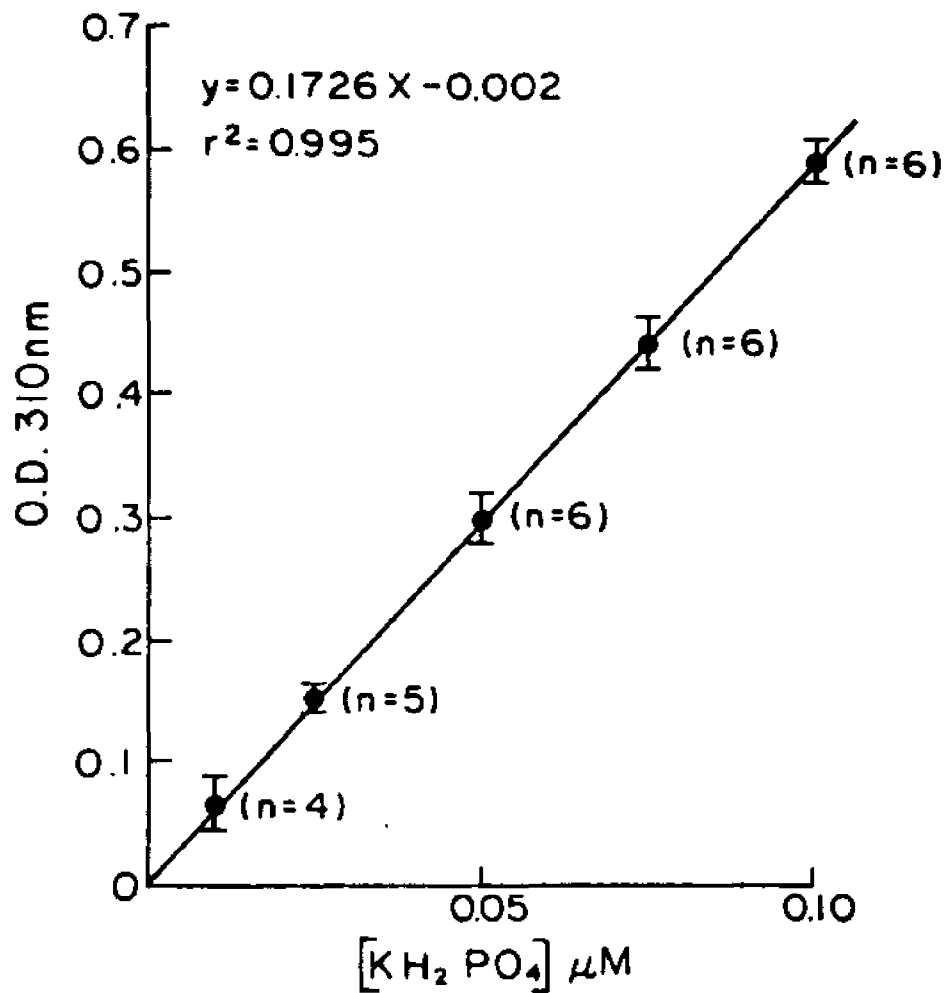


Fig. 4. Regression analysis of standard curve generated to estimate ATPase activity by measuring the liberation of inorganic phosphate. Assays were run as described in methods except that protein was omitted and varying concentrations of KH_2PO_4 were included in the reaction mixture. The absorbance at 310 nm is plotted as a function of the concentration of KH_2PO_4 added to the assay tube.

tissue was removed and the muscle was minced and weighed. Muscle was homogenized by three 10 sec bursts of a Waring blender in three volumes of cold myosin extraction buffer: 0.5 M KCl, 0.1 M K_2HPO_4 , pH 7.0.

The mixture was further extracted in the cold for 10 min and then centrifuged for 20 min in a Sorvall RC-2 refrigerated centrifuge at 16,000 RPM (31,000 x g). The supernatant, containing solubilized myosin and actomyosin, was discarded, and 200 ml ice-cold water was added to the pellets. The pH was adjusted to 8.2 - 8.4 with 1 M Na_2CO_3 , and the mixture was again centrifuged at 16,000 RPM. The supernatant was discarded and a further 200 ml deionized water was added to the pellets. The process was repeated (usually 2 or 3 times) until the pellets began to swell. Approximately 250 ml cold acetone was then added to the final pellet, and the extract was stirred in acetone in the cold room for 20 min. The mixture was filtered through Whatman No. 1 paper on a Buchner funnel, and the acetone powder remaining on the filter was extracted with a second 250 ml volume of acetone. After filtering a second time, the acetone powder was removed to Parafilm, lightly covered, and allowed to dry overnight under a fume hood at 23°C.

The acetone powder was used the following day for preparation of purified actin by the method of Spudich et al. (129), modified for use in the MBL physiology course. The method described below depends upon the ability of the protein to undergo the G - F transformation in solutions of varying ionic strength.

After washing the acetone powder in chloroform and allowing it to dry, it was mixed with cold actin extraction buffer, 20 ml/g powder, and extracted

as the monomer for 30 min in the cold. The extraction buffer contained 20 mM Tris-HCl, 0.2 mM ATP, 0.5 mM dithiothreitol (DTT), 0.2 mM CaCl₂, pH 8.0 at 23°C. The mixture was then centrifuged at 16,000 RMP for 20 min, and the supernatant was filtered through glass wool into a graduated cylinder. The soluble G actin was then made 50 mM in KCl and 2 mM in MgCl₂ by adding 2.5 mL 2 M KCl and 0.2 ml 1 M MgCl₂ per 100 ml of extract, respectively. The mixture was then stirred and left to polymerize on the bench at 23°C without stirring for 45 min. The partially polymerized actin was then removed to the cold room for a further 45 min without stirring. After this time the actin was made 0.8 M in KCl and stirred in the cold room for 45 min. The exposure to high salt at the end of the incubation period served to solubilize tropomyosin away from the polymerized actin. The sample was then centrifuged at 35,000 RMP (80,000 x g) for 3 h in a Spinco Model L ultracentrifuge, using a No. 40 rotor. The pelleted actin was washed in actin extraction buffer and then homogenized using a Dounce homogenizer with a tight-fitting pestle in approx. 20 ml of the same buffer until a homogeneous suspension was obtained. The actin was then depolymerized by dialysis against three 2 L changes of buffer over a 3 day period. The solubilized actin was finally then clarified by centrifugation at 35,000 RPM for 1 h. Aliquots were taken for analysis of protein concentration and for SDS-polyacrylamide gel electrophoresis.

The purified actin was lyophilized (Thermo-Vac FD/Port, Coptague, L. L.) and stored dessicated in 5 mg aliquots at -15°C. Typically, 50 g muscle yielded 50-70 mg of purified actin.

Characterization

Rabbit muscle actin isolated as described was characterized by 1) ascertaining its mobility on SDS-polyacrylamide gels; 2) establishing its ability to form filaments under appropriate conditions as monitored by electron microscopy; and 3) assaying its ability to activate actin-dependent, magnesium-activated ATPase of purified rabbit muscle myosin.

Actin isolated by this method migrated as a single band on 5% SDS-polyacrylamide gels, and comigrated with actin isolated by a similar method in the laboratory of Dr. Soll Berl (not shown). In this gel system, the actin has an R_f value of about 0.70.

Figure 5 is an electron micrograph of negatively stained filaments formed by the purified rabbit actin. These were prepared by polymerizing the protein in a solution containing 0.1 M KCl and 2 mM $MgCl_2$. Actin filaments have a diameter of between 50 to 70 Å, and a characteristic beaded appearance. From this micrograph it can also be seen that the actin filaments tend to associate alongside each other.

Table 2 shows that this actin is capable of activating the magnesium-stimulated ATPase activity of rabbit muscle myosin. An aliquot of actin was polymerized and subsequently added in 4 fold excess (mg/mg) to myosin in the assay tube. The mixture was assayed as described in Section IV.



Fig. 5. Electron micrograph of purified rabbit muscle actin after polymerization and negative staining with uranyl acetate. x 136,500

Table 2. Actin-activated Mg^{++} -ATPase Activity of

Muscle Myosin		
<u>Mg^{++}-ATPase, $\mu M/min/mg$ myosin</u>		
	<u>+20 μg actin</u>	<u>-actin</u>
Myosin, 5.5 μg	0.27	0.03

These data indicate that the protein purified as described above has the physical properties associated with purified rabbit skeletal muscle actin.

Rabbit Muscle Myosin

Rabbit muscle myosin was used as a standard protein for gel electrophoresis, for occasional evaluation of ATPase activity stimulated by toad bladder actin preparations, and for the preparation of heavy meromyosin (HMM).

Preparation

The protein was prepared by the method adapted from Kielley et al. (71) as used in the physiology course at the MBL. The flow sheet for this procedure was given to me by Mooseker and is described here (104). The method depends on the selective solubility of myosin in high and low salt solutions, and its behavior in solutions of varying ammonium sulfate content.

Initial steps in the isolation procedure were identical to those described for the isolation of rabbit muscle actin. Approximately 50 g of psoas muscle was dissected from a white New Zealand rabbit as previously described. Minced muscle, washed in 0.9% saline, was homogenized by three 10 sec bursts in a Waring blender in three volumes of ice-cold myosin extraction buffer containing 0.5 M KCl, 0.1 M K_2HPO_4 , pH 7.0. All subsequent proce-

dures were performed at 4°C. The homogenized muscle was first incubated in extraction buffer for 10 min to solublize the myosin. The extract was then centrifuged in a Sorvall RC 2 refrigerated centrifuge at 20,000 RPM (48,000 x g). The supernatant was used for isolation of myosin; when needed, the pellet was saved for later extraction of rabbit muscle actin.

The supernatant containing myosin was adjusted to pH 6.6 - 6.8 with 0.5 M acetic acid, and the volume was measured. The sample was then slowly diluted with 10 volumes of ice-cold water which was dripped into the myosin solution from a separatory funnel, while the mixture was continuously stirred. After allowing the protein to settle to the bottom of the flask, as much fluid as possible was poured off, and the precipitated myosin was then centrifuged at 10,000 RPM (10,400 x g) for 20 min. The supernatant was discarded, and the myosin was dissolved in 2 M KCl, 50 mM imidazole, pH 7.0, allowing 1 ml per gram of myosin. This procedure was designed to give a final KCl concentration of about 1 M. The pH of the solution was measured and when necessary adjusted to 6.7 - 6.8 with 1 M NaHCO₃. The mixture was then diluted with one volume of water in order to obtain a KCl concentration of 0.5 M. The mixture was then carefully diluted with water to obtain a final KCl concentration of 0.28 M. This procedure allowed the selective precipitation of any acto-myosin present while leaving the uncomplexed myosin in the soluble form. The mixture was centrifuged again at 20,000 RPM for 30 min, and the pellet was discarded. The supernatant, containing the dissolved myosin, was then precipitated by the addition of 7 volumes of distilled water. The myosin was

spun at 10,000 RPM for 20 min, and this time the supernatant was discarded. The myosin-containing pellet was weighed and dissolved in 2.0 M KCl, 50 mM imidazole, pH 7.0, and the mixture was corrected with water to give a final KCl concentration of 0.5 M KCl in the solution.

Myosin was extracted from this mixture by $(\text{NH}_4)_2\text{SO}_4$ precipitation. Cold, saturated ammonium sulfate containing 10 mM EDTA was added to a concentration of 40% with stirring. This amounted to the addition of 2/3 volume $(\text{NH}_4)_2\text{SO}_4$ to one volume of myosin solution. The mixture was centrifuged at 15,000 RPM for 20 min, and the pellet was discarded. Ammonium sulfate was added to the supernatant to bring the myosin solution up to 50% saturation. This was achieved by adding a further 1/5 volume of ammonium sulfate. The mixture was allowed to stand on ice for several minutes until no further precipitation of myosin was observed, and was then centrifuged at 15,000 RPM (27,000 x g). The supernatant was discarded, and the pellet containing purified myosin was dissolved in the smallest possible amount 0.5 M KCl, 20 mM imidazole. The mixture was dialyzed overnight against 2 L of 0.5 M KCl, 20 mM imidazole, 2 mM dithiothreitol, 10 mM EDTA to eliminate the $(\text{NH}_4)_2\text{SO}_4$. The next morning the myosin was clarified by centrifugation at 15,000 RPM; the supernatant was made 50% in glycerol and the protein was stored at -15°C in this solution.

Characterization

Rabbit muscle myosin prepared as described was characterized 1) by ascertaining its behavior on SDS-polyacrylamide gels; 2) by observing electron micrographs of negatively stained myosin filaments; and 3) by testing its

intrinsic ATPase activities.

When 5% SDS-polyacrylamide gels of rabbit muscle myosin, isolated by the procedure described above, were run using as a standard, authentic myosin prepared in the laboratory of Prof. Soll Berl, the heavy chain of both these myosins comigrated in this gel system, and had a mobility of 0.16 (not shown). Light chains were not resolved on these gels since 5% gels of this type do not resolve the low molecular weight light chains. Ten percent gels of myosin run to determine the presence of light chains revealed, in addition to the heavy chain, a 25,000 dalton species only (not shown). Lower molecular weight light chains were not resolved because the gel was not sufficiently loaded to detect their presence by staining with Coomassie Brilliant Blue.

When myosin is incubated at a neutral pH in 0.1 M KCl, bipolar filaments are formed that are visible in the electron microscope. Figure 6 is an electron micrograph of a negatively stained sample of myosin incubated in this manner. Filaments similar to those described by Huxley are the only visible structures present in these samples (65).

Three types of ATPase activity have been demonstrated in myosin (14). Table 3 demonstrates that the K^+ -EDTA and Ca^{++} -stimulated ATPase activities are present in samples of this purified protein. Mg^{++} -activated ATPase was demonstrated only when a 4 fold excess of actin was added to the assay mixture.

Taken together, the results from gel electrophoresis, electron micro-

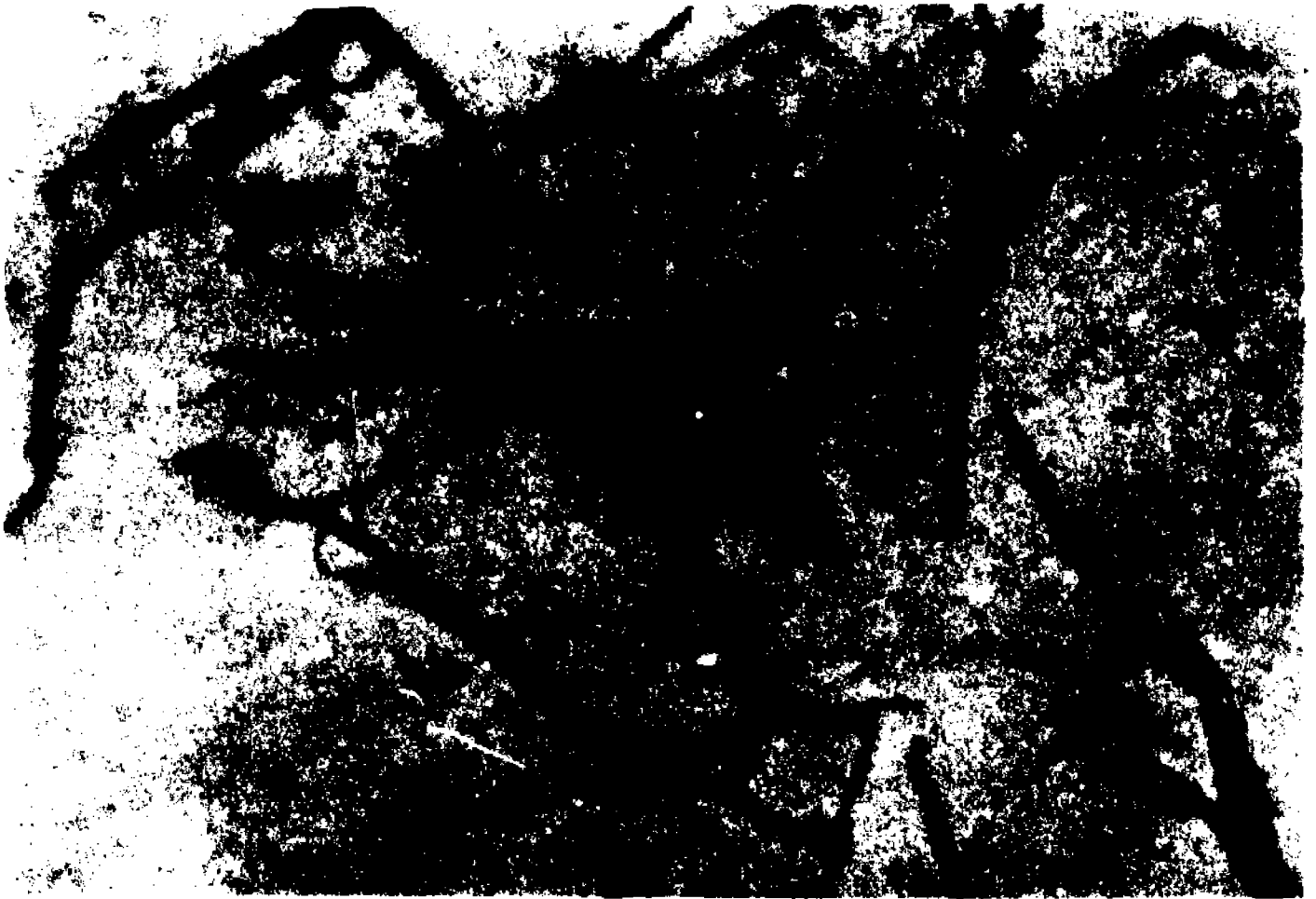


Fig. 6. Electron micrograph of purified rabbit muscle myosin after incubation in 0.1 M KCl and negative staining with uranyl acetate. x 68,500

scopy and measurement of the ATPase activity of purified myosin indicated that the molecule was isolated intact and free from contamination by muscle actin.

Table 3. ATPase Activity of Rabbit Muscle Myosin

<u>Date</u>	<u>Activity, $\mu\text{M}/\text{min}/\text{mg}$ myosin</u>			
	<u>K^+ EDTA</u>	<u>Ca^{++}</u>	<u>Mg^{++}</u>	<u>Mg^{++} + Actin</u>
10/31/77		0.26	0.01	0.23
12/7/77		0.50	0.01	0.20
12/20/77		0.27	0.00	0.17
12/22/77	1.32	0.84		
12/27/77	1.24	0.66		
12/23/78	0.70	0.46	0.03	0.27

(See Myosin ATPase Activities Section for details)

Heavy meromyosin (HMM) was prepared by the method of Lowey and Cohen (90), as adapted for use in the MBL physiology course. The procedure was communicated to me by Mooseker and is described here (104). This method depends upon the controlled digestion of myosin by trypsin to yield 1) HMM, which contains the actin-binding and ATPase activities of myosin, and 2) light meromyosin (LMM), which contains the myosin tails. These fragments are then isolated according to their solubility differences in solutions of varying ionic strength.

Tryptic Digestion

Five milligrams of bovine pancreatic trypsin (Sigma type XII, twice crystallized) was dissolved in 10 ml of 0.001 N HCl, to give a concentration of

0.5 mg/ml. Five milligrams of soybean trypsin inhibitor (Sigma type 1-s) was dissolved in 5 ml of water, and the pH was adjusted to 7.4 with 0.1 N NaOH. The concentration of inhibitor was 1.0 mg/ml. An aliquot of myosin, approximately equivalent to 13 mg/ml, was dissolved in 0.1 M sodium phosphate buffer, 0.5 M KCl, pH 7.0. One volume of trypsin was added to 10 volumes of myosin, and the mixture was stirred for 5 min at 23°C. The reaction was stopped by adding one volume of soybean trypsin inhibitor and placing the test tube in an ice bath.

Isolation of HMM

The tryptic digest was placed into dialysis against 7 mM imidazole, 0.75 mM β -mercapto-ethanol, pH 7.0, in order to precipitate the LMM together with any undigested protein. The sample was then centrifuged for 30 min at 35,000 RPM (80,000 x g). The supernatant containing the HMM was subjected to ammonium sulfate treatment and the 40-55% ammonium sulfate-precipitable fraction was collected. The HMM was then dissolved in a small amount of 10 mM imidazole buffer, pH 7.0, and the mixture was dialyzed overnight to remove the ammonium sulfate. The purified HMM was clarified by centrifugation at 35,000 RPM. The fragment was either used immediately or mixed with 2 mg enzyme grade sucrose per ml of HMM, lyophilized, and stored at -15°C.

Characterization of HMM

HMM was assayed by its ability to form characteristic arrowhead figures when incubated with preformed actin filaments (65). The arrowhead-forming interaction of actin with HMM is depicted in Figure 7. HMM bound



Fig. 7. Electron micrograph of purified rabbit muscle actin filaments after incubation with heavy meromyosin prepared from purified rabbit muscle myosin; negative staining with uranyl acetate. x 136,500

to rabbit actin with a periodicity of 320 ± 20 A, in fair agreement with the figure of 366 ± 15 A given by Huxley (65) for the acto-HMM interaction in negatively stained specimens. The arrowheads were displaced if the acto-HMM was subsequently rinsed in 6 mM neutralized ATP (c. f. Figures 27, 37, reversibility in toad bladder smooth muscle and epithelial cells).

Isolation of Actin from Toad Bladder Epithelial Cells

Isolation of Epithelial Cells

Epithelial cells were isolated from bladders as described in Sapirstein et al. (121a). Female Bufo marinus toads were doubly pithed and the hemibladders were dissected out and placed in a beaker containing bicarbonate buffered Ringer's solution of the following composition: NaCl 111 mM, NaHCO₃ 2.5 mM, KCl 3.4 mM and CaCl₂ 0.89 mM, pH 8.1, at 25°C. Hemibladders were tied to the outlets of Luer Lock syringe tips (A.H. Thomas, Philadelphia, Pa.) with surgical silk, and the bags were filled with about 5 ml of Ringer's solution of the same composition except that the calcium was removed and 2.0 mM ethylenediaminetetraacetic acid (EDTA) was added to the solution. The solution was titrated to pH 8.2 with NaOH. Hemibladders were attached to syringes and placed in a beaker containing about 200 ml of the EDTA-Ringer's solution, gassed with air, and allowed to incubate at room temperature, about 23°C, for 45 min. At the end of this period a few milliliters of solution was aspirated from each hemibladder, and the hemibladders were gently massaged to detach the loosened epithelial cells. The aspirated fluid was then returned to the bladder bag and the entire contents of the hemibladder finally aspirated, and

placed in 40 ml plastic centrifuge tubes on ice. The bags were washed with a few milliliters of EDTA-Ringer's solution, and the wash was added to the centrifuge tubes. Subsequent procedures were performed at 4°C.

The isolated epithelial cells were then centrifuged in a Sorvall RC2 refrigerated centrifuge at 3500 RPM (1500 x g) for 20 min. The supernatant was discarded and the pelleted cells resuspended in a few milliliters of Ringer's solution containing 0.89 mM calcium from which the EDTA was omitted. The pellet was gently aspirated several times with a Pasteur pipette to suspend and separate the cells. The separated cells was washed by centrifugation in a tared centrifuge tube at 3500 RPM in at least 20 ml of the calcium-containing Ringer's solution. The supernatant was again discarded and the test tube containing the epithelial cells was weighed. Cells were stored frozen at -15°C, under N₂. Cells were used within 1-21 days of isolation. No differences between freshly isolated and stored cells were detected during subsequent isolation of actin-like protein.

Extraction of toad bladder actin

The method which follows, adapted from Gordon et al. (48), was the final method adopted and was scaled down by about 100 fold for use with small volumes of starting material.

Isolated toad bladder epithelial cells were thawed and resuspended in one volume of extraction buffer, buffer G (48), which contained 3 mM imidazole, Sigma grade I (pH 7.5); 0.1 mM CaCl₂; 0.5 mM ATP; and 0.75 mM β-mercapto-ethanol, and to which 0.1 mM phenylmethylsulfonylfluoride (PMSF) and 0.2% Aprotinin (Trasylol) were added to inhibit proteolysis. The

mixture was homogenized with three 10 sec bursts of an MSE Ultrasonic Disintegrator (Instrumentation Associates, Inc., N. Y., N. Y.), and the homogenate was centrifuged at 35,000 RPM (80,000 x g) in the No. 40 rotor of a Spinco Model L ultracentrifuge. The high-speed supernatant obtained in this manner was chromatographed on DEAE-cellulose within a few hours of its preparation, as outlined by Gordon et al. (48).

DEAE-cellulose chromatography

Diethylaminoethyl cellulose ion exchange resin was purchased from Whatman (DE-32) and swelled according to the package directions. Swelled resin was restored refrigerated in water at pH 9.5. A fresh DEAE column was prepared 24-48 h before each extraction. Ten grams of swelled DEAE was weighed out. The resin was soaked in saturated NaCl for at least 30 min, rinsed, and filtered twice with about 80 ml deionized water in a Buchner funnel. The washed resin was then added to 7.5 ml buffer D (48), 10 mM imidazole (pH 7.5); 0.1 mM CaCl_2 ; 0.5 mM ATP; 0.75 mM β -mercapto-ethanol; 0.1 mM KCl. The pH of the mixture was adjusted to 7.5 with HCl, and 0.50 g ATP (sodium salt) was then added as the dry powder. (It was necessary to saturate the column with ATP to avoid denaturing the actin.) DEAE was allowed to equilibrate with ATP at 23°C for 15 min with intermittent stirring. The mixture was again titrated to pH 7.5 with NaOH, and the resin was poured into a Bio Rad disposable column to a bed height of about 8 x 0.7 cm. The bed volume was 3.1 cm³. The column was removed to the cold room and allowed to equilibrate overnight with buffer D. All subsequent procedures were performed at 4°C.

During preparation of high-speed supernatant, 3 ml of buffer G was passed into the DEAE column to facilitate the tendency of the actin-like protein to bind the ion exchanger as the monomer. The sample supernatant (3-4 ml) was then applied to the column followed by another 3 ml buffer G. Five milliliters buffer D containing 0.1 M KCl was then passed through the column. Lastly, thirty milliliters of a 0.1 to 0.5 M KCl solution in buffer D was applied as a gradient to elute the actin-like protein from the column. Fractions of about 1 ml were collected in an LKB minifraction collector. Protein elution was monitored by measuring the absorbance of the fractions at 290 nm. (A_{290} was chosen in order to minimize the component due to nucleotide.) The KCl gradient was monitored by measuring the conductance of the fractions with a type CDM 2e conductivity meter (Radiometer, Copenhagen).

Polymerization of actin-like protein

Initially, to localize actin-like protein in the elution pattern of the DEAE column, aliquots of selected fractions were analyzed by SDS-polyacrylamide gels. The appropriate fractions containing the 45,000 dalton protein were pooled, an aliquot was frozen for analysis, and the pooled sample was prepared for polymerization by dialysis against buffer G containing 0.1 M KCl and 2 mM $MgCl_2$. After overnight dialysis the sample was allowed to incubate at 23°C for 2 h. The polymerized sample was then centrifuged at 35,000 RPM (81,000 x g) at 25°C for 3 h in the Ti 50 rotor of a Beckman L-265-B ultracentrifuge. The cloudy, gelatinous pellet was homogenized in a small volume of buffer G plus 0.02% NaN_3 and dialyzed 3 days against at least three changes of dialysis buffer in order to depolymerize the protein.

The sample was then clarified by centrifugation at 35,000 RPM for 1 h in the No. 40 rotor of the Spinco Model L ultracentrifuge. The clarified supernatant was then used for electron microscopy of actin filaments; in one experiment, this supernatant was further purified by gel filtration on G150 Sephadex, as described by Gordon et al. (48).

Preparation of G-150 column

One gram Sephadex G-150 (Pharmacia Fine Chemicals, Uppsala, Sweden) was weighed out and placed in a beaker that contained buffer G, 3 mM imidazole (pH 7.5), 0.5 mM ATP, 0.75 mM β -mercapto-ethanol, 0.1 mM CaCl_2 , plus 0.02% NaN_3 . The resin was allowed to swell for three days, at room temperature. The solution was periodically changed, and at this time the fines that did not settle within about 15 min of having stirred the suspension were decanted. The swelled resin was then degassed in buffer G for several hours in a water aspirator, and the resin was refrigerated.

A Bio Rad disposable column (0.9 x 15 cm) was fitted with PE 90 tubing connected to its outlet by a fitting made from a 100 μ l disposable pipette tip. A tight seal was achieved at this end by attaching the sawed-off end of the pipette tip to the column outlet with melted candle wax. The column was filled half-way with cold buffer G, and when all the bubbles were flushed out of the tubing, the outlet was closed. To achieve uniform packing, all the resin was poured into the column at one time, by attaching a reservoir at its top end. The resin was allowed to settle to the bottom of the column until it had gone about one-third of the way; at this time the column outlet was opened and the resin

allowed to settle with buffer moving through it. The uniformity of the packing was checked by passing a light behind the column and observing the bed through the light. When no bubbles or other inconsistencies were observed, a cork stopper fitted with PE 90 tubing was fitted to the top of the column, and the packed column was allowed to equilibrate at 4°C in buffer G.

The flow was set at about 1.0 ml/h, and calibrated with rabbit actin (see Results).

Chromatography of actin-like protein on G-150 Sephadex

The clarified supernatant retrieved after one cycle of polymerization was applied to the gel filtration column and eluted in buffer G. Fractions of 0.5 ml were collected every 30 min on an LKB minifraction collector. The absorbance of the effluent was monitored at A_{290} , and those fractions which eluted from the column in the same position as rabbit skeletal muscle actin were pooled. The elution pattern of toad actin-like protein was compared with that of authentic rabbit actin, and these data are shown in Results. The pooled fractions were concentrated by dialysis against dry Sephadex, and aliquots were taken for measurement of protein content and for SDS gels.

The remaining pooled sample was dialyzed overnight in a polymerizing medium (25 mM imidazole, pH 7.0, 0.1 M KCl, 2 mM $MgCl_2$) to prepare the protein for electron microscopy. Samples of polymerized protein were applied to carbon-coated grids and negatively stained. The grids were then examined in the electron microscope to ascertain the presence of actin filaments.

MORPHOLOGICAL STUDIES

Glycerination and Heavy Meromyosin Treatment of Toad Urinary

Bladders.

The method for in situ arrowhead-labeling of toad bladder actin with heavy meromyosin (HMM) was modified from the technique of Ishikawa et al. (66). This procedure relies on the incubation of experimental tissues with glycerol to render the cell membranes permeable to HMM. To modify the procedure for use in the toad bladder, it was necessary only to decrease the duration of the glycerol incubation period, and to include calcium in all incubation mixtures, in order to preserve minimum integrity of the tissue during sample preparation. The addition of calcium did not interfere with the binding of HMM to actin of either epithelial cell or smooth muscle origin.

Glycerination of toad bladders was carried out in 5 mM sodium phosphate buffer, pH 7.0, that contained in addition, 2 mM $MgCl_2$, 0.1 mM $CaCl_2$ and 0.1 M KCl. Several hundred milliliters of this solution was mixed with glycerol (Baker) to make solutions of 5%, 25% and 50% glycerol. These were stored at 4°C prior to use. Heavy meromyosin, either freshly prepared or reconstituted from the lyophilized powder, was dialyzed against the glycerination buffer and reclarified by centrifugation immediately before use. The HMM was used at concentrations of between 2.5 and 5 mg/ml.

For each experiment, two toads were pithed and their bladders excised. For convenience of handling, the bladder openings were tied to the outlets of Luer Lock syringe tip adapters, as described previously. All incubations were performed at 4°C. The bladders were rinsed several times with cold glyceri-

nation buffer, and both experimental and control hemibladders were then incubated in graded glycerols. In early experiments, the initial incubation was performed in 50% glycerol for 4 h. This was followed by incubating the hemibladders for 1 h each in 25% and 5% glycerol solutions for a total incubation time of 6 h. In later experiments, it was found that optimal tissue preservation was achieved if the hemibladders were incubated in graded glycerols in both the increasing and decreasing directions, as described below.

Each hemibladder was filled with 5 ml 5% glycerol and suspended in 25 ml of the same solution. After 1 h the solutions were changed to 25% glycerol and the bladders again incubated for 1 h. The solutions were then replaced with 50% glycerol, and the incubation was continued for 2 h. Hemibladders were then incubated in 25% and 5% glycerol for 1 h each; thus the total time of exposure to glycerol was maintained at 6 h.

After glycerol incubation, the apex of each hemibladder (about 1.5 cm in diameter) was cut off and allowed to fall into a Petri dish containing glycerination buffer. Each hemibladder apex was rinsed in this buffer and cut into 4 segments. Each segment was placed in a test tube containing either 1) HMM, 2.5 - 5.0 mg. ml in glycerination buffer, 2) HMM to which 6 mM neutralized ATP had been added as a control to inhibit the acto-HMM interaction (65, 66), 3) 6 mM ATP in glycerination buffer, or 4) glycerination buffer alone. Bladders were incubated in these solutions overnight at 4°C. Each portion of bladder tissue was then washed in glycerination buffer (to remove excess HMM), fixed in glutaraldehyde (see below) and processed for observation by thin section transmission electron microscopy.

Sample Preparation for Electron Microscopy

Thin Section Electron Microscopy

Bladder tissue was prepared for thin section electron microscopy by a method modified from the procedure used by Marovitz et al. (97). This procedure was adapted for use in the toad bladder by decreasing the concentration of glutaraldehyde to 0.8% in the initial fixation medium. For observation of bladder tissue treated with glycerol and HMM, 0.2% tannic acid was also included in the initial fixation solution, as this treatment better preserves actin filaments, and enhances the visibility of arrowheads formed by the interaction of actin with HMM (10). Glycerinated samples were fixed at 4°C. All other fixations were performed at room temperature.

Fixation

Samples were well rinsed in cacodylic acid buffer, 0.1 M, pH 7.0. Rinsed bladders were then incubated at least 4 h in medium containing 0.8% glutaraldehyde (Ladd Research Industries, Burlington, Vt.) buffered with 0.1 M cacodylic acid, pH 7.0, and in some cases 0.2% tannic acid. Specimens were then well rinsed in 2 changes of excess cacodylic acid buffer and finally treated for 10 min (glycerinated samples) or 1 h (intact tissue) in 1.0% OsO₄ in 0.1 M cacodylic acid buffer at room temperature. The osmium was stored at -15°C.

Dehydration

The osmicated samples were again rinsed in cacodylic acid buffer and dehydrated in graded ethanols. The procedure for dehydration included two

10 min periods, one each in 50% and 75% absolute ethanol, followed by one 15 min period in 88% ethanol. The specimens were then rinsed twice in 100% ethanol and incubated for three consecutive 20 min periods in this solvent. Samples were then incubated for three 20 min periods in propylene oxide.

Embedding

Epoxy resin for embedment of samples for transmission electron microscopy was obtained from Ladd Research Industries. Stock resin was prepared in 50 ml batches after the method of Luft (92) and stored at -15°C until use. To 19.75 ml Epon was added 17.50 ml DDSA (Ladd), and the mixture was allowed to stir 15 min. At this time 10 ml of NMA (Ladd) hardener was added to the resin, and this was followed by the addition of 2 ml DBP (dibutyl phthalate). The mixture was allowed to stir a further 30 min before the addition of DMP 30 (Ladd). The complete mixture was stirred for 30 min before it was stored in a plastic container at -15°C .

Samples that had been dehydrated through propylene oxide were transferred to a mixture containing 1:1 propylene oxide:epon, and allowed to incubate on the bench overnight. Caps were left loosely covering the samples to allow the propylene oxide to evaporate. The next morning, samples were transferred to room temperature Epon, and finally embedded in flat molds in a fresh change of Epon. The mixture was cured at 60°C for at least 24 h.

Sectioning

Silver to gold sections were cut on a Sorvall MT-2B ultramicrotome using glass or diamond knives. Sections were stained for 10 min in saturated

uranyl acetate and for 15 min in Reynolds lead citrate (118) and examined on a Zeiss Model 9S2 electron microscope operated at 60 KV.

Negatively Stained Samples

Morphologic observation of the structures formed by solutions of contractile proteins were made by transmission electron microscopy of unfixed specimens after the method of Schwartz et al. (124), similar to that described by Huxley (65).

Actin was dialyzed overnight in 25 mM Tris HCl, pH 7.0; 0.1 M KCl; 2 mM MgCl₂; myosin or HMM was dialyzed in 10 mM imidazole, 0.75 mM β-mercapto-ethanol and clarified by centrifugation just prior to use. Solutions of protein were prepared containing 0.2 mg/ml actin or myosin and 0.4 mg/ml HMM.

Copper EM grids, 200-300 mesh (Ladd) were coated with a thin film of collodion and stabilized by an 800 Å thick coating of colloidal carbon. Grids were stored at 23°C until use, and were used within 3 months of preparation.

For observation of actin filaments, a drop of the actin-containing solution was placed on a clean sheet of Parafilm, and a grid was floated coated side down on the drop of solution. The grid was left in place for 2 min and then rinsed by dipping the grid 10-15 times in a solution of 25 mM Tris HCl, pH 7.0; 0.1 M KCl; 2 mM MgCl₂. The grid was then floated on a drop of 1% aqueous uranyl acetate which had been stored at 4°C, brought to room temperature and passed through a Millipore filter just prior to use. After incubation in uranyl acetate for 2 min, the grid was removed, and the edge was blotted with a small piece of filter paper to draw off excess stain. A similar procedure

was carried out for observation of myosin filaments.

When purified actin was reacted with HMM, the grid was incubated on a drop of the actin solution, as above, and rinsed. It was then placed on a drop of HMM, and allowed to incubate for 2 min. The grid was then rinsed free of excess HMM by dipping it in 50 mM Tris, pH 7.5; 0.1 M KCl and stained as usual in 1% uranyl acetate.

Observations were made either on a Phillips 300 electron microscope operated at an accelerating voltage of 80 KV or on a Zeiss Model 9S2 electron microscope operated at 60 KV.

RESULTS

I. Effect of Dihydrocytochalasin B on Osmotic Water Movement in Isolated Toad Bladders.

Toad urinary bladders were exposed to dihydrocytochalasin B (H_2CB) to determine whether or not the effect of this agent upon vasopressin-induced osmotic water flow was similar to that of CB.

Effect on Basal Water Flow

The results of a 90 min exposure of paired hemibladders to either 5 or 10 $\mu\text{g/ml}$ (10.6 and 21.2 μM) H_2CB on the basal rate of water flow in the absence of vasopressin are shown in Table 4. H_2CB had no demonstrable effect on the basal rate of osmotic water flow across the bladders. As shown in Table 4, in bladders exposed to either 5 or 10 $\mu\text{g/ml}$ H_2CB , the basal rate of water movement was not significantly different from that in their paired controls exposed to 0.1% or 0.2% DMSO. Thus, bladders exposed to 0.1% DMSO lost an average of 0.73 ± 0.08 mg/min compared with 0.63 ± 0.07 mg/min lost by hemibladders exposed to H_2CB in DMSO ($n=3$, n. s.). Control bladders receiving 0.2% DMSO lost an average of 1.5 ± 0.06 mg/min compared with 2.0 ± 0.3 mg/min lost by experimental hemibladders receiving H_2CB in 0.2% DMSO ($n=3$, n. s.). These data indicate that exposure to DMSO caused an increase in the basal rate of water flow across the bladders over that which is normally observed (Taylor and Pearl, unpublished observation). Although in the experiments in which 0.2% DMSO was used, there was a tendency for the experimental hemibladders to have a greater rate of basal water movement than the controls, even in this small sample there was no consistent difference

Table 4. Effect of Dihydrocytochalasin B and DMSO on Basal

Osmotic Water Movement

<u>Incubation conditions</u>	<u>Water flow, mg/min</u>		<u>Average water flow, mg/min</u>	
	<u>DMSO</u>	<u>H₂CB</u>	<u>DMSO</u>	<u>H₂CB</u>
0.1% DMSO or 10.6 μ M H ₂ CB in DMSO	0.6	0.7	0.73 \pm 0.13	0.63 \pm 0.12
	1.0	0.8	p < 0.8, n. s.	
	0.6	0.4		
0.2% DMSO or 21.2 μ M H ₂ CB in DMSO	1.6	3.0	1.5 \pm 0.06	2.0 \pm 0.3
	1.3	1.7	p < 0.5, n. s.	
	1.6	1.3		

in the rate of water transfer between experimental and control hemibladders.

Effect on Vasopressin-Induced Water Flow

The effect of H₂CB on the hydrosmotic response to 20 mU/ml vasopressin is shown in Figure 8 and Table 5. Incubation of hemibladders in H₂CB for 90 min prior to the addition of vasopressin resulted in a marked inhibition of the response to the hormone in all of the hemibladders tested. Figure 8 depicts the response to vasopressin in 3 pairs of hemibladders in which one member of each pair had been exposed to 10 µg/ml H₂CB for 90 min.

The inhibition induced by H₂CB was dose-dependent. Because exposure of bladders to H₂CB resulted in a progressive loss of the osmotic gradient across the bladder, the degree of inhibition of vasopressin-stimulated water flow was estimated by normalizing water flow to the average osmotic gradient to which the bladders were exposed during the 60 min period following challenge with hormone (see Methods). As shown in Table 5, the mean inhibition of vasopressin-stimulated osmotic water flow was $20.9 \pm 2.8\%$ (n=3, p<0.02) and $43.9 \pm 3.1\%$ (n=3, p<0.001) for bladders exposed to 10.6 µM and 21.2 µM H₂CB, respectively.

II. Isolation and Purification of Actin-like Protein from Toad Bladder Epithelial

Cells

Preliminary approaches

Hartwig and Stossel Procedure

Initial attempts to purify actin from extracts of isolated toad bladder epithelial cells were made using the method developed by Hartwig and Stossel

EFFECT OF DIHYDROCYTOCHALASIN B
ON VP-INDUCED OSMOTIC WATER MOVEMENT

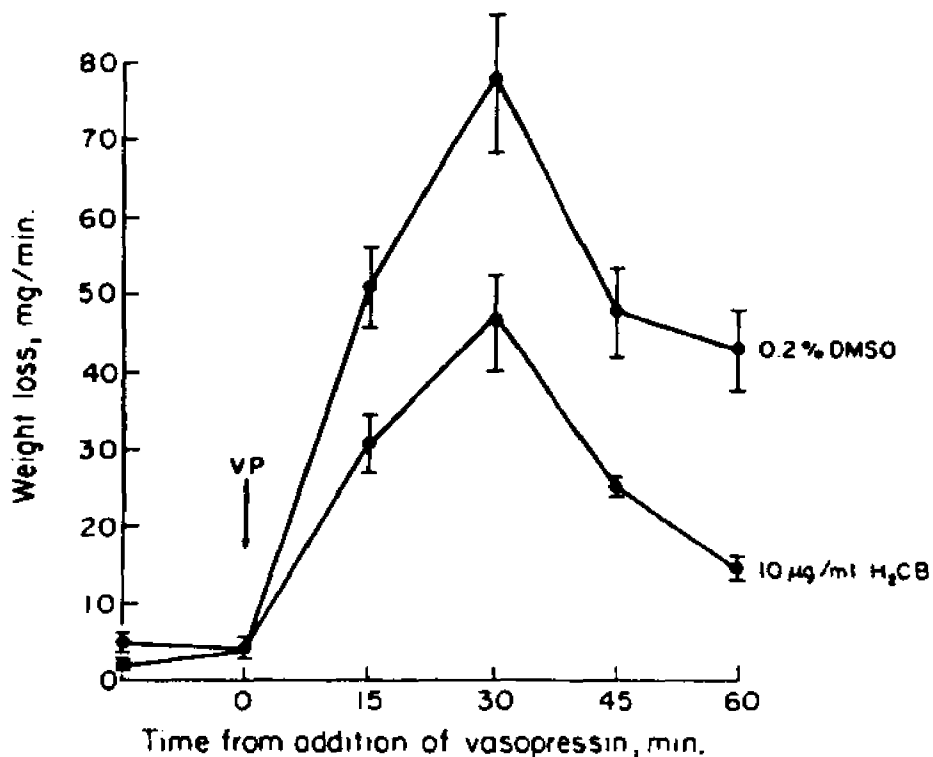


Fig. 8. Water loss in mg/min from paired hemibladders in the presence and absence of H₂CB is plotted as a function of time following the addition of 20 mU/ml vasopressin to the serosal solution bathing each hemibladder.

Table 5. Effect of Dihydrocytochalasin B on Vasopressin-Stimulated Water Movement

Incubation conditions	Mean gradient, mOsm/kg H ₂ O		Water flow, mg/min/mOsm/kg H ₂ O		% inhibition 1-E/C x 100
	DMSO	H ₂ CB	DMSO	H ₂ CB	
0.1% DMSO or 10.6 μM H ₂ CB in DMSO	205	164	0.238	0.196	26.1
	205	175	0.219	0.202	16.4
	209	194	0.232	0.202	20.3
Average inhibition, %					20.9 ± 2.53
p					p < 0.02
0.2% DMSO or 21.2 μM H ₂ CB in DMSO	230	192	0.196	0.117	40.3
	219	205	0.271	0.159	41.3
	223	223	0.294	0.147	50.1
Average inhibition, %					43.9 ± 3.13
p					p < 0.001

(55) for the purification of actin from macrophages. In the procedure used by these investigators, macrophages were mixed with 2 volumes of a low salt buffer containing 0.34 M sucrose, 10 mM DTT, 0.5 mM ATP, 1 mM EDTA, and 20 mM Tris-maleate, pH 7.0. The cells were homogenized in this medium, and a 100,000 x g supernatant was prepared. The extract supernatant was made 0.075 M in KCl and 0.002 M in $MgCl_2$ and was incubated at 25°C for 1.5 h to allow the actin to polymerize. The extract was then centrifuged at 12,000 x g for 10 min; this procedure pelleted the actin complexed with a high molecular weight actin-binding protein. When the pellet was dissolved in 0.6 M KCl and centrifuged at 80,000 x g for 3 h, the actin pelleted leaving an actin-binding protein in the supernatant. Actin was then subjected to two complete cycles of polymerization. Hartwig and Stossel (55) reported that highly purified actin could be isolated from macrophages using these procedures.

Accordingly, an identical method was first employed in an attempt to isolate actin from toad bladder epithelial cells. In a pilot experiment, cells were isolated from 10 toads following exposure to EDTA, as described in Methods. The cells were first homogenized in low salt buffer, and then subjected to the various extraction procedures described above. At each purification step, aliquots were taken for gel electrophoresis and protein estimations. Analysis of 5% SDS-polyacrylamide gels stained with Coomassie Brilliant Blue revealed that a dense band comigrating with authentic rabbit muscle actin (45,000 daltons) was present in the initial high speed supernatant, i. e., this species was a major component of the soluble fraction of the epithelial cells.

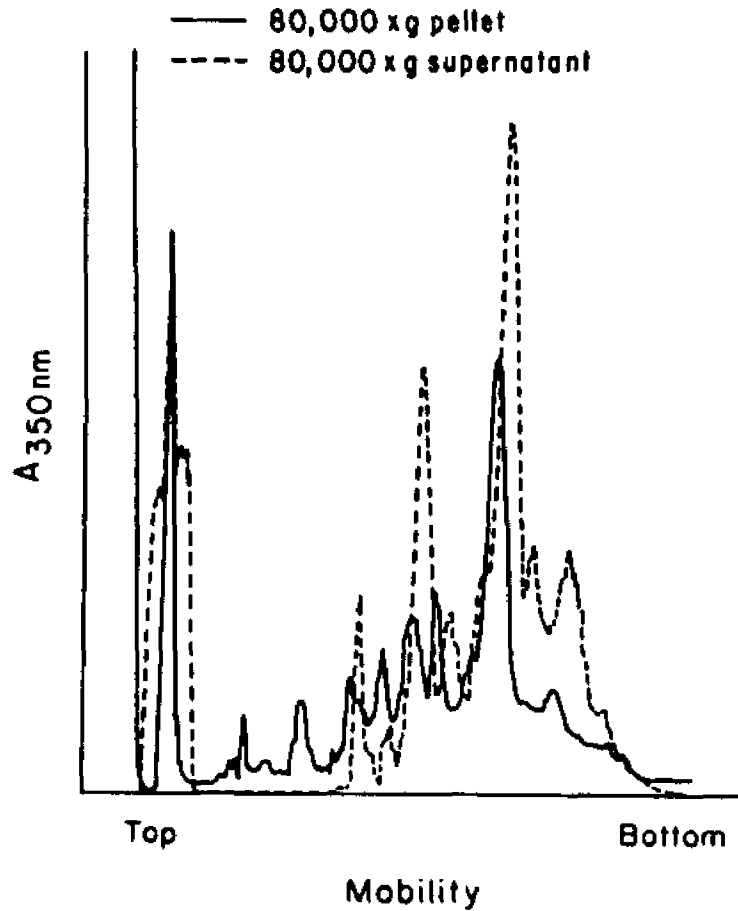
However, unlike the situation in macrophages reported by Hartwig and Stossel, the toad bladder material remained in the supernatant after the 12,000 x g spin (data not shown).

A method frequently employed to pellet polymerized actin is centrifugation at 80,000 x g for 3 h at 4°C (115). Therefore, to determine whether the species comigrating with rabbit muscle actin would pellet after centrifugation at high speed, the Hartwig and Stossel procedure was repeated using this modification in place of the 12,000 x g spin. Densitometer tracings of 5% SDS-polyacrylamide gels of the supernatant and pelleted fractions resulting from such a preparation are shown in Figure 9. These scans show that some of the material comigrating with rabbit actin was indeed recovered in the post-polymerization, high-speed pellet, although the major proportion of this material still remained in the supernatant fraction.

It seemed possible that the low yield of pelleted material was due to a failure to maintain a critical concentration of G actin during the polymerization process. It was therefore decided to reduce the volume of extraction buffer in which the cells were homogenized, to favor the G - F transformation and presumably, therefore, the polymerization of actin from the high-speed supernatant. When this was done, however, there was still no further enrichment of the 45,000 dalton protein. An outline of this modified procedure is shown in Figure 10. Gel samples from such an experiment are shown in Figure 11. These gels were run on aliquots taken from the supernatant and pelleted material following polymerization in KCl and Mg and centrifugation at high speed.

TOAD BLADDER ACTIN ISOLATION

(Modified after Hartwig et al.)



J. Biol. Chem. 1975. 250, 5696

Fig. 9. Densitomer tracings of 5% SDS gels of polymerized pellet and supernatant of toad bladder actin-like protein prepared by the method of Hartwig et al. (55). The arrow indicates the electrophoretic position of rabbit muscle actin. Electrophoresis was performed in phosphate buffer, as described by Weber et al. (143). Gels were stained in Coomassie brilliant blue, and scanned at 550 nm.

Figure 10

Toad Bladder Actin Isolation (modified after
Hartwig et al.)

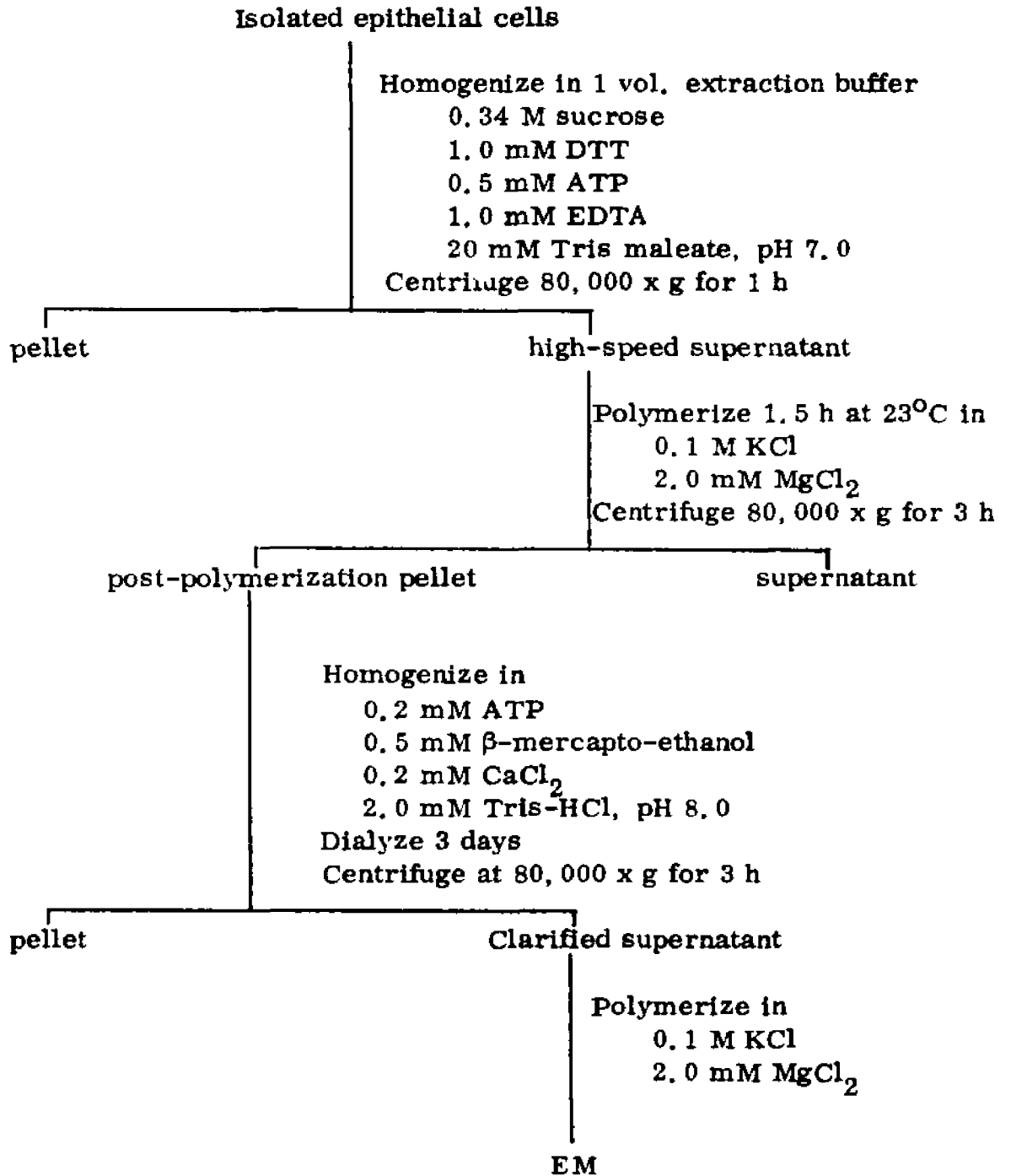




Fig. 11. 5% SDS gels of actin-like protein prepared by the method outlined in Fig. 10. The high speed supernatant was exposed to polymerizing conditions and centrifuged at 80,000 x g for 3 h at 4°C. 1) Supernatant; 2) pellet recovered after polymerization; 3) standard rabbit muscle actin.

It is clear that despite the reduction in volume of the extraction buffer, most of the 45,000 dalton band did not pellet, but remained in the supernatant fraction. (This occurred even though the extract supernatant, containing 7.2 mg/ml protein, would greatly have favored the polymerization of actin from a preparation of skeletal muscle, since a critical concentration of only 0.02 mg/ml is necessary (1).)

A small gelatinous pellet (similar in appearance to the pellet that can be collected from the centrifugation of polymerized rabbit actin) was retrieved after the 3 hour high-speed spin, and this material contained a small fraction of 45,000 dalton protein (see Fig. 11, gel 2). The pellet was homogenized in low salt buffer, dialyzed against this depolymerizing medium, and recentrifuged at high speed. The 45,000 dalton band was recovered in the clarified supernatant comprising 2% of the protein contained in the initial high speed supernatant. The gel pattern of the clarified supernatant was also not substantially different from that of Figure 11, gel 2, demonstrating that the 45,000 dalton protein amounted to only a small fraction of this 2%.

To determine whether this sample would form actin-like filaments visible in the electron microscope, the clarified protein solution was reincubated in polymerizing medium, and an aliquot was examined by electron microscopy after negative staining with uranyl acetate (see Methods for details). The results of this observation revealed that no filaments were present in the sample, although filaments were observed in samples of rabbit muscle actin polymerized in an identical manner, and observed at the same time. Thus, either actin was not present in the sample, or it was present in an unpolymerized but never-

theless aggregated and sedimentable form.

Although the results of these experiments demonstrated that toad bladder epithelial cells contained a soluble protein with the electrophoretic mobility of actin on SDS gels, they also clearly showed that it was not possible to further purify this protein by polymerization from the crude, high-speed supernatant. Inability to polymerize a significant fraction of actin from similar crude supernatant fractions has been a problem in the purification of actin from many types of nonmuscle cells (see 48). The failure to polymerize actin from nonmuscle cells has been attributed to the presence of actin-binding proteins that act as natural inhibitors of actin polymerization (20, 95, 135). In certain instances these actin-binding proteins have been identified (20, 95, 135). Their roles in interacting with actin are presently under investigation and will be discussed below.

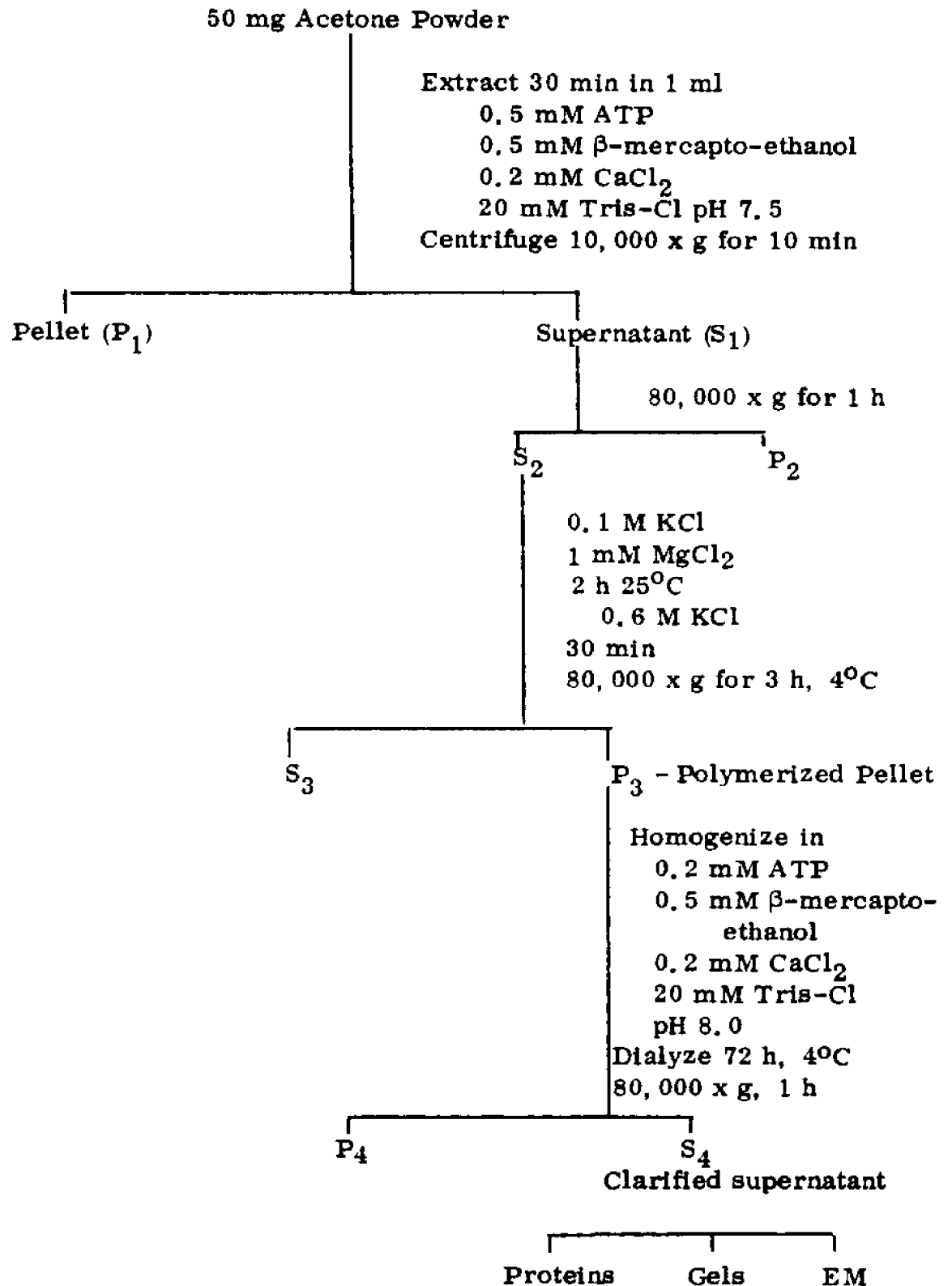
Extraction from Acetone Powder

The possibility was suggested that successful purification of toad bladder actin might be achieved using an acetone powder, on the theory that whatever factor was inhibiting the polymerization might be denatured by the acetone treatment, leaving the actin free to polymerize*. The method that was used for acetone extraction of actin from isolated toad bladder epithelial cells was modified from the procedures used by Spudich and Watt (129) for the extraction of rabbit muscle actin, and from that of Yang and Perdue (150) for the extraction of actin from cultured chick embryo fibroblasts. The procedure developed for toad bladder is summarized in Figure 12.

* M. Mooseker, personal communication

Figure 12

Isolation of Toad Bladder Actin-like Protein from Acetone Powder



Cells were collected from 12 toads in the usual fashion, washed once in calcium-containing Ringer's solution, and resuspended in a small volume of Ringer's. The cell suspension was added to about 100 ml cold acetone and stirred at 4°C for 30 min. Insoluble material was collected on a Buchner funnel, and the acetone treatment was repeated. The residue remaining on filter paper after two acetone treatments was dried overnight at -15°C under vacuum. This material was used for the extraction of actin on the following day. The extraction procedure was similar to that presented above (Hartwig procedure), in that it involved the solubilization of actin in a low salt buffer, and purification by centrifugation followed by cycles of polymerization. Modifications included the omission of sucrose in the extraction buffer, which contained 20 mM Tris-HCl, pH 7.5; 0.5 mM ATP; 0.5 mM β -mercapto-ethanol; and 0.2 mM CaCl₂ (see Figure 12).

SDS-polyacrylamide gels of this extraction are shown in Figure 13. Although a protein with the electrophoretic mobility of actin was progressively enriched during this procedure, most of the 45,000 dalton band again remained associated with the supernatant when centrifuged after incubation in polymerizing medium. Protein concentrations determined for this extraction revealed that out of 8 mg protein in the starting material, only 0.06 mg protein was recovered in the final supernatant (S4). About one-half the protein remained in the post-polymerization supernatant (S3), representing a recovery of 0.75% of the total soluble protein, similar to that obtained by others (see below).

The clarified supernatant (S4) was exposed to polymerizing medium

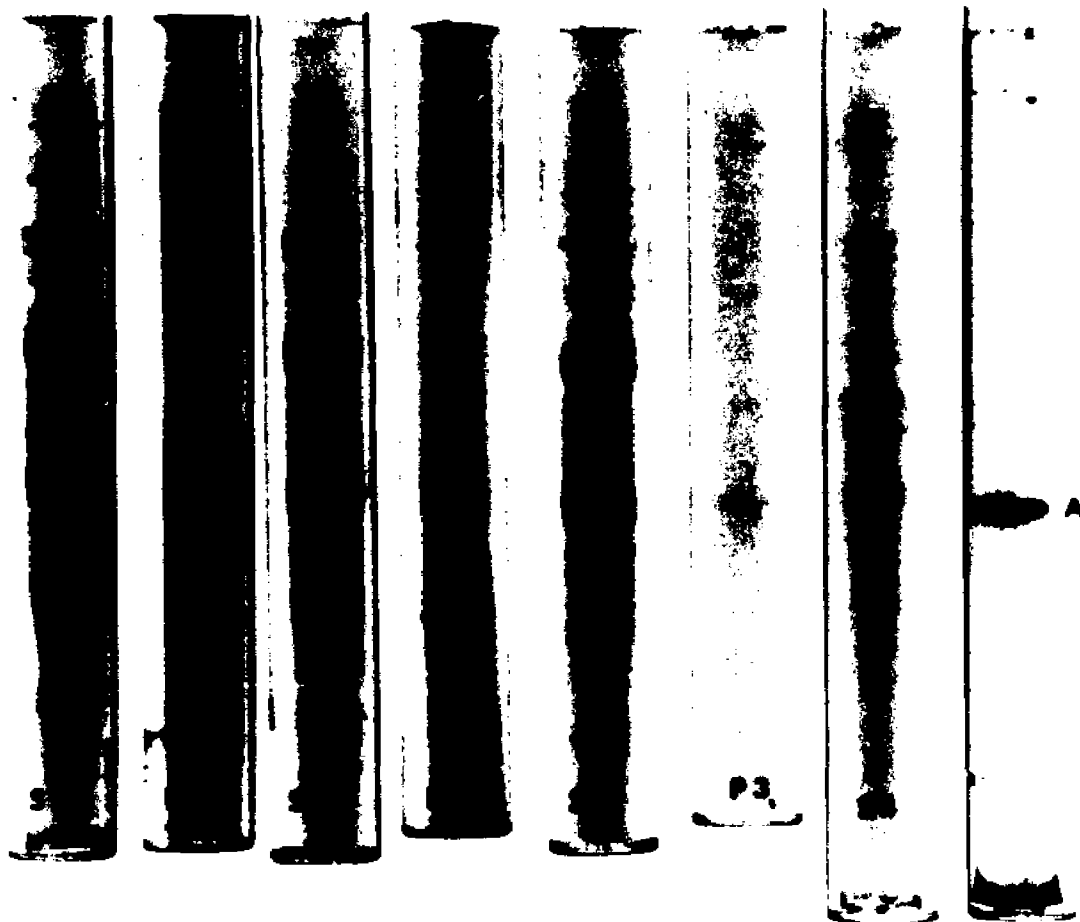


Fig. 13. 5% SDS gels derived from the procedure outlined in Fig. 12. Comparison of gels 5(S_3) and 6(P_3) reveal that almost none of the 45,000 dalton band sedimented after exposure to polymerizing medium. Gel 7 (S_4) was run after concentrating the sample; here, a light 45,000 dalton band is visible; Gel 8 is standard rabbit muscle actin.

(0.1 M KCl, 2 mM MgCl₂ in 20 mM Tris-HCl, pH 8.0, 0.2 mM ATP, 0.5 mM β-mercapto-ethanol, 0.2 mM CaCl₂), and samples transferred to grids in preparation for electron microscopy. Some samples were treated with HMM. Control samples of polymerized rabbit actin, with and without HMM, were prepared similarly. Electron microscopy of the rabbit actin samples revealed that filaments and HMM-decorated arrowheads were present in the control rabbit actin samples. However, no filaments or evidence of HMM decoration were observed in the toad bladder samples. Correspondingly, SDS gels of this sample (S4) revealed that little 45,000 dalton protein was recovered in this sample.

Isolation of Actin-like Protein by Column Chromatography

Both the isolation procedures used so far in this work have depended upon the KCl-induced polymerization of actin from a crude, high-speed supernatant (55), or from a solubilized, acetone-precipitable fraction derived from whole cells (150). In other systems, e.g., macrophages (55), these methods employed 30-100 g of packed cells as starting material and yielded purified protein amounting to less than 2.5% of the estimated amount of cell actin (see 48). The greatest losses of protein in these procedures apparently occurred during the polymerization step, with most of the 45,000 dalton band remaining in an un-sedimentable form (2, 55, 150, see 48). Although it has never been conclusively shown that actin accounts for all of the low-salt extractable, 45,000 dalton material in nonmuscle cells, there is now considerable evidence that much of the actin in these cells is kept in a non-polymerizable form (135, 136), complexed with actin-binding proteins. In some cases, such proteins that in-

hibit actin polymerization have been identified (20, 95, 135, see below). Therefore, in the toad bladder, because of the relatively small amount of available starting material, and because large losses were to be expected during polymerization of a crude supernatant, it seemed desirable to use a procedure for isolation of toad bladder actin that did not depend on polymerization as the initial purification step.

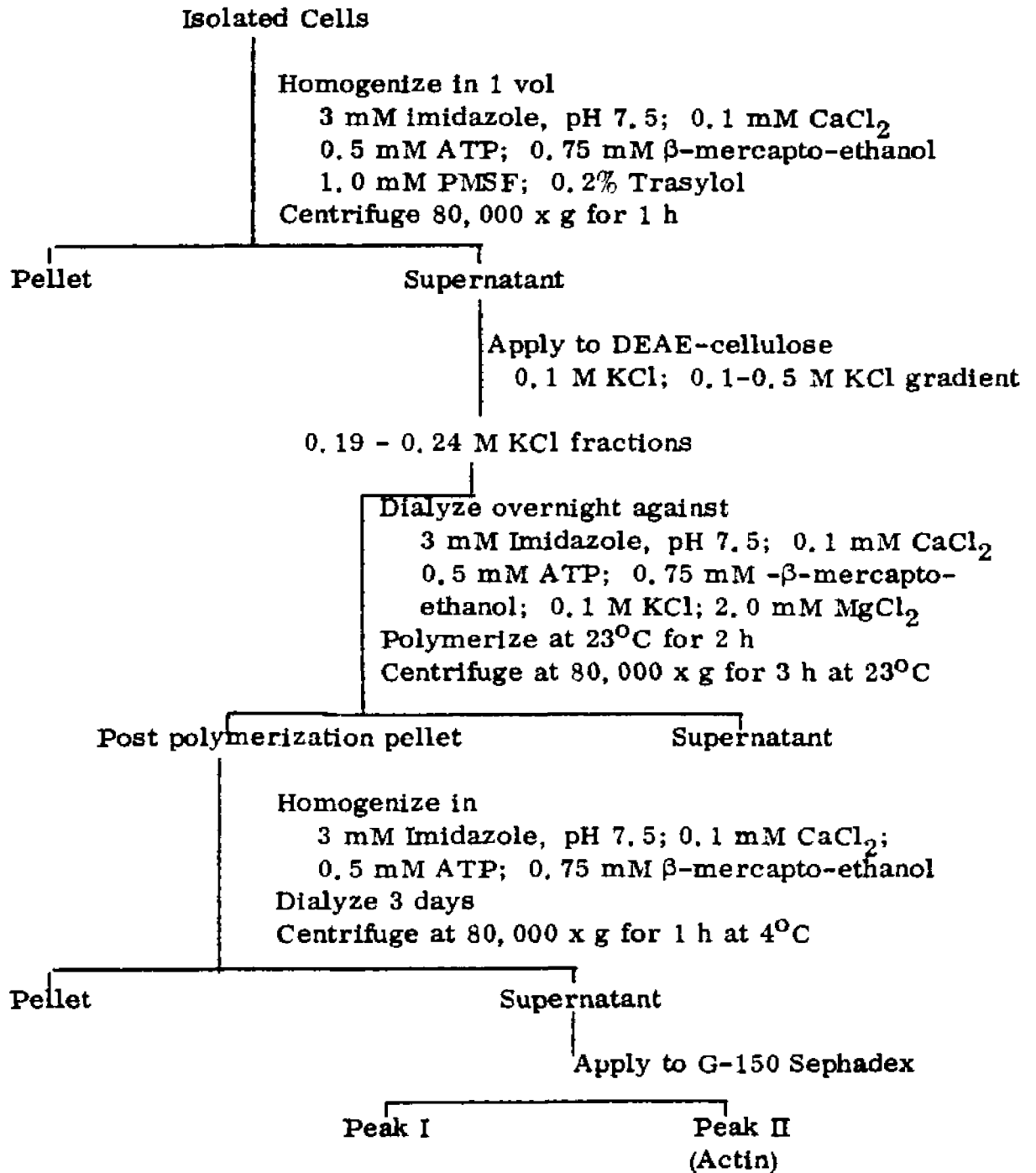
Such a procedure has been described by Gordon et al. (48) for the purification of actin from Acanthamoeba. This method relies upon the selective retention of actin on DEAE-cellulose in solutions of low ionic strength. Actin-binding proteins presumably elute before actin, leaving the latter available for polymerization after collection in the effluent from a KCl gradient. Ion exchange chromatography is followed by one cycle of polymerization, and subsequent gel filtration on G-150 Sephadex.

In order to adapt this method for use in the toad bladder, it was necessary to scale down the volumes used by about two orders of magnitude. The preparation of DEAE-cellulose ion exchange and G-150 Sephadex gel filtration columns are described in Methods, as is the complete description of the purification procedure. Figure 14 outlines the purification of toad bladder actin by this method.

DEAE-Cellulose Chromatography

Epithelial cells were isolated in the usual fashion from 10-20 toads, homogenized by sonication, and the 45,000 dalton protein was extracted into the 80,000 x g supernatant. This sample was applied to DEAE-cellulose and the

Fig. 14. Isolation of Toad Bladder Actin by Column Chromatography
(after Gordon et al.)



column was eluted with successive solutions containing no KCl, 0.1 M KCl, and a linear 0.1 - 0.5 M KCl gradient. Determinations of the optical densities of the eluted fractions and their conductivities were made, and SDS gels of selected fractions were run to determine the position of the 45,000 dalton band.

Figure 15 A shows the elution profile of rabbit actin from DEAE-cellulose. Figure 15 B shows the elution pattern of a typical toad bladder experiment. SDS gels of fractions eluted from the column are presented in Figure 16. Comparison of these data reveals that the 45,000 dalton component present in the initial high-speed supernatant was selectively retained on the column, eluting in a single, broad peak that corresponded to the elution pattern of authentic rabbit muscle actin. Both these proteins eluted in the KCl gradient at conductivities between about 7.5 and 15 mS corresponding to 0.19 - 0.24 M KCl. These data are in good agreement with those published by Gordon et al. for the elution of Acanthamoeba actin.

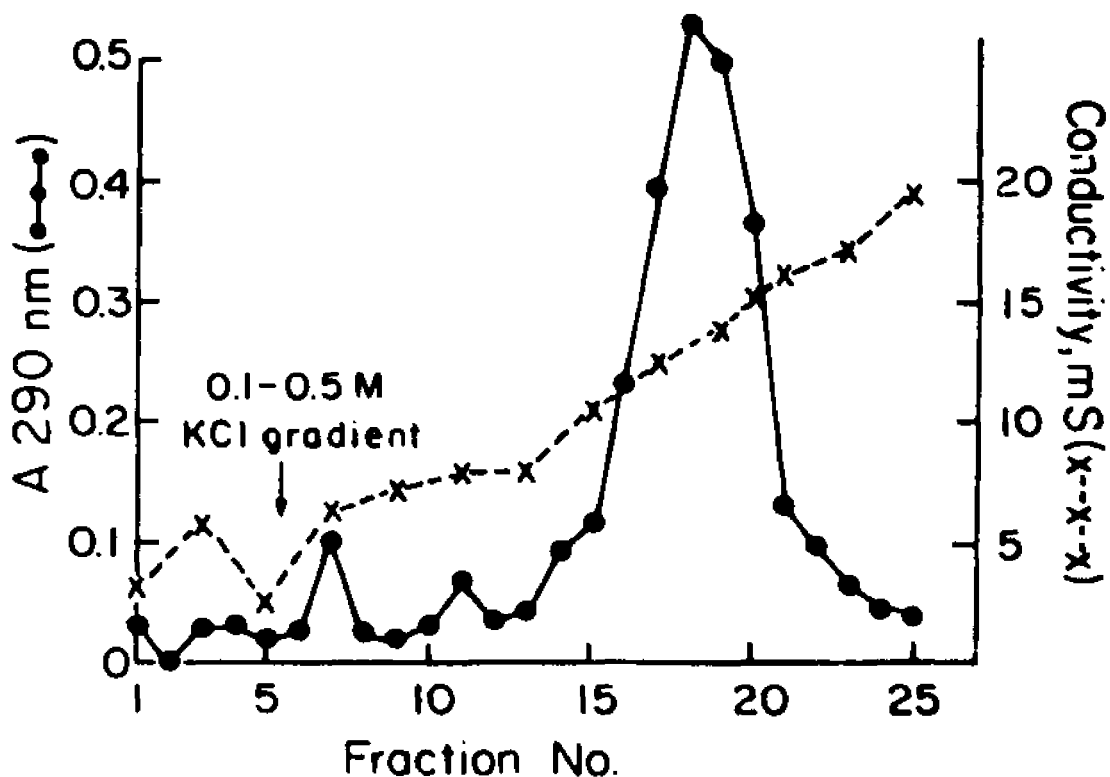
Polymerization Cycle

Fractions containing the 45,000 dalton band were subsequently pooled and dialyzed overnight against polymerizing medium (3 mM imidazole, pH 7.5; 0.1 mM CaCl₂; 0.5 mM ATP; 0.75 mM β-mercapto-ethanol, 0.1 M KCl, 2 mM MgCl₂). The sample was then removed from the cold room and allowed to incubate 2 h at 23°C. After centrifugation at this temperature for 3 h at 80,000 x g, a small gelatinous pellet was recovered. (This material contained the polymerized actin-like protein). The pellet was homogenized in a small volume of depolymerizing medium (as above but KCl and Mg were ex-

Fig. 15A. Elution pattern of rabbit actin from DEAE cellulose. Actin, 2 mg was homogenized in 1 ml buffer (3 mM imidazole, 0.5 mM ATP, 0.1 mM CaCl_2 , 0.75 mM β -mercapto-ethanol, pH 7.5, buffer G, see Methods) and applied to DEAE cellulose saturated with ATP that was equilibrated in 10 mM imidazole, 0.1 mM CaCl_2 , 0.5 mM ATP, 0.75 mM β -mercapto-ethanol, 0.1 M KCl buffer D, see Methods). Prior to sample application, 1 ml buffer G was applied to the column, and a second ml buffer G was applied after the sample. The protein was eluted with a few ml of buffer D and then with 30 ml of a 0.1 - 0.5 M KCl gradient in buffer D. Fractions of 0.5 ml were collected. The absorbance of each fraction was monitored at 290 nm, and the conductivity of the gradient was monitored to determine the position of the protein in the KCl gradient.

Fig. 15B. Elution pattern of toad bladder actin-like protein from DEAE cellulose. About 5 ml of high-speed supernatant was applied to the column equilibrated as in the legend to Fig. 15A. Fractions were collected also as described above.

Figure 15 A and B
**DEAE-CELLULOSE CHROMATOGRAPHY
 OF RABBIT ACTIN**



**DEAE-CELLULOSE CHROMATOGRAPHY OF ACTIN-LIKE
 PROTEIN FROM TUBE**

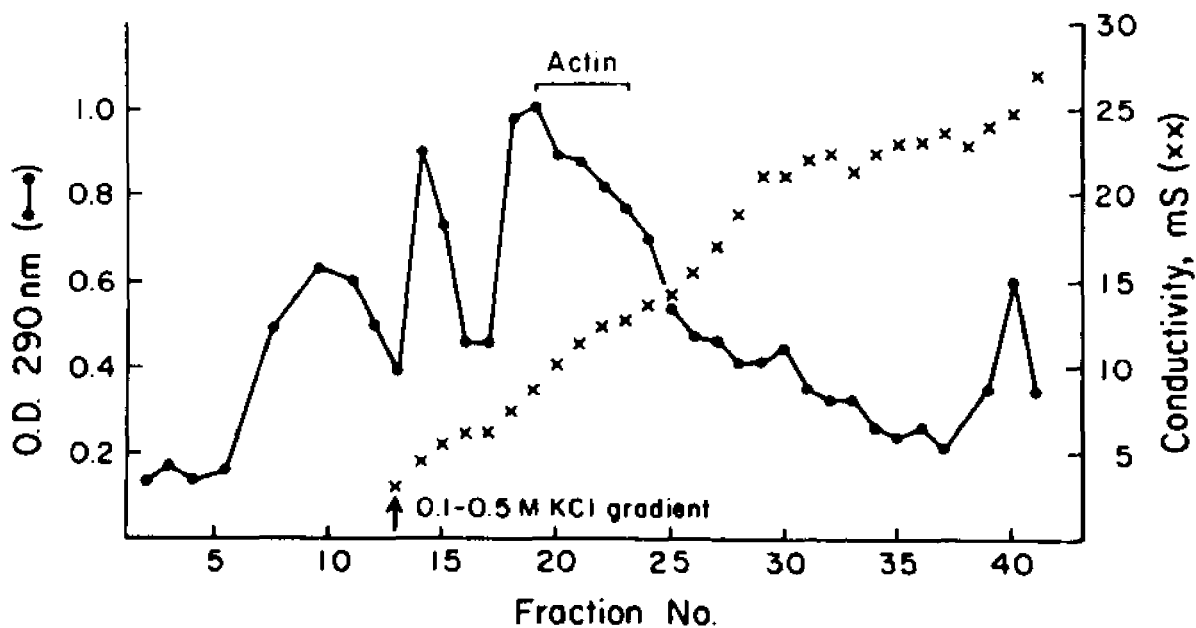




Fig. 16. SDS gels of selected fractions from DEAE-cellulose chromatography of toad bladder epithelial cells. Actin-like protein eluted with the KCl gradient.

cluded and 0.02% NaN_3 was added), and dialyzed against several changes of this solution for 3 days. At this time the sample was centrifuged at 80,000 x g for 1 h at 4°C to sediment any actin-like protein that had not depolymerized, along with any impurities that had cosedimented during centrifugation of the polymerized protein. The clarified, depolymerized protein was then either further purified on Sephadex G-150 (as described in Methods) or used directly for electron microscopy.

Figure 17 shows 5% SDS gels from an extraction in which Sephadex chromatography was not performed. Comparison of the gels reveals that the 45,000 dalton component present in the high-speed supernatant is significantly enriched during chromatography on DEAE-cellulose and by one cycle of polymerization. However, several contaminants remain in the purified sample. The most prominent of these being a protein with the electrophoretic mobility of myosin, and a second species with an apparent molecular weight of approximately 107,000 ($M = 0.38$) daltons.

Chromatography of Toad Bladder Actin-like Protein on

G-150 Sephadex

The clarified supernatant was applied to the Sephadex column in depolymerizing medium and eluted with the same buffer. Figure 18 shows the elution profiles of rabbit actin and toad bladder actin-like protein from this column. Rabbit actin eluted in two peaks (see Legend to Fig. 18). The toad bladder protein also eluted in 2 peaks. These results correspond well with those published by Gordon et al. (48) and others (3) in that actin did not elute



Fig 17. SDS gels profile of purification of toad bladder actin-like protein.

1) 84 μ g high-speed supernatant; 2) 48 μ g of pooled fractions recovered from DEAE-cellulose; 3) 36 μ g of material recovered after one cycle of polymerization; 4) standard rabbit actin (45, 000 daltons) and myosin heavy chains (200, 000 daltons), and purified brain tubulin (55, 000 daltons).

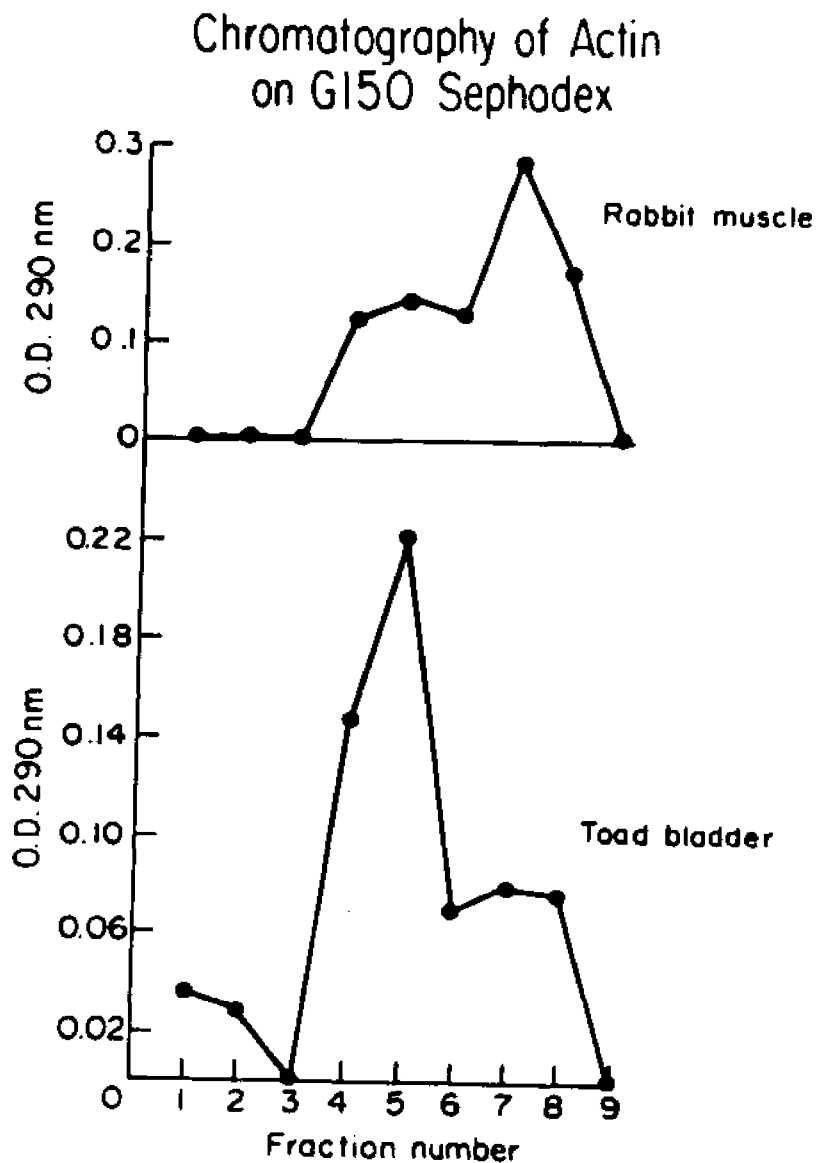


Fig. 18. Elution patterns of rabbit muscle actin and toad bladder actin-like protein on G-150 Sephadex. Rabbit muscle: 2 mg of purified lyophilized actin was homogenized in 1 ml Buffer G (see Fig. 15A) + 0.02% NaN_3 and applied directly to the 0.9 x 15 cm column. 0.5 ml fractions were collected every 30 min. Fractions 3-5 presumably containing oligomeric actin eluted with the void volume (3). Toad bladder: 0.5 mg protein was applied to the column in 0.8 ml Buffer G. Elution was the same as for rabbit actin. Peak I eluted with the void volume; Peak II contained actin-like protein.

from the column as a sharp peak. Gel electrophoresis of samples from each peak recovered from the toad bladder sample revealed that the second peak contained the major proportion of the 45,000 dalton band.

In Figure 19 are depicted gels of an extraction which was similar to that shown in Figure 17, but included Sephadex gel filtration. Examination of gels from aliquots of peaks I and II of the Sephadex column shows that the actin-like protein was further purified by this treatment (peak II) while the higher-molecular weight contaminants were largely retrieved in Peak I. The major molecular weight species eluting with actin-like protein had apparent molecular weights of 79,000 ($M = 0.49$) and 93,000 ($M = 0.43$) daltons, compared with 69,000, 93,000 and 107,000 ($M = 0.54$, 0.43 , and 0.38 , respectively) eluted in Peak I.

Filament Formation

When the clarified supernatant obtained from toad bladder epithelial cell extracts after ion exchange chromatography and one cycle of polymerization was dialyzed against polymerization medium and allowed to incubate for 1 or 2 h at room temperature, filaments formed that were visible in the electron microscope. Negatively stained samples prepared as described in Methods were examined, and in every preparation, numerous 50-70 A filaments were seen. An electron micrograph of one of these preparations is shown in Figure 20. These filaments had the characteristically beaded appearance of actin filaments, and the inter-bead distance measured about 50 A, close to the value of 55 A given by Huxley (65) and for the size of the beaded monomer

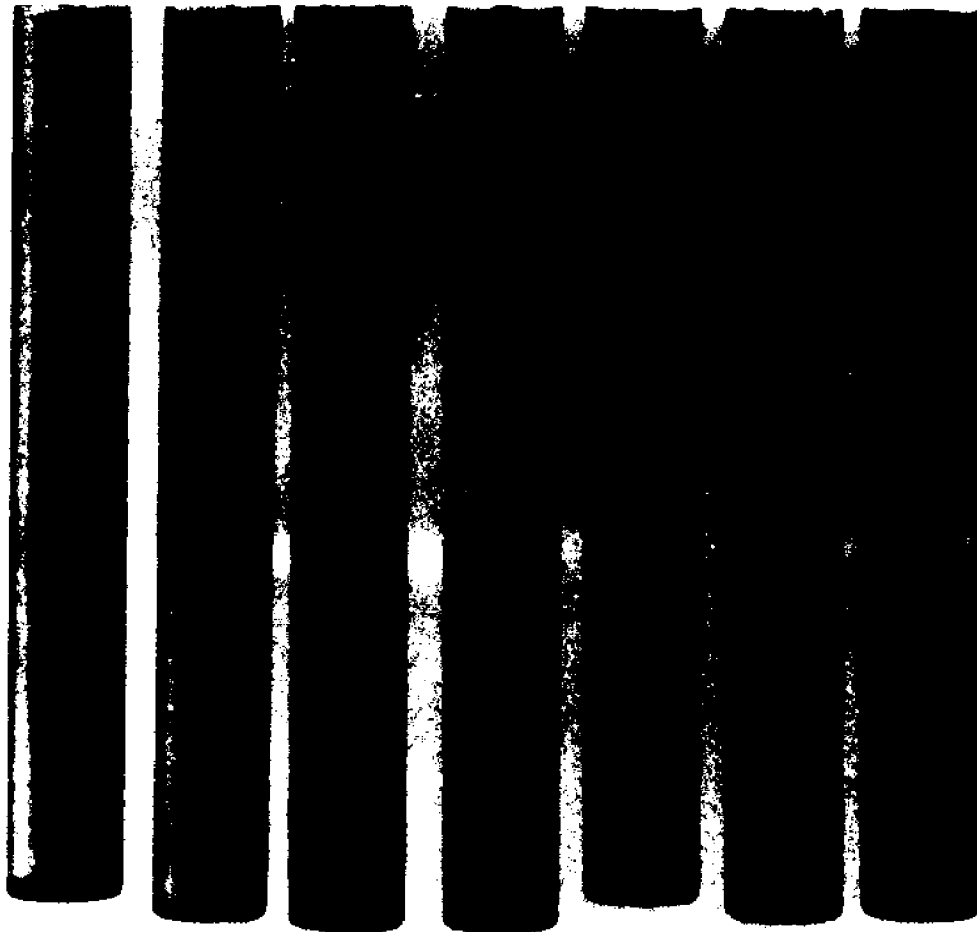


Fig. 19. Purification of toad bladder actin-like protein by chromatography on DEAE-cellulose and G-150 Sephadex. 1) 86 μg high speed supernatant; 2) 48 μg fractions 31-36; 3) 36 μg material recovered in pellet after polymerization; 4) 32 μg material recovered in supernatant after depolymerization; 5) 10 μg Peak I recovered from G-150 Sephadex; 6) 10 μg Peak II from G-150 Sephadex; 7) Standard actin, tubulin, myosin.

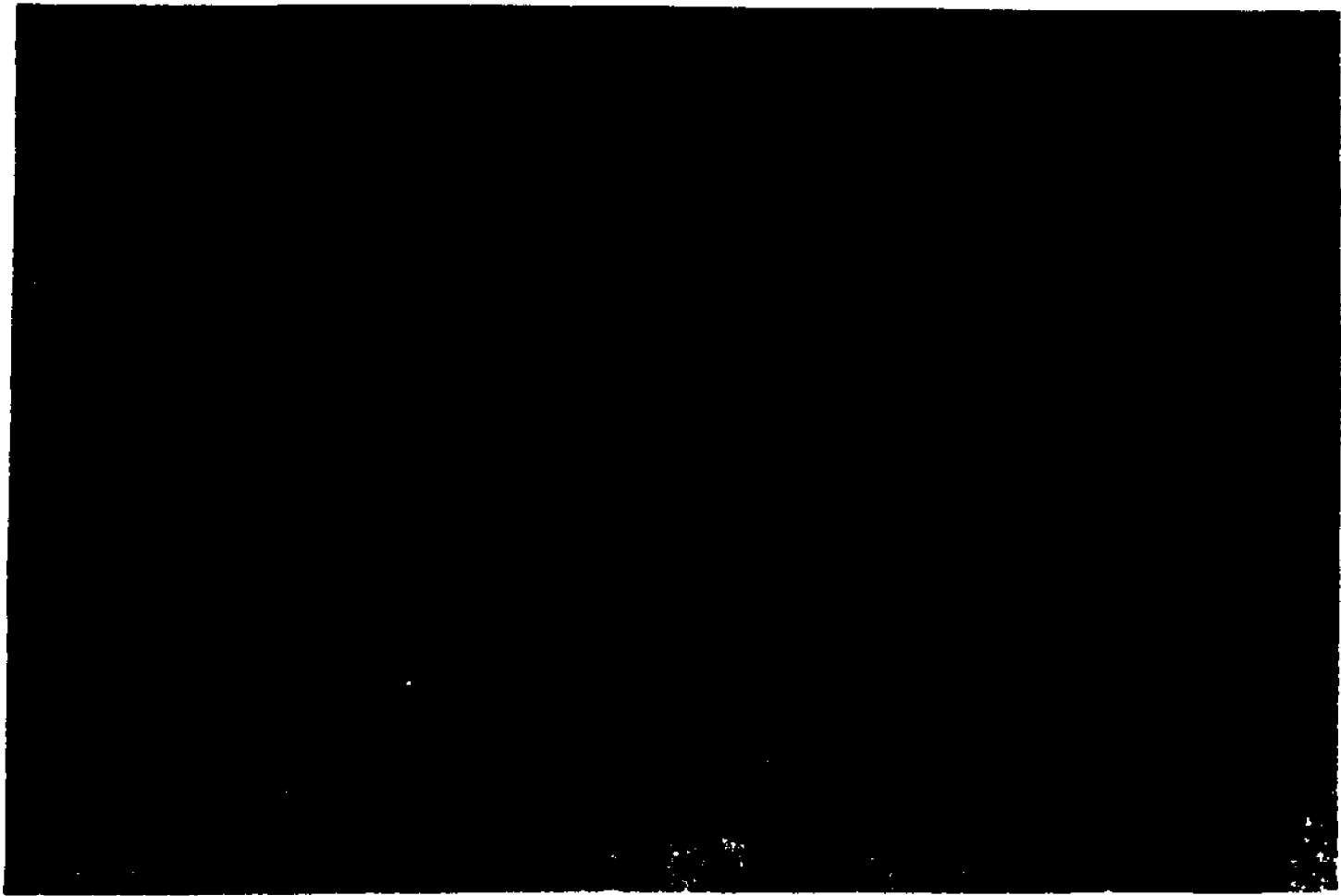


Fig. 20. Electron micrograph of negatively stained toad bladder actin-like protein purified by DEAE-cellulose and one cycle of polymerization. Beaded filaments (arrows) have the diameter and appearance of actin (arrows).

Thick-bipolar filaments appear myosin-like (*) x 136,500

comprising the actin filament. Material that copurifies with toad bladder actin-like protein is also present in this electron micrograph. Much of the material contaminating this sample has the appearance characteristic of myosin filaments.

Attempts to decorate toad bladder actin-like protein prepared by this method resulted in no discernible binding. The possible reasons for failure to decorate this actin preparation will be presented in the Discussion. A further attempt at HMM decoration was made with material that had been further purified by gel filtration.

Aliquots of both peaks eluted from the Sephadex column were subjected to polymerization in preparation for electron microscopy. Electron micrographs of these samples are shown in Figures 21 through 23. A micrograph from Peak I is presented in Figure 21. This material formed very few filaments; the majority of the protein in the sample seemed to have no obvious morphologic characteristics. No changes in the morphology of this sample was observed after treatment with HMM.

Figure 22 depicts polymerized material formed from Peak II of the gel filtration column. Actin-like filaments can be seen which are similar to those described above, that were formed from samples taken prior to Sephadex chromatography. No myosin-like filaments were observed in this preparation.

Figure 23 shows the result of incubating samples from Peak II with HMM. No 50-70 A filaments are now visible and the sample has taken on the appearance of a filamentous network. No discernible arrowhead figures with quantifiable

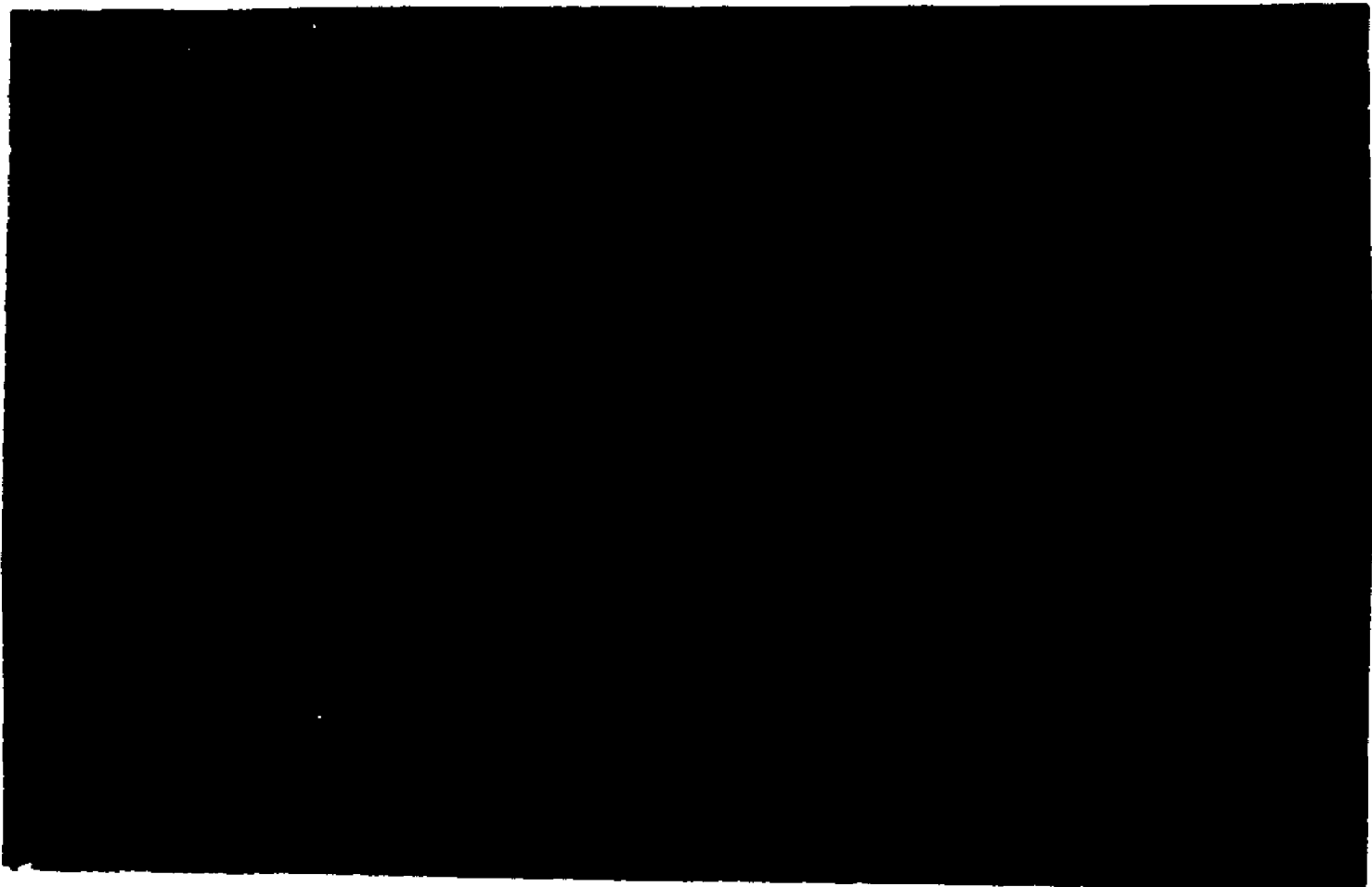


Fig. 21. Electron micrograph of Peak I from G-150 Sephadex column after exposure to polymerizing conditions. Few filaments are apparent; SDS gels of this peak show little 45,000 dalton material. Only aggregated globs appear to be present. x 139,600

Figures 22 and 23

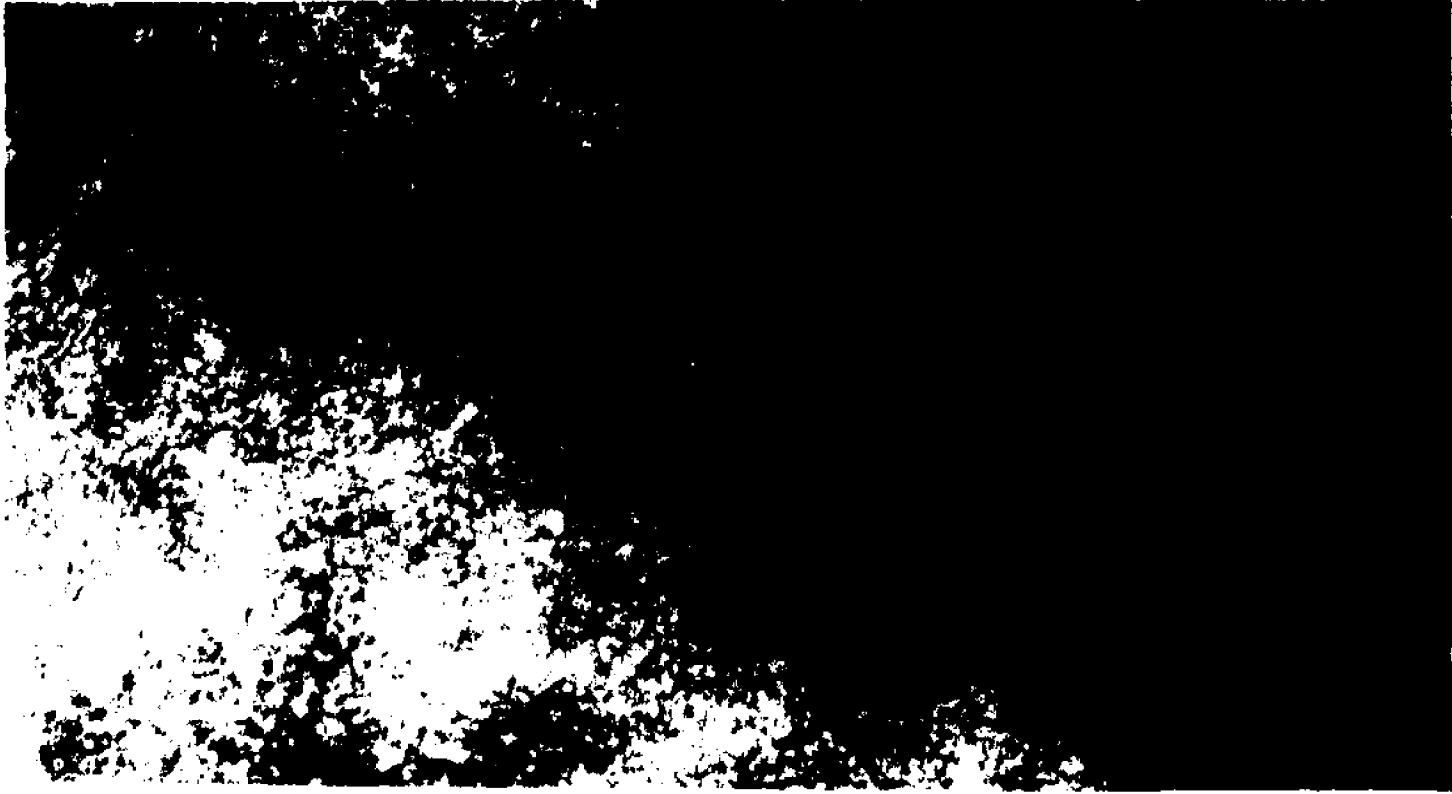


Fig. 22. Electron micrograph of negatively stained preparation of Peak II from G-150 Sephadex after exposure to polymerizing medium. A fine network of negatively stained filaments with the appearance of actin is visible. Few other structures are apparent in this micrograph. x 139,600

Fig. 23. Same as in Fig. 22 but treated with HMM. Note the thickened appearance of the filament networks through which individual actin-like filaments can sometimes be observed. x 139,600

dimensions are observed, although it is clear that HMM-treatment has had some effect on this material.

Estimates of Actin Content and Yields

The content of actin in nonmuscle cells has been estimated at between 5 and 10% of the total cell protein (144). Estimates of the actin content of toad bladder epithelial cells were made using data obtained from SDS gels. Densitometric tracings were made of initial high-speed supernatants prepared during extraction of actin-like protein by the method of Gordon (48). Xerox copies of the scans were cut out and weighed on a Mettler balance. The weight of the actin band was divided by the weight of the entire cut out scan, and this figure was normalized to the fraction of total protein contained in the supernatant fraction. Measurements made from two separate extractions gave figures of 10 and 12%, respectively, for the proportion of total protein represented by the 45,000 dalton component.

These figures were used to construct a table of theoretical and observed yields for the various extraction methods used (Table 6, see p. 94 for legend).

Table 6. Theoretical and Observed Yields of Actin-like Protein

Extraction Method	High-Speed Sup. Total Protein (mg)	Final Protein (mg)	% Yield Protein	% Yield Actin (if pure)*
Modified Hartwig	23.0	0.4	2	17 ⁺
Acetone	7.2	0.06	0.83	11 ⁺
DEAE 1	27.3	0.18	0.66	15 ⁺
2	22.1	0.31	1.4	14 ⁺
3	38.0	1.2	4.1	31 ⁺
DEAE + G-150	34.4	0.1 ⁺⁺	0.29	2.9

- * Theoretical 100% yield of actin-like protein was estimated assuming actin accounts for 10% of the protein present in the high-speed supernatant.
- + Actual yield of actin was really much lower than this due to the large number of other proteins contaminating the final sample.
- ++ The loss of 43,000 dalton protein occurred during chromatography on G-150 Sephadex, because of the difficulties encountered in quantitatively recovering the already tiny volume of sample applied.

III. In Situ Labeling of Actin Filaments with Heavy Meromyosin

To determine unequivocally whether actin was present in toad bladder epithelial cells, the method of in situ labeling of actin with heavy meromyosin (HMM) was employed. The procedure for glycerination of tissue and subsequent incubation with HMM was developed by Huxley using muscle tissue (65) and modified by Ishikawa et al., who extended the technique to demonstrate actin filaments in nonmuscle cells (66).

Isolated toad bladders were incubated in graded glycerols and exposed to HMM. In control experiments, either HMM was omitted or 6 mM neutralized ATP was included in the HMM incubation mixture. The details of this procedure are described in Methods. Bladder segments were then fixed in glutaraldehyde containing 0.2 % tannic acid. (Inclusion of tannic acid in the primary fixative has been shown by Begg et al. (10) to enhance the photographic appearance of arrowheads formed by the interaction of actin with HMM.) The samples were subsequently embedded in Epon and thin sections of both epithelial cells and smooth muscle were then examined by transmission electron

microscopy.

The morphologic fine structure of the intact toad urinary bladder has been described (19, 24, 109). Fig 24 is a transmission electron micrograph of a thin section of a typical intact bladder preparation. A layer of epithelial cells faces the lumen of the bladder, and is separated at its basal surface from supporting tissues by a basement membrane. These structures rest upon a submucosa in which collagen fibrils and an occasional fibroblast can be seen. A layer of smooth muscle cells underlies the collagen layer, which is covered, at the serosal surface of the bladder, by an incomplete layer of mesothelium (not shown).

In this micrograph, three types of epithelial cells can be seen. Granular (G) cells, which account for 80-90% of the cells in the epithelium, contact both the lumen and the basement membrane, and can be identified by their numerous short microvilli and by the electron-dense, membrane-limited granules at their apical surface. Mitochondria-rich cells make up 5-10% of the cells in the epithelium (24, 109) and are identified by the long, finger-like microvilli at their apical surface and numerous mitochondria that in some sections have an elongated appearance. This cell type also spans the entire epithelium, having its basal surface abutting the basement membrane. In contrast, basal epithelial cells do not contact the bladder lumen but lie between the basement membrane and other epithelial cells. Typically, basal cells have long or multi-lobed nuclei which occupy a large proportion of the cell cytoplasm.

Figure 24



Figure 25



Fig. 24. Transmission electron micrograph of section of normal toad bladder. The epithelium shows granular cells (G) containing numerous electron-dense granules (arrow), mitochondria-rich cells (M) and basal cells (B). Collagen (Co) separates the epithelial basement membrane from the smooth muscle layer (S). x 9,500

All micrographs are of thin sections stained with uranyl acetate and lead citrate as described in Methods.

Fig. 25. Electron micrograph of apical region from section of granular epithelial cell. The microvilli and apical cortical region contain a dense microfilament network (mf). Membrane-limited granules (G) and a microtubule segment (mt) are located in the apical cytoplasm, as are vesicles of rough (rE) and smooth (sE) reticulum, and free ribosomes. A junctional complex consisting of a zonula occludens (zo) and part of a macula adherens (ma) are also visible; bundles of 100 Å filaments (arrows) also occur in the apical cytoplasm. x 57,500

Results of HMM Labeling of Epithelial Cells

The Granular Cell

Figure 25 is a high power electron micrograph of the apical region of a granular epithelial cell (from an untreated bladder). The apical surface of the cell shows the characteristically webbed appearance of the microvilli. Subtending this surface is a microfilamentous network having a fuzzy appearance that consists of apparently randomly oriented (or in some sections, oriented) filaments. Measurements made on oriented filaments have demonstrated their diameter to be 50-70 A, similar to that described for actin filaments. In the subjacent cytoplasm are prominent 100 A filaments. (In other epithelial cells, such filaments have been identified as prekeratin (45).) A microtubule segment that courses through the apical cytoplasm has one end embedded in the apical subplasmalemmal region (terminal web).

Underneath, and embedded in, the cortical microfilament network, are the membrane-limited granules (for which the cell is named) and also various types of unidentified vesicles. Some of the latter may constitute cisternae of smooth endoplasmic reticulum, and others may be endocytic vesicles (99). Occasional mitochondria are also present in the apical cytoplasm, as well as cisternae of rough and smooth endoplasmic reticulum, and numerous free ribosomes.

The apical region of a granular cell from a glycerinated control toad bladder preparation is shown in Figure 26. Extensive disruption of the normal morphology has occurred, but the apical membrane with its cortical filamentous layer is still clearly identifiable, and appears to be continuous with the

Figure 26



Figure 27



Fig. 26. Apical region of a glycerinated control granular epithelial cell. Microvilli (mV) contain electron-dense filamentous material (f), and the apical surface is covered by the glycocalyx (g). Numerous vesiculated structures and 100 A filaments (arrows) are present in the apical cytoplasm.
x 57,500

Fig. 27. Apical region of a glycerinated granular cell treated with HMM and ATP (as control for HMM). Vesiculated organelles appear embedded in a network of 100 A filaments (arrows) and lightly stained 50-70 A filaments with the beaded structure of actin (*). Some vesicles appear to have attached ribosomes (R) and may thus represent rough endoplasmic reticulum.
x 114,000

microvillus core. The microvilli are thrown into folds (plicae), and in this micrograph, the glycocalyx surrounding the apical membrane has been well preserved. It may be noted that the morphologic appearance of the glycocalyx differs from that of the fine filamentous fuzz composing the subplasmalemmal microfilament network. Numerous unidentifiable granules and vesicles are present in the cytoplasm and appear to be enmeshed in a prominent network of randomly oriented 100 A filaments.

Figure 27 is a higher power micrograph of the apical region of a granular cell from a control preparation treated with glycerol and with HMM in the presence of 6 mM ATP. Numerous granular and vesicular organelles are again visible and appear to be embedded in the cytoskeletal matrix, as in the glycerinated control shown in Figure 26. Close observation of this high power micrograph reveals that two types of filaments are present. The darkly stained 100 A filaments, which appear both individually and in randomly oriented bundles, criss-cross the entire field. Upon close inspection, a second class of filaments, having a diameter about one-half that of the 100 A filaments, i. e., 50 A can be observed. These filaments do not stain as darkly as the 100 A filaments. This figure reveals that these filaments with a diameter of between 50 and 70 A are beaded. They are seen to form an interconnecting network with the 100 A filaments and other organelles in this control micrograph.

The effects of HMM incubation of glycerinated toad bladders are shown in the micrographs of granular cells presented in Figures 28 through 30. Figure 28 is the apical region of a granular cell from a glycerinated bladder treated with HMM in which the luminal surface is

Figure 28



Figure 28 A and B



Fig. 28 A. Apical region of glycerinated granular cell treated with HMM.

Cortical actin microfilaments form a decorated network. Arrowhead-decorated filaments are associated with the microvilli, and apical membrane (arrows) and with cytoplasmic membrane-limited organelles (starred). 100 A filaments do not bind HMM. x 57,500

Fig. 28 B. shows decorated microvillus and associated terminal web region at higher magnification. HMM-decorated actin filament network is clearly visible in the microvillus core and associated with the apical membrane. x 115,000

Fig. 28 C. shows starred area at higher magnification. Arrowhead-decorated filaments are associated with the membrane surrounding a cytoplasmic organelle. x 115,000.

visible. Numerous cytoplasmic granules and vesicles are also seen. The microvilli and subplasmalemmal regions contain randomly oriented arrowhead-decorated filaments characteristic of the acto-HMM interaction. These structures are prominent in the microvillus cores and apparently extend from the membrane into the apical cytoplasm. The presence of acto-HMM arrowheads in this preparation can be viewed to better advantage in Figures 28 B and C. Figure 28 B shows a high power view of a sheared microvillus and the subplasmalemmal cortical region; decorated microfilaments appear to be associated with the microvillus membrane and to form a latticework within the microvillus core. In cases where the orientation of the decorated filaments can be discerned, rows of arrowheads originating from the membrane can be observed pointing either away from or toward the interior of the microvillus. The association of actin microfilaments with organelles is depicted in Figure 28 C.

This figure also shows the arrowhead-decorated microfilaments which make up a large proportion of the cytoplasm in the apical subplasmalemmal (terminal web) region. In this micrograph (Figure 28) it is not possible to distinguish with certainty the orientation of these cytoplasmic HMM-decorated filaments. However, it is clear that these filaments form a fibrous latticework in the cytoplasm, surrounding granules and vesicles present in the area of the epithelial cell. It is noteworthy that 100 A filaments are present in the subcortical cytoplasm but are not decorated with HMM.

A similar situation exists in the granular cell shown in Figure 29. This micrograph shows the basolateral surface of a granular epithelial cells. Arrow-

Figure 29



Figure 30



Fig. 29. Basolateral surface of a glycerinated granular epithelial cell treated with HMM. The nucleus and interdigitated area of a neighboring cell (T) are visible. Decorated actin filaments course beneath the membrane to which they occasionally appear to be attached (arrows). Directions of individual arrowheads can be discerned. x 114,000.

Fig. 30. Apical surface of a granular epithelial cell treated with HMM. Underlying the bladder lumen (L) in the apical cytoplasm, a network of HMM-decorated actin filaments (F) is associated with a membrane-limited electron-dense granular structure. x 114,000

head-decorated filaments course beneath the membrane and appear in close association with the membrane in certain areas. Decorated actin filaments also appear to be associated with the membranes limiting cytoplasmic organelles. In this micrograph the specific orientation of the decorated filaments can be determined. Filaments with rows of arrowheads pointing in various directions can be observed. However, all the arrowheads of a single filament always have the same orientation, as is characteristic of HMM-decorated preparations of actin filaments from all cell types (65, 66, 94).

The association of actin filaments with organelle membranes is again apparent in Figure 30. Underlying the apical plasma membrane of this granular cell treated with HMM is a granule surrounded by a network of arrowhead-decorated actin filaments. 100 A filaments are also prominent in this micrograph but do not decorate with HMM.

Other Epithelial Cells

HMM-decorated filaments were observed in all types of toad bladder epithelial cells. However, the glycerination procedure to which the bladders were subjected resulted in too extensive a disruption of cellular elements to allow detailed characterization of the microfilaments in cells other than the granular cells.

Mitochondria-Rich Cell

Figure 31 is a micrograph showing the normal morphology of the apical region of a mitochondria-rich (MR) cell. The microvilli are longer than those of the granular cell, but their cores have a similar finely filamentous appearance. The apical boundary of this cell is highly irregular; the terminal web area contains numerous vesicles of varying sizes. Few 100 A filaments are visible.

Figure 31

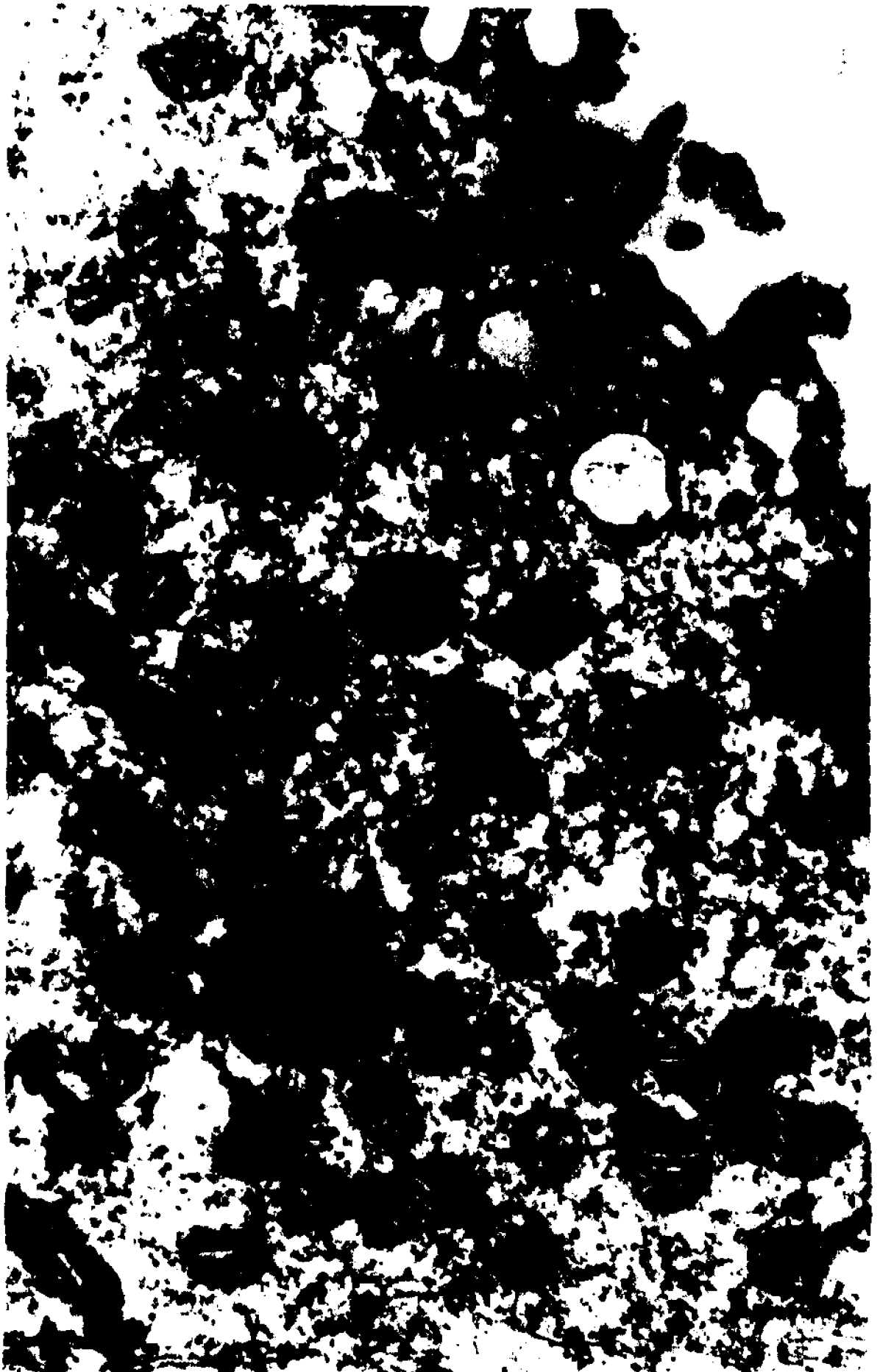


Fig. 31. Normal morphology of an untreated MR cell. The apical surface consists of numerous microvilli and vesicles (V). Microtubule segments (arrows) are embedded in the apical microfilamentous matrix. In the cytoplasm, mitochondria (M) have been sectioned along both transverse and longitudinal axes. A centriole (C) and electron-dense granules (G) are also present, along with ribosomes (R). The basolateral membrane is interdigitated with that of a neighboring cell, rich in 100 A filaments. A desmosome (ma) occurs in this region. x 57,500

The central cytoplasm, contains abundant mitochondria that appear to be embedded in a filamentous matrix.

After the glycerination procedure, an occasional MR cell can be tentatively identified. Figure 32 A shows the apical region of such a cell (identified by its narrow luminal border, typical of this cell type). The microvillar region of this cell has been disrupted by the glycerol treatment, but the junctional complexes by which it is attached to neighboring cells are clearly visible. The apical membrane appears to have billowed out, forming, as it were, a giant microvillus. The apical cytoplasm contains a network of decorated filaments, which appear to be attached to the plasma membrane in some areas. Some decorated filaments also are associated with the tight junction. Figure 32 B shows this area at higher magnification. HMM-decorated filaments are clearly demonstrated with the periodic arrowhead structure characteristic of the acto-HMM interaction. Where they are attached to the membrane, these filaments seem to point away from the surface.

Figure 33 shows a central area of the same epithelial cell. The heavily vesiculated cytoplasm appears to contain a similar HMM-decorated filamentous network.

Basal Cells

The normal morphological appearance of a basal epithelial cell is demonstrated by the micrograph in Figure 34. This cell overlies the basement membrane of the epithelium, but unlike the granular or mitochondria-rich cell, does not contact the luminal surface. Its apical aspect instead forms an interdigitated

Figure 32 A



Figure 32 B



Figure 33



Fig. 32 A. Apical region of a tentatively identified MR cell treated with glycerol and HMM. The apical cytoplasm appears to consist almost entirely of a network of HMM-decorated filaments forming a latticework attached in some places to the plasma membrane. A few undecorated 100 A filaments are also visible in the apical cytoplasm (F). Decorated filaments appear to be associated with the zonula occludens (zo). x 57, 500

Fig. 32 B shows apical region at higher magnification. HMM-decorated filaments are associated with the plasma membrane. Arrows point to the direction of filament decoration. x 115, 000

Fig. 33. Central cytoplasm of same (?) MR cell decorated with HMM. Network of decorated actin filaments (F) appears to be associated with vesiculated organelles. Other 100 A filaments (arrows) do not decorate with HMM.
x 115, 000

Figure 34



Figure 35



Fig. 34. Normal morphology of a basal epithelial cell. The apical surface (A) is interdigitated with the basolateral membrane of a neighboring epithelial cell; the basal surface rests on the basement membrane (B). The cytoplasm surrounding the prominent nucleus (N) contains 100 A filaments cut in longitudinal (L), and transverse (T) and oblique (O) sections. Numerous vesicles (V), including a coated vesicle (arrow) are apparent in the basal cytoplasm. The perinuclear cytoplasm has a granular appearance and contains many free ribosomes. x 57, 500

Fig. 35. Portion of a basal cell treated with glycerol and HMM. This cell was relatively well preserved, although its apical surface has detached from the neighboring granular cell. Prominent 100 A filaments are seen in the cytoplasm which do not decorate with HMM. The perinuclear region contains a lattice of HMM-decorated actin filaments (F). x 57, 500

structure with the membranes of other epithelial cells (24). The nucleus is prominent and elongated, and appears to occupy a large proportion of the cell volume. The cytoplasm is characterized by a granular matrix in which bundles of 100 A filaments can be observed cut in longitudinal, oblique, and cross sections. These do not decorate with HMM. Occasional mitochondria occupy the perinuclear region. Vesicles including coated vesicles are abundant in the area of the basal plasma membrane. These are believed to be formed by pinocytic events at this surface (99).

A portion of a basal cell from a bladder treated with glycerol and HMM is shown in Figure 35. An extensive array of 100 A filaments within this cell is clearly demonstrated and occupies much of the cell cytoplasm. These filaments do not decorate with HMM. However, the perinuclear region now contains a prominent network of HMM-decorated filaments, which again form a latticework arrangement. Arrays of such decorated filaments were repeatedly observed in basal epithelial cells of HMM-treated toad bladders.

Smooth Muscle Cells

Because glycerination and HMM-treatment were performed on whole toad bladders, it was possible to use the results of HMM interaction with the bladder smooth muscle as an internal control.

Figure 36 shows an area of smooth muscle from a toad bladder not exposed to glycerol. The dense packing of the muscle filaments demonstrates the normal morphology of this cell type.

Figure 37 shows the morphology of a control preparation treated with

Figure 36

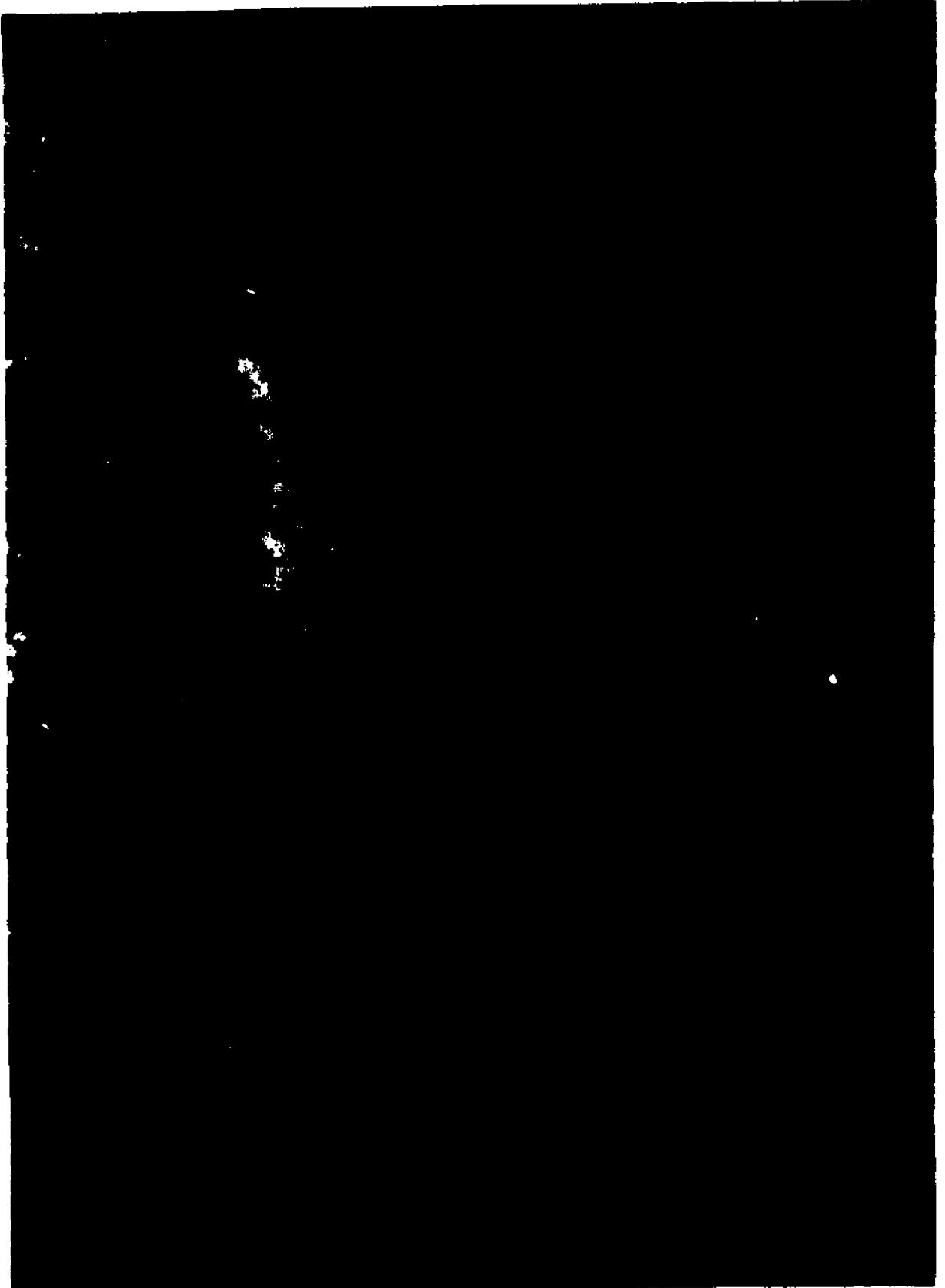


Figure 37



Figure 38 A



Figure 38 B

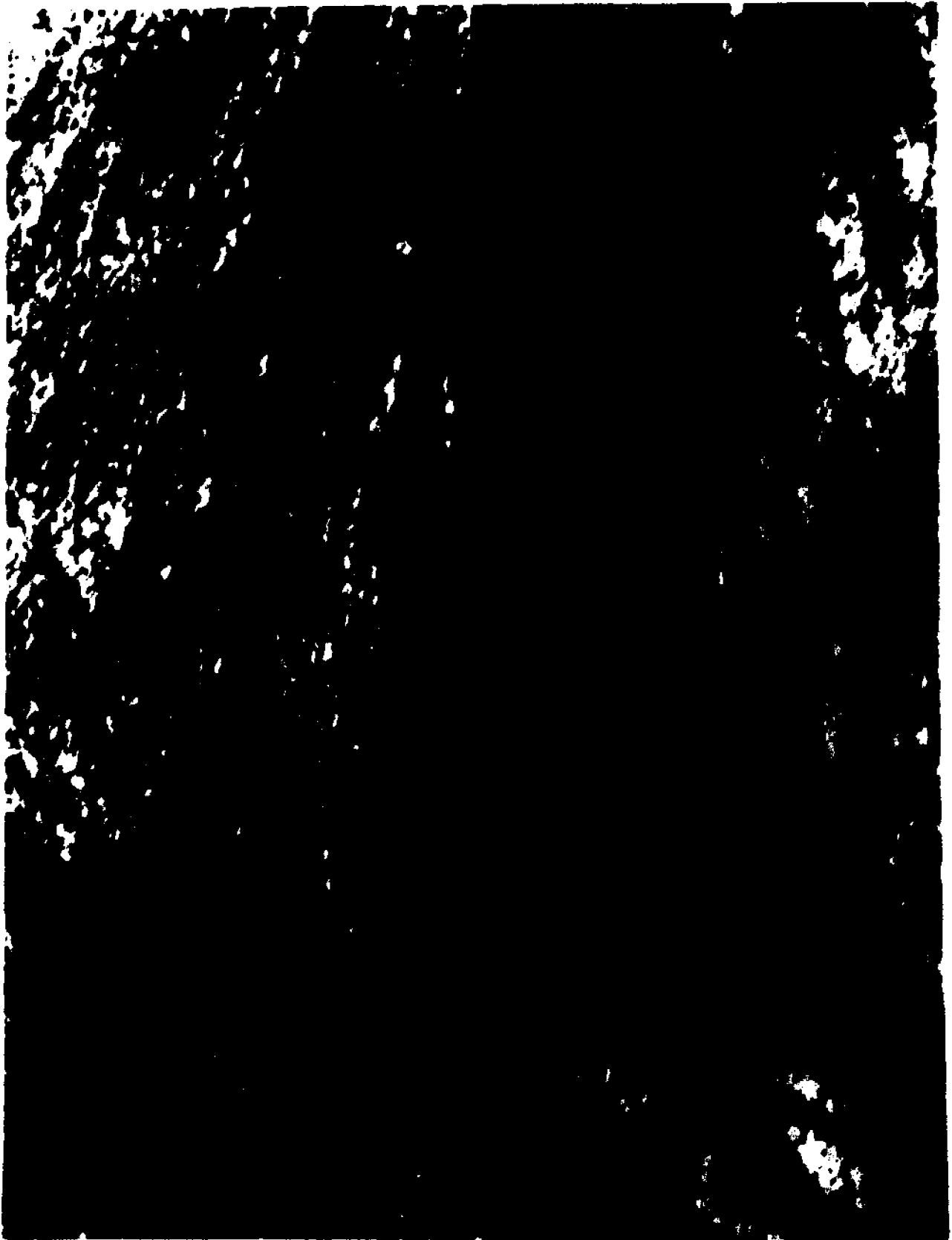


Fig. 36. Normal morphology of bladder smooth muscle. The cytoplasm is densely filamentous, and the muscle filaments have been cut in transverse (T) and oblique (O) sections. x 57,500.

Fig. 37. Morphology of glycerinated bladder smooth muscle treated with HMM and 6 mM ATP (as HMM control). The cytoplasm is much less dense than in the usual EM preparation, as a result of the glycerol treatment. Muscle filaments have been well preserved, and are cut mainly in longitudinal sections. x 57,500

Fig. 38. Bladder smooth muscle treated with glycerol and HMM. The density of the cytoplasm has been enhanced by HMM binding to the actin filaments.

A. Micrograph at magnification comparable to those of Figs. 36 and 37. showing rows of decorated filaments (F). Bundles of collagen (C) have been sectioned transversely. x 57,500

B. High power micrograph of decorated smooth muscle. The arrowhead-decorated filaments are prominently demonstrated, occupying the entire field. x 178,000

HMM and 6 mM ATP. Much of the normal structure is disrupted by the glycerol treatment. However, the muscle filaments have been reasonably well preserved. No HMM decoration is visible in this control micrograph.

Figure 38 A shows a similar preparation of toad bladder smooth muscle treated with HMM in the absence of ATP. The cytoplasm has become much more dense, due to the binding of HMM to the muscle actin filaments. The rows of arrowhead-decorated filaments can be seen to better advantage in the higher power micrograph in Figure 38 B.

Dimensions of Toad Bladder Acto-HMM

The periodicity of the binding of HMM to actin filaments in epithelial cells was measured, and the results are presented in Table 7. The head-to-head spacing of the myosin fragments was found to occur with a periodicity of 342 ± 8.27 A, and the width of the decorated filaments was 270 ± 8.71 A. Both of these estimates are in good agreement with published values for the dimensions of decorated filaments of both muscle and nonmuscle origins (10, 65). There was no difference in the dimensions of decorated filaments from smooth muscle cells when they were compared with those of epithelial origin.

Table 7. Filament Periodicity and Width of Toad Bladder Epithelial Cell Acto-HMM

<u>Filament</u>	<u>Arrowhead Periodicity, A</u>	<u>Arrowhead Width, A</u>	
1	311	278	
2	311	244	
3	289	200	
4	344	278	
5	356	311	
6	333	278	Periodicity
7	356	289	X=342±8.27 A
8	356	289	
9	356	300	Width
10	388	256	X=270±8.71 A
11	377	278	
12	333	244	

Measurements were made on glycerinated bladders treated with HMM. All measurements were taken from micrographs at a magnification of 90,000, using a micrometer loupe with 0.1 mm divisions.

DISCUSSION

The studies described herein have demonstrated that dihydrocytochalasin B inhibits vasopressin-stimulated water movement in toad urinary bladder and that the contractile protein, actin, is present in the bladder epithelial cells. In view of recent data on the specificity of the interaction between cytochalasins and actin, these data suggest that toad bladder epithelial cell actin plays a functional role in the hormone-induced increase in water permeability.

I. Functional Studies with Dihydrocytochalasin B.

The present series of studies indicates that H₂CB is as effective as CB in inhibiting the hydrosmotic response to vasopressin in the toad bladder. At concentrations of 5 $\mu\text{g}/\text{ml}$ and 10 $\mu\text{g}/\text{ml}$ (10.6 and 21.2 μM), H₂CB reduced hormone-stimulated water flow by 21 and 43%, respectively. These values correspond closely to those obtained by Taylor et al. (132) for inhibition of the response to vasopressin by CB in the toad bladder. Since it is known that H₂CB does not affect hexose transport (86), these findings demonstrate that inhibition of vasopressin-induced water movement by these macrolide antibiotics can not be mediated through binding sites similar to those described in studies of the inhibition of hexose transport by cytochalasin B.

The results of the functional studies with H₂CB essentially paralleled those previously described for the effect of CB in the anuran bladder (19, 29, 33, 130, 132). In the small sample studied (n=3), H₂CB at 5 $\mu\text{g}/\text{ml}$ did not significantly increase basal water movement beyond the slight increase in this parameter induced in paired controls by DMSO alone; however, at the higher

concentration used (10 $\mu\text{g}/\text{ml}$) a trend toward increased basal water flow was noted.

Upon treatment with vasopressin, the hemibladders incubated in H_2CB showed a progressive increase in the osmolality of their mucosal solutions. A similar observation was also noted by Taylor et al. (130, 132). Such a leakage of ions into the mucosal bathing medium, and hence reduction in the osmotic gradient, may, in part, account for the discrepancy in published values of the effectiveness of CB in inhibiting the vasopressin response (see Introduction). If incubation of bladders in CB resulted in a quantitatively similar amount of ionic leakage into the mucosal solution in the studies reported by DeSousa et al. (33), then the effective osmotic gradient during the vasopressin response would also have been diminished. Since no correction was made in DeSousa's studies for loss of the osmotic driving force, the inhibitory effectiveness of CB would have been overestimated.

The results of the present studies with H_2CB suggest that actin-related binding sites are involved in cytochalasin inhibition of vasopressin-stimulated water flow. Available evidence on the inhibition of cell motility by cytochalasins has led to the hypothesis that these drugs interfere with actin in nonmuscle cells. Difficulties in interpreting data with cytochalasin B have stemmed from the fact that until recently, a direct effect of cytochalasin B upon actin had not been satisfactorily demonstrated. However, recently, a group of elegant studies on the interaction of nonmuscle actin with cytochalasins by Lin et al (88, 89), and others (16, 17), has begun to shed some light on the specific binding properties of the cytochalasins.

The development of H₂CB permitted Lin and coworkers to isolate and characterize actin-related cytochalasin binding sites in extracts of human erythrocyte ghosts (88, 89) and bovine brain (44). A high molecular weight complex was isolated from extracts of erythrocyte ghosts. This complex contained actin, spectrin, and other minor components, including two polypeptides with the electrophoretic mobility of erythrocyte band 4.1. The complex bound CB and H₂CB in the submicromolar range (89), and this binding was unaffected in the presence of glucose. When this material was added to a low salt solution of monomeric (G) actin, the viscosity of the solution increased, and electron microscopy of the negatively stained solution revealed the presence of (F) actin filaments, i. e., the complex induced polymerization. The high molecular weight complex appeared to participate only in the initiation of actin polymerization, since less than 1 μg of complex converted 0.4 mg of G actin to the filamentous form. An increase in the complex to actin ratio resulted only in an increase of the rate at which the actin polymerized; the final extent of polymerization remained unchanged. The ability of this complex to initiate polymerization was blocked in the presence of cytochalasins. Binding studies performed with the mixture showed that the cytochalasin-binding complex became associated with the actin during polymerization. Furthermore, it was shown that polymerization in the presence of cytochalasin B, C, E or dihydrocytochalasin B was inhibited to the relative extent of each of these congener's capability to impair cell motility-related functions. Thus, it appeared that cytochalasins specifically inhibited polymerization of actin initiated by this membrane-bound complex. These authors therefore suggested that the mem-

brane-associated cytochalasin binding complex may mediate some or all of the effects of these drugs upon motility-related functions.

The data of Lin and coworkers have now been confirmed and extended in recent studies by Brenner and Korn (16). These investigators isolated a similar spectrin-actin complex from sheep erythrocyte membranes, and showed that the complex, composed only of these two proteins, was sufficient to nucleate actin polymerization in low ionic strength medium. Polymerization of G actin by the spectrin-actin complex was inhibited by substoichiometric concentrations of cytochalasin D, in a manner similar to that described by Lin et al. Interestingly, the polymerization of actin by this complex was also inhibited in the presence of the actin-binding protein, profilin (16). These authors have now suggested that actin polymerization occurs by a treadmill process similar to that described by Margolis and Wilson (96) for microtubules, and that cytochalasins inhibit actin polymerization by binding to the polymerizing end of the actin filament. These results have been further substantiated by work of Brown and Spudich (17), who found that actin polymerization was blocked in the presence of submicromolar concentrations of cytochalasin D. Taken together, these studies therefore conclusively demonstrate a specific interaction between actin filaments and cytochalasin. (For a recent review, see Bray (15)).

In the light of these recent studies on the specific effect of cytochalasins on actin polymerization, the results of studies with CB in the toad bladder can be reassessed. The experiments with H₂CB described here, permit the conclusion that inhibition of the vasopressin response by the cytochalasins

is dependent upon their interaction with actin.

II. Biochemical Studies

Isolation of Actin-like Protein

The biochemical studies described above revealed that isolated epithelial cells of the toad urinary bladder contain a low ionic strength soluble species with the electrophoretic mobility of rabbit muscle actin, which accounts for about 10 percent of the soluble protein of these cells.

Attempts at further purification of this putative actin-like protein using methods which required that it polymerize from either low ionic strength extracts or from an acetone powder did not give any appreciable enrichment (as would have been expected of muscle actin incubated under these conditions). Inspection of SDS gels of samples prepared both by the method of Hartwig and Stossel (55), and after acetone extraction (129, 150), revealed that several other molecular weight species copurified with the 45,000 dalton band (Figs. 11, 13). There is a growing literature on the presence, in nonmuscle cells, of an unpolymerizable form of actin that is complexed with other (?actin-binding) proteins (20, 55, 70, 95, 135). Thus, it seemed likely that failure to polymerize the protein prepared by these methods may have occurred because of the presence of one of the copurifying species.

The method of Gordon et al. (48) was therefore employed in an attempt to separate an actin-containing fraction free of possible binding proteins, prior to the polymerization. This procedure afforded considerable enrichment of the toad bladder actin-like protein before polymerization.

During an average experiment, about 30 ± 4 mg of high speed supernatant was applied to the DEAE column, and 6.4 ± 2 mg (21%) was recovered in the pooled fractions containing the 45,000 dalton band. When the pooled fractions containing the 45,000 dalton protein were subsequently incubated in polymerizing medium, between 15 and 20% of the protein recovered from DEAE-cellulose became sedimentable. This represented a much higher yield of toad bladder actin-like protein than with either of the other two methods used. Presumably, therefore, some inhibitor of polymerization was released from the ion exchange column at low ionic strength, and came off in the early peaks (Figs. 15B, 16), whereas the actin-like protein was retained until the column was eluted with high ionic strength buffer (0.19 - 0.24 M KCl, Fig. 15B). These results closely paralleled those obtained by Gordon et al. (48) for DEAE-cellulose chromatography of Acanthamoeba actin. Thus, these workers recovered 15% of the protein applied to the DEAE column in the actin-containing fractions, of which 27% was again recovered after one cycle of polymerization. That the entire extraction procedure proved extremely successful in purifying toad bladder actin-like protein is clear from the SDS gel pattern of protein recovered using this method (Figs. 17, 18).

The actin-like protein thus isolated formed filaments after incubation of the purified protein in polymerizing medium. The diameter of the filaments was 50-70 A, the same as that reported for actins isolated from a variety of nonmuscle sources (115). The filaments were composed of elements having a beaded appearance; in muscle actin, this morphology is said to arise from

the association of the globular monomers in forming the filamentous structure (65). The individual beads occurred about every 50 A, close to the value of 55 A reported by Huxley (65) for the spacing of monomers in filaments polymerized from isolated rabbit muscle actin.

When this fraction was incubated with heavy meromyosin prepared from rabbit muscle, no arrowhead-labeled figures could be discerned upon electron microscope observation of negatively stained samples. However, this result was not surprising, since the actin-like protein had not been purified to homogeneity.

Further purification of the toad bladder actin-like protein using column chromatography on G-150 Sephadex was therefore attempted. This gel filtration step was employed in the method of Gordon et al. (48) in order to remove high molecular weight contaminants from the actin. The toad bladder sample was applied to a 0.9 x 15 cm Sephadex column after one cycle of polymerization. Protein eluted in two major peaks; a sharp peak migrated with the excluded volume of the column, and a second, broader peak eluted at the same position as monomeric rabbit muscle actin. These results correspond well to those obtained by Gordon et al. (48) and others (3), in that the actin-like protein eluted from the column as a broad, slowly rising peak which then rapidly declined. Only about 60% of the protein applied to the column was recovered in these two peaks; however, only 0.8 ml of sample containing about 0.5 mg protein had been applied. The relatively low recovery of protein was related to the fact that the size of the column was not optimal for the small amount of sample available.

Examination of the Coomassie-Blue stained gels of both column peaks (Fig. 19) revealed relatively good separation between actin-like protein and higher molecular weight species. Three major species (in addition to a small amount of actin-like protein) were present in the fractions eluting with the void volume (peak I), having mobilities of 0.38, 0.43, and 0.54 (compared with 0.70 for actin). These represented apparent molecular weights of 107,000, 95,000 and 69,000 daltons, respectively. Gels corresponding to protein eluted in the molecular weight range of actin (Peak II) showed one major band, which comigrated with authentic rabbit muscle actin. Two minor bands were also present on these gels, and had mobilities of 0.43 and 0.49 (95,000 and 79,000 daltons). These were present in peak I in greater amount. While it is not possible to identify the proteins that eluted either with actin or from peak I, it is of interest that proteins having molecular weights of 70,000, 95,000 and 105,000 daltons have been identified in isolated preparations of intestinal brush border microvilli and are known to be closely associated with actin from this source (105).

Samples of both peaks eluted from G-150 Sephadex were dialyzed against 0.1 M KCl, 2 mM MgCl₂ and observed by electron microscopy of negatively stained grids. No actin-like filaments were observed in samples from peak I. On the other hand, electron microscopy of grids from peak II revealed filaments having the diameter and beaded appearance of actin.

Heavy meromyosin binding studies were attempted using samples from both column peaks. As expected, the protein eluting in the high molecular

weight range (peak I) showed no evidence of binding. Surprisingly, no clear evidence of arrowhead formations was visible in the sample eluting in the molecular weight range of actin (peak II) either. The failure to observe arrowhead-labeled filaments in samples from peak II is somewhat unsettling, since actins of all known origins readily bind this myosin fragment under similar experimental conditions (65, 124), and because definite binding was observed in the control samples containing a mixture of rabbit muscle actin and HMM examined at the same time. It is quite possible, however, that the acto-HMM formed from the toad bladder samples was hidden by the presence of contaminants in the toad bladder actin-like protein sample (vide supra). Any proteins copurifying with actin throughout the entire purification procedure would probably have been rather tightly bound to actin, and might therefore have obscured any arrowheads formed in these samples. Thus, either an actin-binding protein or perhaps proteolytic fragments of a myosin-like protein may have interfered with the visualization of HMM binding. It is unlikely that the binding reaction would have been altogether prevented, since the actin-like protein was present in large excess over the other molecular weight species contaminating the sample. Indeed, there was some change in the appearance of the material on the grids after incubation with HMM (cf. Figs. 22 and 23).

Unfortunately, because of the small amount of material that was recoverable in these experiments, it was not possible to attempt further biochemical characterization of the toad bladder actin-like protein. These limited results of actin purification from isolated toad bladder epithelial cells can only

show, therefore, that a protein is present within the epithelial cells that 1) has the electrophoretic mobility of actin on SDS gels; 2) has solution properties similar to actin from other nonmuscle sources, as assessed by its behavior in high and low salt media; and 3) is capable of undergoing the G - F transformation when the purified protein is incubated under conditions similar to those which transform muscle actin into filaments.

While these results do not allow one to state unequivocally that the protein which was isolated actually was actin, enough similarities exist between the protein in the purified sample and actin from skeletal muscle to suggest that the two are very similar in their molecular weight and ionic and chemical properties. Taken together with the results of purification studies of many nonmuscle actins (2, 48, 55, 56, 149), these results also demonstrate similarities in the nature of the protein isolated from toad bladder and actins isolated from a wide variety of nonmuscle sources (2, 78, 115). It is thus quite likely that this protein represents a toad bladder epithelial cell actin that is similar to actins which have been described in other nonmuscle cells.

Evidence for a Toad Bladder Myosin-like Protein

The results of purification of actin-like protein from isolated toad bladder epithelial cells indicate that other contractile proteins may also occur in these cells. Thus, in these studies, some evidence was coincidentally obtained that a myosin-like protein was present in the toad bladder fractions.

In this regard, gel electrophoresis of samples prepared by the method of Gordon et al. (48) revealed that a 200,000 dalton polypeptide

(Fig. 18) was present in the toad bladder extracts. Correspondingly, electron micrographs of the repolymerized actin-like protein after purification by chromatography on DEAE-cellulose and one cycle of polymerization revealed bipolar, myosin-like filamentous structures, in addition to F actin (Fig. 20). These data therefore indicate that a protein similar to myosin may have been present in the sample. Contamination of the sample by a myosin-like protein would also account for the inability to bind HMM to these actin-like filaments, since myosin would compete with HMM for binding sites on actin.

The presence of a myosin-like protein in toad bladder epithelial cells was further suggested from measurements of myosin ATPase activity made on an early sample of partially purified actin-like protein. A fraction containing a 45,000 dalton species prepared by the method of Hartwig et al. (55) was used in an ATPase assay to determine whether the fraction could activate the Mg-ATPase activity of muscle myosin. Unfortunately, results of simultaneous control assays revealed that this batch of myosin had lost its actin-stimulatable ATPase activity. However, samples containing either toad protein plus rabbit myosin, or toad protein alone, exhibited a small but reproducible Mg-ATPase activity, amounting to $0.02 \pm 0.002 \mu\text{M}/\text{min}/\text{mg}$ total protein. If this represented ATPase activity of an endogenous myosin contaminating the toad bladder "actin" preparation, the quantitative value of the myosin ATPase activity would have been greatly underestimated, since the myosin-like component would have represented only a minor proportion of the total protein in the sample. However, it is also possible that this activity could have arisen from a non-myosin ATPase.

Taken together, these findings are at least consistent with the hypothesis that a complete actomyosin system is present in toad bladder epithelial cells.

III. Morphological Studies: In situ Labeling with HMM

Early electron microscopic studies on toad bladder epithelial cells by Choi (24) and Peachey et al. (109) revealed that the cortical subplasmalemmal region of these cells is constituted of an array of filaments that appear randomly dispersed, with individual diameters between 50 and 70 A. In later studies, Carasso et al. (19) described both 50-70 A and 100 A microfilaments in epithelial cells of the frog urinary bladder. Such an array of cortical microfilaments is now known to be a feature common to most eukaryotic cells. In many cases, heavy meromyosin binding studies have demonstrated that the filamentous cortex is composed, in large part, of actin (10, 22, 66, 103, 121, 126). This finding has now been confirmed in the epithelial cells of the toad bladder.

Glycerin Treatment

The technique available for heavy meromyosin labeling requires that cells be made permeable to the myosin fragment. For work at the electron microscope level, this is usually accomplished by incubating tissues with glycerin prior to exposure to HMM (66). The incubation buffer used in the glycerination procedure is similar in ionic strength and composition to polymerization solutions used in the purification of actin, and should stabilize the ultrastructure of cytoskeletal elements, including polymerized actin, 100 A filaments and structures with which they may be associated, such as

membranes (26, 43, 94, 101, 136, 139) and cytoplasmic organelles (124, 148). However, glycerination renders the membranes permeable to molecules at least as large as HMM (about 150,000 daltons) and allows various cytoplasmic elements, including unpolymerized actin (18, M. Pearl, unpublished observation), and tubulin (125) to diffuse out of the cells. The combined effects of the glycerination buffer to stabilize microfilaments, while allowing loss of other cytoplasmic elements, thus enhances the visibility of 50-70 A and 100 A microfilaments in these preparations.

In glycerinated control preparations not treated with HMM, or exposed to HMM in the presence of 6 mM ATP, the toad bladder granular epithelial cells were seen to contain lightly stained filaments that measured 50 - 60 A in diameter. These filaments were often associated with darker staining filaments measuring 100 A. Clusters of actin-like and 100 A filaments were most commonly observed in peripheral areas of the cell cytoplasm. Actin-like filaments also composed the cores of the broad, ridge-like microvilli of these cells. The fingerlike projections that form the lateral interdigitations between the epithelial cells were characterized by both 50-60 A and 100 A filaments. It is noteworthy that 50-60 A filaments occurred in all types of epithelial cells. In basal cells, prominent clusters of 50-60 A filaments were observed in the perinuclear cytoplasm.

The 50 - 60 A filaments that form part of the cortical matrix of the toad bladder epithelial cells appeared to be short, branching filaments that formed polyhedral structures with other, most likely protein, components of the cytoskeleton. Such polyhedral arrays were often seen in images of sec-

tions cut tangential to the epithelial cell cortex, or in perinuclear regions of the cytoplasm. The sides of the polyhedrons appeared to be composed of actin-like filaments and 100 A filaments, while their vertices were visualized as darker staining, globular structures.

Heavy Meromyosin Decorated Bladders

Observations made on bladder tissue treated with HMM confirmed the hypothesis that the 50-60 A filaments in the epithelial cells were composed of actin. HMM-decorated filaments were identified in all types of toad bladder epithelial cells.

In granular cells, actin-containing filaments were demonstrated to occur in abundance in cortical regions of the cells. In many instances, arrowhead-decorated filaments appeared to connect the cell membranes to organelles, and to other filamentous structures within the peripheral cytoplasm. Numerous arrowhead-decorated filaments were also observed to make up a large proportion of the cytoplasm abutting the membranes of the lateral interdigitations.

It was not possible to identify the mitochondria-rich cells with complete certainty. However, those tentatively identified as such cells were extremely rich in filaments which formed a decorated latticework in both the apical and central cytoplasm. Unlike the case in the granular cell, the apical filamentous network of this cell type was remarkably devoid of 100 A filaments. Instead, the filaments of the cortical lattice appeared to be composed almost entirely of actin (Fig. 32).

Basal cells were identified according to their position in the epithelial

cell layer, by their characteristic shape, and by the presence of prominent bundles of 100 A filaments (24, 79, 109). The basal cells also contained a prominent latticework of 50 - 60 A filaments in their perinuclear region, that formed decorated arrays of arrowheads in bladders that were treated with HMM.

Comparisons with Other Studies on Toad Bladder Actin

In a recent study, Kraehenbuhl and coworkers reported that epithelial cells of the toad urinary bladder bind fluorescent anti-actin antibodies (79). Their results therefore demonstrated, at the light microscope level, that the bladder epithelial cells contain actin. In a companion study of isolated epithelial cells, separated by centrifugation on a density gradient (120), these workers provided evidence that the basal epithelial cell layer is composed of two populations of cells -- those which incorporated tritiated thymidine and were therefore true basal cells, and those which did not take up thymidine, but which contained a prominent array of 100 A filaments (microfilament-rich cells). The study by Kraehenbuhl et al. (79) further demonstrated that the great proportion of fluorescent anti-actin antibody was bound to these microfilament-rich basal cells.

The results presented here confirm, at the level of the electron microscope, the fluorescent antibody studies of Kraehenbuhl et al. (79) in that basal cells containing numerous 100 A filaments also contained actin; however, in this type of preparation it was not possible to identify two populations of basally located epithelial cells. The results of the present study differ from those of Kraehenbuhl and coworkers in that prominent arrays of actin filaments were observed in all types of bladder epithelial cells, whereas

in Kraehenbuhl's study little fluorescent antibody was bound by the mitochondria-rich or granular cells (79).

The differences between the two sets of results may have arisen from the use of different methods to solubilize the cell membranes. Both glycerin treatment and fixation for immunofluorescence staining (1:1 ethanol:ether) open cell membranes to the passage of high molecular weight polypeptides. Thus, the unpolymerized actin (as well as other soluble components) are lost from epithelial cells during their preparation. In the studies presented here, the glycerination buffer (KCl, phosphate) was designed to preserve the integrity of polymerized actin; in the fluorescent study, fixed cells were rehydrated in an unspecified phosphate-saline buffer. Thus, the discrepancy between these two studies may be due to a relatively larger loss of actin from granular and mitochondria-rich cells in the immunofluorescence study. Using this assumption, it is not surprising that these workers found a relatively greater amount of actin in the basal epithelial cells. Actin in the mitochondria-rich and granular cells appeared to be located primarily in the peripheral cytoplasm in both these studies, while that in the basal cells occurred primarily in the perinuclear region in the HMM-treated bladders. In both cases 100 A filaments appear to have been relatively well preserved. Under these conditions, if loss of unpolymerized (and depolymerized) actin were to occur by diffusion through the cell membrane, more actin would have been preferentially lost from cortical regions not protected by 100 A filaments than from central (perinuclear) areas of the cytoplasm, where actin would have been stabilized by its association with the 100 A filament protein(s).

Organization of the Microfilament Lattice

The most striking finding in these glycerination studies was the configuration of the actin filaments. Instead of the "stress fibers" characteristic of actively motile cultured cells (61, 66, 81), or the long actin fibers of muscle, the actin filaments of certain areas of the toad bladder epithelial cells were often organized into a latticework in both control and HMM-treated preparations. The filaments themselves were rather short and terminated in the cytoplasm, connected with other actin or 100 A filaments, and/or with membranes. To discover whether this phenomenon really occurred as often as was thought, a random sample of decorated filaments from four preparations was measured to obtain an estimate of the average lengths of the filaments. These data are presented in Table 8.

Table 8. Average Lengths of HMM-Decorated Filaments

Prep. No.	<u>Length of filaments, mm (x 30, 800)</u>			
1	5.2	6.3	7.8	6.8
2	11.5	6.0	8.1	9.0
3	7.0	5.0	6.1	5.5
4	5.0	9.9	8.9	7.5

The mean and standard deviation of the mean were calculated from the data. The lengths of the decorated filaments averaged 240 ± 16 nm. It seems quite unlikely that such consistency in filament length could have been caused by an artifact of sectioning, particularly when decorated smooth muscle filaments

sometimes in the same section, had the long appearance associated with actin filaments from muscle cells.

Correlations and Conclusions

The Cytoskeletal Lattice

Over the past several years, many workers have described the biochemical and morphological characteristics of cytoskeletal elements in non-muscle cells (1, 47, 115). Filamentous networks composed of actin and other proteins have been demonstrated in the cytoplasm of many kinds of cells. Together with microtubules, these nonmuscle contractile proteins play a dual role to stabilize cell shape and to form the basis of a contractile system which functions to move organelles and/or membranes within the cells. The emerging evidence from such studies suggests that the filament networks and microtubules may correspond to part of the "microtrabecular lattice", reported by Wolosowick and Porter (148), that is likely to constitute the cytoplasmic matrix (or ground substance) of all cells. According to Wolosowick and Porter (148), the lattice forms a three-dimensional network which supports the cytoplasmic organelles suspended within the matrix, and is bounded by amorphous material subjacent to the plasma membrane from which it appears to arise. In several instances, organelle movement has been demonstrated to be dependent upon the functional integrity of elements within the structural matrix (see article by Porter in ref. 47).

Microfilament-membrane Associations

There is now ample evidence demonstrating an intimate association between actin microfilaments and cell membranes in a wide variety of cell

types (47). For example, Metzels and coworkers (101) have shown that the filamentous cortex arising from the plasma membrane of the squid giant axon is composed of actin-containing filaments. In epithelial cells, Mooseker et al. (103, 105) have determined that actin filaments comprise the major proportion of protein in the cores of intestinal brush border microvilli; the filament bundles are attached to the microvillus membrane at both their apical and lateral aspects. Actin filaments are also known to be associated with lymphocyte (26, 43, 76) and choroid plexus (94) membranes.

However, it is not known whether all the actin associated with cell membranes is in a filamentous form. Recent work by Tilney and coworkers (135, 136) has demonstrated that actin associated with the membranes of certain sperm may exist in an oligomeric form, complexed with an actin-binding protein, profilin; the profil-actin complex is not competent to polymerize. (Actin has also been isolated from pancreas (95) and calf thymus and spleen (20) associated with binding proteins.) In certain functional states, the actin may be dissociated from its binding protein, the inhibitory effect upon polymerization reversed and filaments formed (135, 136). Furthermore, according to recent data of Brenner and Korn (16) such proteins are capable of inhibiting actin polymerization normally induced by the membrane-bound cytochalasin-binding complex of erythrocytes. In sum, these studies provide evidence that cell membranes may play a role in controlling membrane-associated actin polymerization in many cells.

Thus, the present findings in the toad bladder are particularly exciting in light of the recent results of Lin and coworkers (86, 88, 98) and others

(16, 17, 44). Considered together with these studies, one may conclude that toad bladder epithelial cell actin is at least present in areas where it may play a role in altering apical membrane function and thus may be of critical importance in mediating the hydrosmotic response to vasopressin. These studies in the toad bladder have therefore provided the groundwork upon which this hypothesis may be further investigated. It is tempting to speculate that vasopressin (and cAMP) may control the insertion of the intramembranous particles into the apical membrane of the granular cell by a process which locally alters actin polymerization at this site. Conceivably, this could occur through the action of a membrane-bound cytochalasin-binding complex such as that described above in erythrocytes and bovine brain (16, 17, 44, 86, 88, 89).

The data presented in this thesis show that actin is present in toad bladder epithelial cells in both polymerizable and nonpolymerizable forms and that actin filaments are associated in this tissue with the cytoplasm, membranes, and membrane-limited organelles. Taken together with the demonstration that dihydrocytochalasin B inhibits vasopressin-stimulated water transfer across the toad bladder, and that the cytochalasins interact specifically with actin (16, 17, 44, 86, 88, 89), these findings support the hypothesis that actin microfilaments play a functional role in mediating the hydrosmotic response to vasopressin.

REFERENCES

1. Adelman, M.R. 1974. The actin- and myosin-like proteins of primitive motile systems: how similar are they to their striated muscle counterparts? *Excerpta Medica*, 333, 79-102.
2. Adelman, M.R. and E.W. Taylor. 1969. Isolation of an actomyosin-like protein complex from slime mold plasmodium and the separation of the complex into actin- and myosin-like fractions. *Biochemistry*, 8: 4964-4975.
3. Adelstein, R.S., J.E. Godfrey and W.W. Kielley. 1963. G-actin: preparation by gel filtration and evidence for a double stranded structure. *Biochem. Biophys. Res. Commun.*, 12: 34-38.
4. Allison, A.C., P. Davis and S. de Petris. 1971. Role of contractile microfilaments in macrophage movement and endocytosis. *Nature (New Biol.)*, 232: 153-155.
5. Altura, B.M. 1977. Comparative cellular and pharmacologic actions of neurohypophyseal hormones on smooth muscle. *Fed. Proc.* 36: 1840-1878.
6. Andersen, B. and H.H. Ussing. 1957. Solvent drag on non-electrolytes during osmotic flow through isolated toad skin and its response to anti-diuretic hormone. *Acta Physiol. Scand.* 39: 228-239.
7. Andreoli, T.E., J.J. Grantham and F.C. Rector, Jr., eds. 1977. Disturbances in Body Fluid Osmolality, Am. Physiol. Soc. Bethesda, Md.

8. Andreoli, T.E. and J.A. Schafer. 1976. Mass transport across cell membranes. The effects of antidiuretic hormone on water and solute flows in epithelia. *Ann. Rev. Physiol.*, 39: 451-500.
9. Atlas, S.J. and S. Lin. 1978. Dihydrocytochalasin B. Biological effects and binding to 3T3 cells. *J. Cell Biol.*, 76: 360-370.
10. Begg, D.A., R. Rodenwald and L.I. Rebhun. 1978. The visualization of actin filament polarity in thin sections. Evidence for the uniform polarity of membrane-associated filaments. *J. Cell Biol.*, 79: 846-852.
11. Bentley, P.J. 1958. The effect of neurohypophyseal extracts on water transfer across the wall of the isolated urinary bladder of the toad *Bufo marinus*. *J. Endocrinol.*, 17: 201-209.
12. Bentley, P.J. 1966. The physiology of the urinary bladder of amphibia. *Biol. Rev.*, 41: 275-316.
13. Bentley, P.J. 1968. Amiloride: a potent inhibitor of sodium transport across the toad bladder. *J. Physiol. (Lond.)* 195: 317-330.
14. Bowen, W.J. 1971. Myosin ATPase and ITPase. In: *Contractile Proteins and Muscle*, K. Laki, ed., Marcel Dekker, Inc., New York, pp. 221-226.
15. Bray, D. 1979. Cytochalasin action. *Nature*, 282:671.
16. Brenner, S.L. and E.D. Korn. 1979. Substoichiometric concentrations of cytochalasin D inhibit actin polymerization. Additional evidence for an F-actin treadmill. *J. Biol. Chem.* 254: 9982-9985.

17. Brown, S.S. and J.A. Spudis. 1979. Cytochalasin inhibits the rate of elongation of actin filament fragments. *J. Cell Biol.*, 83: 657-662.
18. Cande, W.Z., E. Lazarides and J.R. McIntosh. 1977. A comparison of the distribution of actin and tubulin in the mammalian mitotic spindle as seen by indirect immunofluorescence. *J. Cell Biol.*, 72: 552-567.
19. Carasso, N., P. Favard, and J. Bourquet. 1973. Action de la cytochalasine B sur la réponse hydrosmotique et l'ultrastructure de la vessie de la grenouille. *J. Microscopie*, 18: 383-400.
20. Carlsson, L., L.E. Nyström, U. Lindberg, K.K. Kannan, H. Cid-Dresdner, S. Lövgren and Hans Jörnvall. 1976. Crystallization of a non-muscle actin. *J. Mol. Biol.*, 105: 353-366.
21. Cass, A. and A. Finkelstein. 1967. Water permeability of thin lipid membranes. *J. Gen. Physiol.*, 50: 1765-1984.
22. Chang, C-M and R.D. Goldman. 1973. The localization of actin-like fibers in cultured neuroblastoma cells as revealed by heavy meromyosin binding. *J. Cell. Biol.*, 57: 867-874.
23. Chevalier, J., J. Bourquet and J.S. Hugon. 1974. Membrane associated particles: distribution in frog urinary bladder epithelium at rest and after oxytocin treatment. *Cell Tiss. Res.* 152: 129-140.
24. Choi, J.K. 1963. The fine structure of the urinary bladder of the toad, *Bufo marinus*. *J. Cell Biol.*, 16: 53-72.

25. Clarke, M. and J. A. Spudich. 1977. Nonmuscle contractile proteins: the role of actin and myosin in cell motility and shape determination. *Ann. Rev. Bioch.* 46: 797-822.
26. Condeelis, J. 1979. Isolation of concanavalin A caps during various stages of formation and their association with actin and myosin. *J. Cell Biol.*, 80: 751-758.
27. Dainty, J. and C. R. House. 1966. "Unstirred layers" in frog skin. *J. Physiol. (Lond.)* 182: 66-78.
28. Davis, W. L., D. B. P. Goodman, J. H. Martin, J. L. Matthews and H. Rasmussen. 1974. Vasopressin-induced changes in the toad urinary bladder epithelial surface. *J. Cell Biol.*, 61: 544-547.
29. Davis, W. L., D. B. P. Goodman, R. J. Schuster, J. H. Martin, and H. Rasmussen. 1974. The effect of cytochalasin B on the response of the toad bladder to vasopressin. *J. Cell Biol.*, 63: 986-997.
30. Davis, W. L., D. B. P. Goodman, R. G. Jones and H. Rasmussen. 1978. The effects of cytochalasin B on the surface morphology of the toad urinary bladder epithelium: a scanning electron microscope study. *Tissue & Cell*, 10: 451-462.
31. DeLorenzo, R. J., K. G. Walton, P. F. Curran and P. Greengard. 1973. Regulation of phosphorylation of a specific protein in toad-bladder membrane by antidiuretic hormone and cyclic AMP, and its possible relationship to membrane permeability changes. *Proc. Nat. Acad. Sci.*, 70: 880-884.

32. DeLorenzo, R.J. and P. Greengard. 1973. Activation by adenosine 3', 5' -monophosphate of a membrane-bound phosphoprotein phosphatase from toad bladder. *Proc. Nat. Acad. Sci.* 70: 1831-1835.
33. deSousa, R. C., A. Grosso, and C. Rufener. 1974. Blockade of the hydrosmotic effect of vasopressin by cytochalasin B. *Experientia* 30: 175-177.
34. deSousa, R. C. 1975. Mechanismes de transport de l'eau et du sodium par les cellules des epithelia d'amphibiens et du tubule rénal isolé. *J. de Physiologie*, 5A-71A.
35. DiBona, D.R., M. M. Civan, and A. Leaf. 1969. The cellular specificity of the effect of vasopressin on toad urinary bladder. *J. Membrane Biol.*, 1: 79-91.
36. Dousa, T. P., H. Sands and O. Hechter. 1972. Cyclic AMP-dependent reversible phosphorylation of renal medullary plasma membrane protein. *Endocrinology*, 91: 757-763.
37. Dousa, T.P. and L.D. Barnes. 1974. Effects of colchicine and vinblastine on the cellular action of vasopressin in mammalian kidney. *J. Clin. Invest.*, 54: 252-262.
38. Durham, A. C. H. 1974. A unified theory of the control of actin and myosin in nonmuscle movements. *Cell*, 2: 123-136.
39. Edelman, G. M. 1976. Surface modulation in cell recognition and cell growth. *Science*, 192: 218-226.

40. Ferguson, D. R. and B. R. Twite. 1974. Effects of vasopressin on toad bladder membrane proteins: relationship to transport of sodium and water. *J. Endocrinol.*, 61: 501-507.
41. Finkelstein, A. 1976. Water and nonelectrolyte permeability of lipid bilayer membranes. *J. Gen. Physiol.*, 68: 127-135.
42. Finkelstein, A. 1976. Nature of the water permeability increase induced by antidiuretic hormone (ADH) in toad urinary bladder and related tissues. *J. Gen. Physiol.*, 68: 137-143.
43. Flanagan, J. and G. L. E. Koch. 1978. Cross-linked surface Ig attaches to actin. *Nature*, 273: 278-281.
44. Flanagan, M. D., 1979. A high-affinity cytochalasin B binding complex from bovine brain. *Fed. Proc. Fed. Am. Soc. Exp. Biol.*, 38: 339a.
45. Franke, W. W., E. Schmid, M. Osborn and K. Weber. 1978. Different intermediate-sized filaments distinguished by immunofluorescence microscopy. *Proc. Nat. Acad. Sci.*, 75: 5034-5038.
46. Garrels, J. I. and W. Gibson. 1976. Identification and characterization of multiple forms of actin. *Cell*, 9: 793-805.
47. Goldman, R., T. Pollard and J. Rosenbaum, eds. Cell Motility. Cold Springs Harbor Laboratories, Cold Spring Harbor, New York 1976.
48. Gordon, D. J., E. Eisenberg and E. D. Korn. 1976. Characterization of cytoplasmic actin isolated from Acanthamoeba castellanii by a new method. *J. Biol. Chem.*, 251: 4778-4786.

49. Gronowicz, G., S.K. Masur and E. Holtzman. 1978. Exocytosis, endocytosis and hydroosmosis in the toad bladder. Am. Soc. Cell Biol., 18th Ann. Meeting. 79, St2420a.
50. Gronowicz, G., S.K. Masur, and E. Holtzman. 1979. Quantitative analysis of exocytosis and endocytosis in the hydroosmotic response of toad bladder. J. Membrane Biol., In press.
51. Grosso, A., F. Spinelli and R. C. deSousa. 1978. Cytochalasin B and water transport. A scanning electron microscope study of the toad urinary bladder. Cell Tiss. Res. 188: 375-388.
52. Handler, J.S., R.W. Butcher, E.W. Sutherland and J. Orloff. 1965. The effect of vasopressin and of theophylline on the concentration of adenosine - 3', 5'-phosphate in the urinary bladder of the toad. J. Biol. Chem. , 240: 4524-4526.
53. Handler, J.S. and J. Orloff. 1973. The mechanism of action of anti-diuretic hormone. In: Handbook of Physiology. Renal Physiology. Am. Physiol. Soc., Washington D. C., Sect. 8, Chap. 24, pp. 791-814.
54. Hardy, M.A., Jr., R. Montoreano and M. Parisi. 1975. Colchicine dissociates the toad (Bufo arenarum) urinary bladder responses to antidiuretic hormone and to serosal hypertonicity. Experientia, 31: 803-804.

55. Hartwig, J.H. and T.P. Stossel, 1975. Isolation and properties of actin, myosin, and a new actin-binding protein in rabbit alveolar macrophages. *J. Biol. Chem.*, 250: 5696-5705.
56. Hatano, S., H. Kondo, and T. Miki-Noumura, 1969. Purification of sea urchin egg actin. *Exp. Cell Res.*, 55: 275-277.
57. Hays, R.M. and A. Leaf, 1962. Studies on the movement of water through the isolated toad bladder and its modification by vasopressin. *J. Gen. Physiol.*, 45: 905-919.
58. Hays, R.M. and N. Franki, 1970. The role of water diffusion in the action of vasopressin. *J. Membr. Biol.*, 2: 263-276.
59. Hays, R.M. 1972. Independent pathways for water and solute movement across the cell membrane. *J. Membr. Biol.*, 10: 367-371.
60. Hays, R.M., N. Franki, and L.S. Ross, 1979. Effect of metabolic inhibitors on vasopressin-stimulated transport systems in the toad bladder. *J. Supramolec. Struct.* 10: 175-184.
61. Herman, I.M. and T.D. Pollard, 1978. Actin localization in fixed dividing cells stained with fluorescent heavy meromyosin. *Exp. Cell Res.* 114: 15-25.
62. Hevesy, G., E. Hofer and A. Krogh, 1935. The permeability of the skin of frogs to water as determined by D₂O and H₂O. *Skand. Arch. Physiol.*, 72: 199-214.
63. Huang, C-J. 1979. The role of cyclic AMP mediated dephosphorylation and cyclic AMP mediated phosphorylation in the mechanism of action of anti-diuretic hormone. Ph.D. Thesis. The City University of New York.

64. Huxley, A. F. 1974. Muscular contraction. *J. Physiol.*, 243: 1-43.
65. Huxley, H. E. 1963. Electron microscope studies on the structure of natural and synthetic protein filaments from striated muscle. *J. Mol. Biol.*, 7: 281-308.
66. Ishikawa, H., R. Bischoff and H. Holtzer. 1969. Formation of arrowhead complexes with heavy meromyosin in a variety of cell types. *J. Cell Biol.*, 43: 312-328.
67. Jard, S. and F. Bastide. 1970. A cyclic AMP-dependent protein kinase from frog bladder epithelial cells. *Biochem. Biophys. Res. Commun.* 39: 559-566.
68. Kachadorian, W. A., J. B. Wade and V. A. DiScala. 1975. Vasopressin-induced structural change in toad bladder luminal membrane. *Science*, 190: 67-69.
69. Kachadorian, W. A., S. J. Ellis and J. Muller. 1979. Possible roles for microtubules and microfilaments in ADH action on toad urinary bladder. *Am. J. Physiol.*, 236: F14-F20.
70. Kane, R. E. 1976. Actin polymerization and interaction with other proteins in temperature-induced gelation of sea urchin egg extracts. *J. Cell Biol.*, 71: 704-714.
71. Kielley, W. W. and W. F. Harrington. 1960. A model for the myosin molecule. *Biochim. Biophys. Acta*, 41: 401-421.
72. Kinne, R. and L. L. Schwartz. 1977. Asymmetric distribution of renal epithelial cell membrane function in the action of antidiuretic hor-

- mone and parathyroid hormone. In: Disturbances in Body Fluid Osmolality, T. E. Andreoli et al., eds. op. cit., pp 37-55.
73. Kirchberger, M. A., I. L. Schwartz and R. Walter. 1972. Cyclic 3', 5'-AMP-dependent protein kinase activity in toad bladder epithelium. *Proc. Soc. Exp. Biol. Med.* 140: 657-660.
74. Kletzien, R. F., J. F. Perdue and A. Springer. 1972. Cytochalasin A and B inhibition of sugar uptake in cultured cells. *J. Biol. Chem.* 247: 2964-2966.
75. Kletzien, R. F. and J. F. Perdue. 1973. The inhibition of sugar transport in chick embryo fibroblasts by cytochalasin B. Evidence for a membrane specific effect. *J. Biol. Chem.* 248: 711-719.
76. Koch, G. L. E., and M. J. Smith. 1978. An association between actin and the major histocompatibility antigen H-2. *Nature*, 273: 274-278.
77. Koefoed-Johnsen, V. and H. H. Ussing. 1953. The contributions of diffusion and flow to the passage of D₂O through living membranes. *Acta Physiol. Scand.* 42: 298-308.
78. Korn, E. D. 1978. Biochemistry of actomyosin-dependent cell motility (a review). *Proc. Nat. Acad. Sci.* 75: 588-599.
79. Kraehenbuhl, J. P., J. Pfeiffer, M. Rossier and B. C. Rossier, 1979. Microfilament-rich cells in the toad bladder epithelium. *J. Membrane Biol.*, 48: 167-180.

80. Kuo, J. F. and P. Greengard, 1969. Cyclic nucleotide-dependent protein kinases. IV. Widespread occurrence of adenosine 3', 5' - monophosphate-dependent protein kinase in various tissues and phyla of the animal kingdom. *Proc. Nat. Acad. Sci.*, 64: 1349-1355.
81. Lazarides, E. 1976. Aspects of the structural organization of actin filaments in tissue culture cells. In: Cell Motility, R. Goldman, et al., eds., op. cit. pp. 347-360.
82. Leaf, A. 1965. Transepithelial transport and its hormonal control in the toad bladder. In: Ergebnisse der Physiologie-Reviews of Physiology, vol. 56, Springer-Verlag, Berlin, pp. 215-263.
83. Levine, S., N. Frankl, and R. M. Hays. 1973. Effect of phloretin on water and solute movement in the toad bladder. *J. Clin. Invest.* 52: 1435-1442.
84. Levine, S. D., R. D. Levine, R. E. Worthington, and R. M. Hays. 1976. Selective inhibition of osmotic water flow by general anesthetics in toad urinary bladder. *J. Clin. Invest.* 58: 980-988.
85. Lin, S. and J. A. Spudich, 1974. Biochemical studies on the mode of action of cytochalasin B. Cytochalasin B binding to red cell membrane in relation to glucose transport. *J. Biol. Chem.*, 249: 5778-5783.
86. Lin, S., D. C. Lin, and M. D. Flanagan, 1978. Specificity on the effects of cytochalasin B on transport and motile processes. *Proc. Nat. Acad. Sci.*, 75: 329-333.

87. Lin, S., D.V. Santi, and J.A. Spudich. 1974. Biochemical studies on the mode of action of cytochalasin B. Preparation of (³H) cytochalasin B and studies on its binding to cells. *J. Biol. Chem.*, 249: 2268-2274.
88. Lin, S. and C.E. Snyder, Jr. 1977. High affinity cytochalasin B binding to red cell membrane proteins which are unrelated to sugar transport. *J. Biol. Chem.*, 252: 5464-5471.
89. Lin, D.C. and S. Lin. 1979. Actin polymerization induced by a motility-related high-affinity cytochalasin binding complex from human erythrocyte membrane. *Proc. Nat. Acad. Sci.*, 76: 2345-2349.
90. Lowey, S. and C. Cohen. 1962. Studies on the structure of myosin. *J. Mol. Biol.*, 4: 293-308.
91. Lowry, O.H., N. Rosebrough, A.L. Farr and R.J. Randall, 1951. Protein measurement with the Folin phenol reagent. *J. Biol. Chem.*, 193: 265-275.
92. Luft, J.H. 1963. Improvements in epoxy resin embedding methods. *J. Biophys. Biochem. Cytol.* 9: 409-414.
93. MacRobbie, E.A.C. and H.H. Ussing. 1961. Osmotic behavior of the epithelial cells of frog skin. *Acta Physiol. Scand.* 53: 348-365.
94. McNutt, N.S. 1978. A thin-section and freeze-fracture study of microfilament-membrane attachments in choroid plexus and intestinal microvilli. *J. Cell Biol.*, 79: 774-787.

95. Mannherz, H.G., W. Babsch and R. Leberman, 1977. Crystals of skeletal muscle actin: pancreatic DNAase I complex. *FEBS Letters*, 73: 141-143.
96. Margolis, R. L. and L. Wilson, 1978. Opposite end assembly and dis-assembly of microtubules at steady state in vitro. *Cell*, 13: 1-8.
97. Marovitz, W. F., K. M. Khan, and T. Schulte, 1977. Studies in otic embryogenesis. 2. Ultrastructural development of the early rat otocyst. *Ann. Otol. Rhinol. Laryngol.* 86, suppl. 35, 9-28.
98. Marsh, B.B. 1959. The estimation of inorganic phosphate in the presence of adenosine triphosphate. *Biochim. Biophys. Acta.* 32: 357-361.
99. Masur, S.K., E. Holtzman, I. L. Schwartz and R. Walter, 1971. Correlation between pinocytosis and hydroosmosis induced by neurohypophyseal hormones and mediated by adenosine 3',5' - cyclic monophosphate. *J. Cell Biol.*, 49: 582-589.
100. Masur, S.K., E. Holtzman, I. L. Schwartz and R. Walter. 1972. Hormone-stimulated exocytosis in the toad urinary bladder. Some possible implications for turnover of surface membranes. *J. Cell Biol.*, 52: 211-219.
101. Metzels, J. and I. Tasaki, 1978. Subaxolemmal filamentous network in the giant nerve fiber of the squid (*Loligo pealei* L.) and its possible role in excitability. *J. Cell Biol.*, 78: 597-621.

102. Mills, J. and L. E. Malick. 1978. Mucosal surface morphology of the toad urinary bladder. Scanning electron microscope study of the natriuretic and hydroosmotic response to vasopressin. *J. Cell Biol.*, 77: 598-610.
103. Mooseker, M. S. and L. G. Tilney. 1975. Organization of an actin filament-membrane complex. Filament polarity and membrane attachment in the microvilli of intestinal epithelial cells. *J. Cell Biol.*, 67: 725-743.
104. Mooseker, M., Personal communication. Preparation of muscle acetone powder, actin, myosin, and heavy meromyosin. *Physiology Course, Marine Biological Laboratories, Woods Hole, Mass.*
105. Mooseker, M. S. 1979. Brush border alpha actinin? Comparison of two proteins of the microvillus core with alpha actinin by 2-D peptide mapping. Submitted for publication.
106. Omachi, R. S., D. E. Robbie, J. S. Handler and J. Orloff. 1974. Effects of ADH and other agents on cyclic AMP accumulation in toad bladder epithelium. *Am. J. Physiol.*, 226: 1152-1157.
107. Orloff, J. and J. S. Handler, 1961. Vasopressin-like effects of adenosine 3', 5'-phosphate (cyclic 3' 5'-AMP) and theophylline in the toad bladder. *Biochem. Biophys. Res. Commun.*, 5: 63-66.
108. Orloff, J. and J. S. Handler. 1962. The similarity of effects of vasopressin, adenosine-3', 5'-monophosphate (cyclic AMP) and theophylline on the toad bladder. *J. Clin. Invest.* 41: 702-709.

109. Peachey, L.D. and H. Rasmussen. 1961. Structure of the toad's urinary bladder as related to its physiology. *J. Biophys. Biochem. Cytol.*, 10: 529-553.
110. Pietras, R. J. and E. M. Wright. 1974. Non-electrolyte probes of membrane structure in ADH-treated toad urinary bladder. *Nature*, 247: 222-224.
111. Pietras, R. J. and E. M. Wright, 1975. The membrane action of antidiuretic hormone (ADH) on toad urinary bladder. *J. Membr. Biol.*, 22: 107-123.
112. Pietras, R. J., B. J. Seeler, and C. M. Szego. 1975. Influence of antidiuretic hormone on release of lysosomal hydrolase at mucosal surface of epithelial cells from urinary bladder. *Nature*, 257: 493-495.
113. Pietras, R. J. 1976. Vasopressin-induced redistribution of binding sites for concanavalin A at the surface of epithelial cells from urinary bladder. *Nature*, 264: 774-776.
114. Plagemann, P. G. W., and R. D. Estensen. 1972. Cytochalasin B. VI. Competitive inhibition of nucleoside transport by cultured Novikoff rat hepatoma cells. *J. Cell Biol.*, 55: 179-185.
115. Pollard, T. D. and R. R. Wehing, 1974. Actin and myosin in cell movement. *Crit. Rev. Biochem.*, 2: 1-65.
116. Puszkin, S. and S. Berl. 1968. Actomyosin-like protein isolated from mammalian brain. *Science*, 161: 170-171.

117. Reaven, E., R. Maffly and A. Taylor. 1978. Evidence for involvement of microtubules in the action of vasopressin in toad urinary bladder. III. Morphological studies on the content and distribution of microtubules in bladder epithelial cells. *J. Membr. Biol.*, 40: 251-267.
118. Reynolds, E.S. 1963. The use of lead citrate at high pH as an electron-opaque stain in electron microscopy. *J. Cell Biol.*, 17: 208-212.
119. Robertson, G.L., S. Athar and R.L. Shelton. 1977. Osmotic control of vasopressin function. In: Disturbances in Body Fluid Osmolality, T.E. Andreoli, ed., op. cit., pp. 125-148.
120. Rossier, M., B. Rossier, J. Pfeiffer and J.P. Kraehenbuhl. 1979. Isolation and separation of toad bladder epithelial cells. *J. Membr. Biol.*, 48: 141-166.
121. Rostgaard, J., B.I. Kristensen and L.E. Nielsen. 1972. Electron microscopy of filaments in the basal part of rat kidney tubule cells and their in situ interaction with heavy meromyosin. *Z. Zellforsch.*, 132: 497-521.
- 121a. Sapirstein, V.S. and W.N. Scott. 1973. Cyclic AMP and sodium transport. Quantitative and temporal relationships in toad urinary bladder. *J. Clin. Invest.* 52: 2379-2382.
122. Schroeder, T.E. 1973. Actin in dividing cells: contractile ring filaments bind heavy meromyosin. *Proc. Nat. Acad. Sci.*, 70: 1688-1692.

123. Schwartz, I. L., L. J. Schlatz, E. Kinne-Saffran and R. Kinne. 1974. Target cell polarity and membrane phosphorylation in relation to the mechanism of action of antidiuretic hormone. *Proc. Nat. Acad. Sci.*, 71: 2595-2599.
124. Schwartz, J., S. Berl, W. J. Nicklas, C. Mahendran and W. O. Whetsell, Jr. 1977. Further characterization of brain actin by electron microscopy. *J. Neuropath. Exp. Neurol.* XXXVI, 398-410.
125. Soifer, D. ed, 1975. The Biology of Cytoplasmic Microtubules. *Ann. N. Y. Acad. Sci.*, 253: 1-848.
126. Spooner, B. S., J. F. Ash, J. T. Wrenn, R. B. Frater and N. K. Wessels, 1973. Heavy meromyosin binding to microfilaments involved in cell and morphogenetic movements. *Tissue & Cell*, 5: 37-46.
127. Spudich, J. A. 1972. Effects of cytochalasin B on actin filaments, In: Cold Spring Harbor Symposia on Quantitative Biology, Vol. XXXVII, The Mechanism of Muscle Contraction, Cold Spring Harbor, New York, pp. 585-593.
128. Spudich, J. A. and S. Lin, 1972. Cytochalasin B, its interaction with actin and actomyosin from muscle. *Proc. Nat. Acad. Sci.*, 69: 442-446.
129. Spudich, J. A. and S. Watt. 1971. The regulation of rabbit skeletal muscle contraction. I. Biochemical studies of the interaction of the tropomyosin-troponin complex with actin and the proteolytic fragments of myosin. *J. Biol. Chem.*, 246: 4866-4871.

130. Taylor, A., M. Mamelak, E. Reaven, and R. Maffly. 1973. Vasopressin: possible role of microtubules and microfilaments in its action. *Science*, 181: 347-350.
131. Taylor, A., R. Maffly, L. Wilson and E. Reaven. 1975. Evidence for involvement of microtubules in the action of vasopressin. In: The Biology of Cytoplasmic Microtubules, D. Soifer, ed. Ann. N. Y. Acad. Sci., 253: 723-737.
132. Taylor, A. Role of microtubules and microfilaments in the action of vasopressin. In: Disturbances in Body Fluid Osmolality, T. E. Andreoli, J. J. Grantham and F. C. Rector, eds., Am. Physiol. Soc., Washington, D. C. 1977, pp. 97-124.
133. Taylor, A., M. Mamelak, H. Golbetz and R. Maffly, 1978. Evidence for involvement of microtubules in the action of vasopressin in toad urinary bladder. I. Functional studies on the effects of anti-mitotic agents on the response to vasopressin. *J. Membr. Biol.* 40: 213-235.
134. Tilney, L. G. 1971. The role of actin in non-muscle cell motility. In: Molecules and Cell Movement, S. Inoue and R. E. Stephens, eds., New York, Raven Press, pp. 339-386.
135. Tilney, L. G. 1976. The polymerization of actin. III. Aggregates of nonfilamentous actin and its associated proteins: a storage form of actin. *J. Cell Biol.*, 69: 73-89.

136. Tilney, L. G., D. Kiehart, C. Sardet, and M. Tilney. 1978. Polymerization of actin. IV. The role of Ca^{++} and H^+ in the assembly of actin and in membrane fusion in the acrosomal reaction of echinoderm sperm. *J. Cell Biol.*, 77: 536-550.
137. Ukena, T. E., J. Z. Borysenko, M. J. Karnovsky and R. D. Berlin. 1974. Effects of colchicine, cytochalasin B, and 2-deoxyglucose on the topographical organization of surface-bound concanavalin A. in normal and transformed fibroblasts. *J. Cell Biol.*, 61: 70-82.
138. Ussing, H. H. and K. Zerahn, 1951. Active transport of sodium as the source of electric current in the short-circuited isolated frog skin. *Acta Physiol. Scand.*, 23: 110-123.
139. Vial, J. D. and J. Garrido, 1976. Actin-like filaments and membrane rearrangement in oxyntic cells. *Proc. Nat. Acad. Sci.*, 73: 4032-4036.
140. Wade, J. B. 1979. Hormonal modulation of epithelial structure. In: Current Topics in Membrane Transport, In press.
141. Weber, A. and J. M. Murray. 1973. Molecular control mechanisms in muscle contraction. *Physiol. Rev.* 53: 612-673.
142. Weber, H. H. and H. Portzehl, 1952. Kontraktion, ATP-cyclus und fibrilläre proteine des muskels. *Ergeb. Physiol.*, 47: 369-468.
143. Weber, K. and M. Osborn, 1969. The reliability of molecular weight determinations by dodecyl sulfate-polyacrylamide gel electrophoresis. *J. Biol. Chem.* 244: 4406-4412.

144. Weibing, R. R. 1976. Membrane association and polymerization of actin. In: Cell Motility, R. Goldman et al., eds. op. cit., pp. 671-684.
145. Weibing, R. R. and E. D. Korn. 1971. Acanthamoeba actin. Isolation and properties. Biochemistry, 10: 590-600.
146. Wessels, N. K., B. S. Spooner, J. F. Ash, et al., 1971. Microfilaments in cellular and developmental processes. Science, 171: 135-143.
147. Wilson, L. and A. Taylor. 1978. Evidence for involvement of microtubules in the action of vasopressin in toad urinary bladder. II. Colchicine binding properties of toad bladder epithelial cell tubulin. J. Membr. Biol., 40: 237-250.
148. Wolosewick, J. J. and K. R. Porter. 1979. Microtrabecular lattice of the cytoplasmic ground substance. J. Cell Biol., 82: 114-139.
149. Woolley, D. E. 1972. An actin-like protein from amoeba of Dictyostelium discoideum. Arch. Biochem. Biophys. 150: 519-530.
150. Yang, Y. and J. F. Perdue. 1972. Contractile proteins of cultured cells. The isolation and characterization of an actin-like protein from cultured chick embryo fibroblasts. J. Biol. Chem., 247: 4503-4509.
151. Zusman, R. M., H. R. Keiser, and J. S. Handler. 1977. Vasopressin-stimulated prostaglandin E biosynthesis in the toad urinary bladder. Effect on water flow. J. Clin. Invest., 60: 1339-1347.

152. Zusman, R. M., H. R. Keiser and J. S. Handler, 1977. Inhibition of vasopressin-stimulated prostaglandin E biosynthesis by chlorpropamide in the toad urinary bladder. *J. Clin. Invest.*, 60: 1348-1353.
153. Zusman, R. M. and H. R. Keiser, 1977. Prostaglandin E₂ biosynthesis by rabbit renomedullary interstitial cells in tissue culture. *J. Biol. Chem.*, 252: 2069-2071.